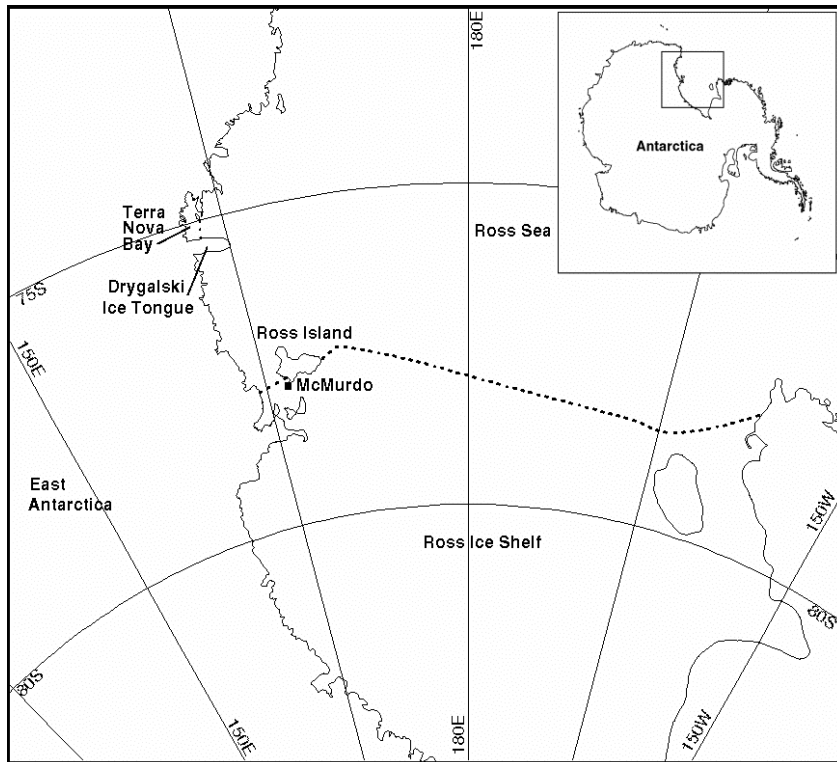


# THE ROSS ISLAND METEOROLOGY EXPERIMENT (RIME)

A Workshop Sponsored by the National Science Foundation

Preprint Volume  
11-13 September 2001

Edited by Andrew J. Monaghan and Lynn R. Everett



BPRC Miscellaneous Series M-422

Polar Meteorology Group  
Byrd Polar Research Center  
The Ohio State University  
Columbus, Ohio 43210

## TABLE OF CONTENTS

### ROSS ISLAND METEOROLOGY EXPERIMENT (RIME) WORKSHOP

#### PAGE

- 1 TOWARDS A SEASONAL FORECAST IN THE ROSS SEA  
Xiaojun Yuan, J. Liu, D. Rind and D. G. Martinson (Lamont-Doherty Earth Observatory, Columbia University)
  
- 4 ICE CORES AND THE ATMOSPHERE: IMPROVING ICE CORE INTERPRETATION THROUGH INTENSIVE STUDY OF WEST ANTARCTIC METEOROLOGY  
David B. Reusch and Richard B. Alley (The Pennsylvania State University, University Park, PA)
  
- 10 MM5 WINTERTIME SIMULATIONS OF THE ANTARCTIC BOUNDARY-LAYER WIND FORCING  
Tom Parish (University of Wyoming, Laramie)
  
- 16 SATELLITE REMOTE SENSING OF ANTARCTIC CLOUD PROPERTIES  
Dan Lubin and Joannes Berque (Scripps Institution of Oceanography, La Jolla, California)
  
- 18 THE ANTARCTIC MESOSCALE PREDICTION SYSTEM (AMPS): POTENTIAL APPLICATIONS FOR RIME  
Ying-Hwa Kuo, Jordan Powers, and James F. Bresch (National Center for Atmospheric Research (NCAR), Boulder, CO)
  
- 21 RIME: IMPROVING MULTISCALE FORECASTING OF ANTARCTIC METEOROLOGY  
David Bacon (SAIC, McLean, VA), Tom Parish (University of Wyoming, Laramie), and Ken Waight (MESO Inc., Raleigh, NC)
  
- 26 AMPS OPERATIONAL UTILITY  
Art Cayette, Chester Clogston, and James Frodge (SPAWAR, Charleston, SC)
  
- 30 IMPROVEMENTS IN DATA SOURCE COLLECTION IN ANTARCTICA  
James Frodge, Chester Clogston, and Art Cayette (SPAWAR, Charleston, SC)
  
- 33 PERFORMANCE OF POLAR MM5 IN SIMULATING ANTARCTIC ATMOSPHERIC CIRCULATION  
Zhichang Guo (Byrd Polar Research Center, Columbus, OH)
  
- 38 PERFORMANCE OF FORECAST MODELS IN THE RESCUE OF DR SHEMENSKI FROM SOUTH POLE IN APRIL 2001  
Andrew Monaghan (Byrd Polar Research Center, Columbus, OH)
  
- 43 USE OF GPS RADIO OCCULTATION DATA IN RIME  
Ying-Hwa Kuo, Tae-Kwon Wee, and William Schreiner (National Center for Atmospheric Research (NCAR), Boulder, CO), David H. Bromwich (Byrd Polar Research Center)
  
- 47 A CASE STUDY OF THE IMPACT OF THE UPPER BOUNDARY CONDITION IN POLAR MM5 SIMULATIONS OVER ANTARCTICA  
Helin Wei, David H. Bromwich Le-Sheng Bai (Byrd Polar Research Center), Ying-Hwa Kuo and Kwon Wee (National Center for Atmospheric Research (NCAR), Boulder, CO)
  
- 54 NOAA/ETL STUDIES IN CONDITIONS RELATED TO THE PROPOSED ROSS ISLAND METEOROLOGY EXPERIMENT (RIME)  
Ola Persson (CIRES/NOAA/Environmental Technology Laboratory, Boulder, CO)
  
- 62 THE UNIVERSITY OF WISCONSIN CONTRIBUTION TO THE ROSS ISLAND METEOROLOGY EXPERIMENT (RIME)  
Matthew Lazzara (AMRC/SSEC, University of Wisconsin, Madison)
  
- 63 APPLICATIONS OF AEROSONDES FOR RIME  
Judith Curry, James Maslanik, James Pinto, Sheldon Drobot, John Cassano (University of Colorado, Boulder) and Gregory Holland (Aerosonde Robot Aircraft)
  
- 66 RIME AND THE DOME C TROPOSPHERIC PROGRAM  
Paul Pettré (Meteo France, Toulouse)
  
- 70 SIMULATION OF IRON DUST TRANSPORT IN THE ROSS SEA  
Hubert Gallée (Laboratoire de Glaciologie et de Géophysique de l'Environnement, Grenoble, France)

# Towards a Seasonal Forecast in the Ross Sea

X. Yuan, J. Liu, D. Rind and D. G. Martinson

Lamont-Doherty Earth Observatory of Columbia University

## 1. Introduction

In a recent study (Yuan and Martinson, 2001), we found that the dominant interannual variance structure in the sea ice edge and surface air temperature fields is organized as a quasi-stationary (in space) wave which we call the “Antarctic Dipole” (ADP). It is characterized by an out-of-phase relationship between the ice and temperature anomalies in the central/eastern Pacific and Atlantic sectors of the Antarctic. The dipole consists of a strong standing mode and a weaker propagating motion within each basin's ice field. It has the same wavelength as the Antarctic Circumpolar Wave (ACW) and dominates the ACW variance. The dipole is clearly associated with tropical El Niño/Southern Oscillation (ENSO) events; it can be predicted with moderate skill using linear regression involving surface temperature two to four months ahead. The prediction performs better in extreme warm/cold years, and best in La Niña years. The Ross Sea is in the Pacific branch of the ADP. The climate variability in the Ross Sea is heavily influenced by the ADP oscillation. The linear regression prediction in Yuan and Martinson (2001) only shows the predictability of sea ice due to its links to the tropical climate variations. To build a more vigorous statistical model, we need to understand what causes anomalies in sea ice and surface temperature. The goal of this study is (1) to examine magnitudes of anomalies in sea ice and surface temperature during tropical warm and cold phases; and (2) to investigate atmospheric circulation in mid to high latitudes and meridional heat transports associated with the circulation. Monthly surface air temperature, meridional heat flux and meridional stream function of mass transport from National Centers for Environmental Prediction / National Center for Atmospheric Research (NCEP/NCAR) Reanalysis data were used in this study. Monthly sea ice concentrations were generated by the bootstrap algorithm from the National Aeronautics and Space Administration (NASA) microwave imager (Comiso et al., 1997). The sea ice edge was then derived from the monthly sea ice concentration.

## 2. Methods and Results

To determine the magnitudes of ENSO impact on Southern Ocean sea ice and surface temperature fields, we generated monthly composition maps of sea ice concentration, ice edge and surface air temperature for EL Niño and La Niña scenarios in the Ross Sea Region. Based on the Niño 3.4 index, we selected five El Niño events in 1980, 1983, 1988, 1992, 1997 and four La Niña events in 1985, 1989, 1996 and 1999. The composite maps were generated starting from the maturing month of each ENSO event, January, through the following December. The differences between El Niño and La Niña scenarios show the maximum ENSO impacts on the sea ice concentration and temperature fields. The large ice concentration differences occur near ice edge. The austral winter months have the largest ENSO impacts on sea ice. The differences in ice concentration between the two states can reach 80% with more ice during the La Niña state in the Pacific. Figure 1 gives such an impact in May as an example. On the other hand, the large ENSO impact in surface air temperature extends further into the ice pack. The temperature differences are more profound from May to September, with a maximum in May (Fig. 2). The largest temperature difference reaches 10°C. These differences reflect the mean anomalies in the two climatological states. Anomalies in the monthly mean and at synoptic time scales could be even larger. Correlation between ENSO index Niño3 and meridional heat transports shows that heat was transported into the Ross Sea region during El Niño periods by both mean circulation and eddy activities (Fig. 3). This is consistent with less sea ice there during/after El Niño events. Moreover, the polarward heat transport is dominant by the mean circulation, which suggests that the mean circulation could be responsible for linking lower and high latitudes. Therefore, we plot the mean meridional mass transport stream function in the Ross Sea region from NCEP/NCAR Reanalysis data for the mean El Niño and mean La Niña state (Fig. 4). In this plot, the mean El Niño state is averaged from May (onset of an El Niño event in the tropics) to the following April (end of the event) and then averaged over five events in the last

twenty years. The mean La Niña state has been treated in the same way. The mean meridional circulation is dramatically different for two extreme states. During El Niño events, the Hadley Cell and Ferrel Cell are relatively equatorward, with an extensive polar cell. Poleward mass transport (therefore heat transport) in the Ferrel Cell occurs from 45° to beyond 65°S. On the other hand, during La Niña events, the Hadley Cell and Ferrel Cell move southward 5 to 7 degrees of latitude with enhanced circulation compared to warm events. However, the polarward mass transport is quite weak beyond 60°S. These characteristic circulation patterns lead the large anomalies in sea ice and air temperature by a couple of seasons. Such a relationship provides an opportunity to build a seasonal forecast model for the area.

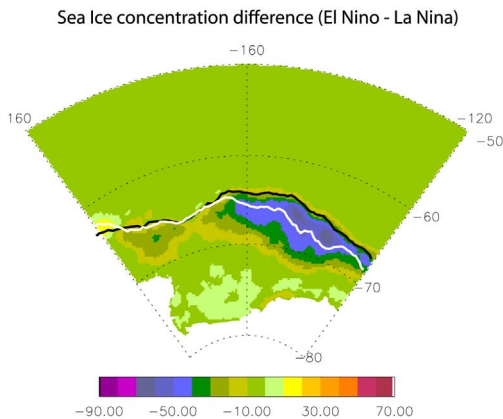


Figure 1 The ENSO impact on sea ice generated by subtracting mean ice concentration in May following 4 La Niña events from the mean ice concentration in May following 5 El Niño events. The white (black) line indicates the mean ice edge following El Niño (La Niña) events.

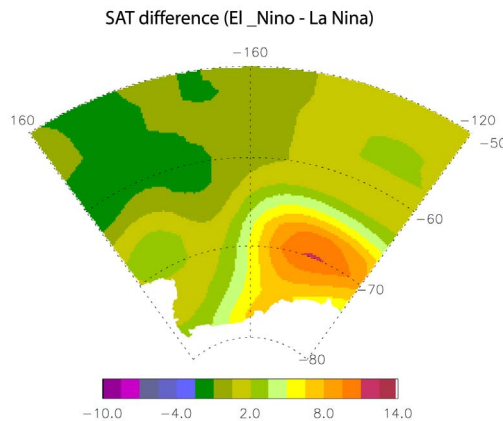


Figure 2 The ENSO impact on surface air temperature generated by subtracting mean air temperature in May following 4 La Niña events from the mean air temperature in May following 5 El Niño events.

### 3. Relevance to RIME

These interannual variabilities in sea ice, air temperature and atmospheric circulation patterns are quite relevant to RIME for following reasons.

1. The magnitudes of interannual variability in the sea ice and surface temperature are large, and are comparable to fluctuations in monthly mean or even synoptic time scales.
2. The temperature simulation in the global climate model is very sensitive to sea ice concentration in polar regions. With wintertime ice concentration contrasts between +50% to -50%, the difference in temperature simulation can exceed 30°C (Parkinson et al. 2001). Therefore, interannual variations in ice concentration with magnitudes up to 40% likely affect regional forecast models significantly.
3. Variation of mean circulation in mid to high latitudes directly influences cyclone distributions in the polar/subpolar regions. In a modeling study, Rind et al. (2001) shows that ENSO-related anomalies in tropical sea-surface temperatures immediately invoke a meridional temperature gradient in the Pacific that alters the intensity of the Hadley Cell, manifested in a meridional shift of the subtropical jet (STJ). For warm events, the STJ moves equatorward in the Pacific, further from the source of available potential energy in the frigid Antarctic (agreeing well with observations in this study). This leads to a reduction in cyclogenesis and polar storm intensity.
4. The interannual variation of mean atmospheric circulation can also trigger regional atmosphere-ice coupling processes that affect storm distribution in the polar/subpolar regions. Such a case was found in 1996 when a wavenumber 3 pattern in the mean atmospheric circulation was coupled with sea ice distribution. The coupling processes provided favorable conditions for cyclogenesis in the open ocean near the sea ice extent maxima (Yuan et al., 1999).

### References

Comiso, J.C., D.J. Cavalieri, C.L. Parkinson, and P. Gloersen, 1997: Passive Microwave Algorithms for Sea Ice Concentration: A Comparison of Two Techniques. *Remote Sens. Environ.*, **60**, 357-384.

Parkinson, C.L., D. Rind, R.J. Healy and D.G. Martinson, 2001: The impact of sea ice

concentration accuracies on climate model simulations with the GISS GCM. *J. Climate*, **14**, 2606-2623.

Rind, D., M. Chandler, J. Lerner, D.G. Martinson and X. Yuan, 2001: The Climate Response to Basin-Specific Changes in Latitudinal Temperature Gradients and The Implications for Sea Ice Variability, *J. Geophys. Res.*, in press.

Yuan, X., D.G. Martinson and W.T. Liu, 1999: Effect of air-sea-ice interaction on Southern Ocean subpolar storm distribution. *Journal of Geophysical Research*, **104**, 1991-2007.

Yuan, X. and D.G. Martinson, 2001: The Antarctic Dipole and its Predictability. *Geophysical Research Letters*, **28**, 3609-3612.

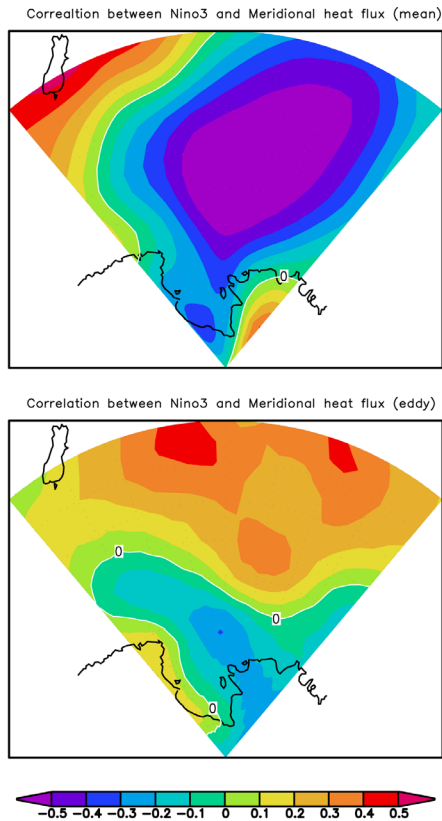


Figure 3 Correlation between ENSO index Nino3 and total meridional heat fluxes due to mean circulation (top) and eddy activities (bottom).

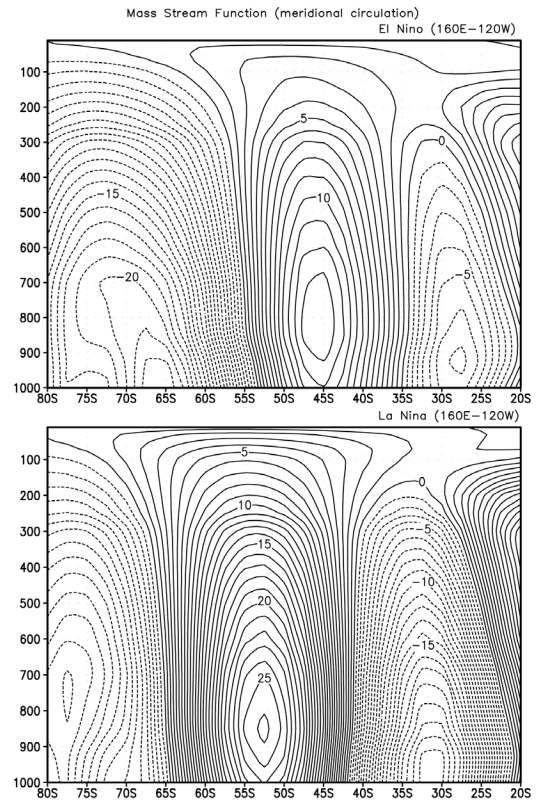


Figure 4 Mass transport stream function for meridional circulation in the Ross Sea region from 160E to 120W. The top panel (bottom panel) is the mean stream function averaged over five El Nino (four La Nina) events from May to following April. The stream function is from NCEP reanalysis.

# ICE CORES AND THE ATMOSPHERE: IMPROVING ICE-CORE INTERPRETATION THROUGH INTENSIVE STUDY OF WEST ANTARCTIC METEOROLOGY

David B. Reusch and Richard B. Alley  
The Pennsylvania State University, University Park, PA

## 1. Introduction

The fundamental postulate of ice-core-based paleoclimate research is that a (probably) non-linear but decipherable relationship exists between the large-scale atmospheric circulation that supplies geochemical tracers and moisture to an ice sheet and paleoclimatic proxy records recovered from ice cores and snow pits. Thus, understanding the meteorology and large-scale circulation in West Antarctica becomes a key prerequisite to improving our knowledge of climate change in this region. In current practice, many different ice-core proxies are interpreted as reflections of changes in atmospheric circulation, but with some uncertainty regarding the mechanisms.

Numerous process studies (e.g., Bergin et al. 1995; Dibb and Jaffrezo 1997; Minikin et al. 1998; Sommer et al. 2000; Wåhlin 1996) have been performed to examine the atmosphere-proxy relationship. However, this work has tended to emphasize specific details of the air-snow transfer process, with a focus on Greenland over Antarctica, rather than relating detailed meteorology to the proxy records. The exceptions to this (e.g., Bromwich and Rogers 2000; Kreutz et al. 1999) have yielded important pointers to what might be possible with an improved understanding of the meteorology.

The Antarctic First Regional Observing Study of the Troposphere (FROST) Project (Turner et al. 1999) has shown the utility of focused meteorological observing campaigns. An extended campaign modeled after FROST and focusing on West Antarctica will bring distinct benefits to the meteorological community studying this region. The benefits could be even larger if the meteorological needs of the ice coring community are also considered.

## 2. Motivation

### 2.1 *Climate Change and Proxy Records*

Natural and human-caused climate change are widely acknowledged to be of great societal importance. Advances in our knowledge of the climate system under the auspices of groups such as the U.S. Global Change Research Program (USGCRP), the International Geosphere-

Biosphere Programme (IGBP), and the World Climate Research Programmes (WCRP) have been remarkable. Yet the global climate system is inherently complex and the details of its functioning remain poorly understood. This ignorance is due in part to our lack of long-term climate records (e.g., Duplessy and Overpeck 1996). Direct observational and instrumental records are limited both spatially and temporally, extending back approximately 200 years in the Northern Hemisphere and only 30-40 years in the Antarctic, not long enough to characterize natural variability. A vital element of climate-change research thus becomes the development of proxy records of climate variables that can be related to modern observable data. These paleoclimate records from ice cores, ocean and lake sediments, tree rings, and other sources, extend our knowledge both deeper into time and into new spatial regions.

### 2.2 *Ice Cores As Paleoclimate Proxies*

Ice cores have been a particularly rich source of paleoclimate proxy data in recent years, providing many new insights into climate from the present back through the last interglacial (ca. 120,000 years ago) and beyond. Ice cores provide information on local climate (snowfall and temperature at a site), regional climate (wind-blown dust, sea-salt, and other materials from beyond the ice sheet), climate in broader regions (through trapped-gas records of carbon dioxide, methane, nitrous oxide and other gases), and even conditions beyond the Earth (concentrations of extraterrestrial dust and cosmogenic isotopes). Ice cores have documented the close tie between greenhouse-gas concentrations and temperature over glacial-interglacial cycles, the common existence of larger, more-rapid climate changes in the past than any experienced by industrial or agricultural humans, and even clean-up of some human-caused pollution (such as the fall of lead concentrations in Greenland snow as the United States phased in unleaded gasoline during the 1970's) (Ice Core Working Group 1998; Sherrell et al. 2000). Global anthropogenic change from biomass burning during the 19th century agricultural revolution has been seen in ice-core records of NH<sub>4</sub><sup>+</sup>, CO<sub>2</sub> and black carbon (soot)

(Holdsworth et al. 1996). Data from the Greenland ice sheet have provided a unique view of atmospheric circulation and chemistry in the northern hemisphere (e.g., Mayewski et al. 1997; O'Brien et al. 1995). Similar work in the Antarctic has shown both the high variability of this region (Reusch et al. 1999) and provided insight into the global nature of the Little Ice Age (Kreutz et al. 1997). The data from the polar regions are also valuable because these areas are usually thought to be more sensitive to climate change (due to ice-albedo feedback effects) than temperate and tropical areas (Peixoto and Oort 1992) and can thus provide unique records of climate.

### **2.3 West Antarctic Ice Core Interpretation Issues**

Ice-core data provide windows on past climates that are critical in understanding and eventually predicting the climate system. Major U.S. efforts are devoted to understanding the time and space variability of climate using West Antarctic ice-core data under the auspices of U.S. ITASE (International Trans-Antarctic Scientific Expedition), WAIS (the West Antarctic Ice Sheet Initiative) and WAISCORES (the WAIS deep ice core project), with important logistical and research investments (Kreutz and Mayewski 1998; U.S. ITASE Steering Committee 1996; WAIS Committee 1995).

Early ice-core data from West Antarctica show large spatial and temporal variability (e.g., Reusch et al. 1999). The "traditional" analysis path, in which ice-core data are examined (by inspection, or by statistical tools including time-series analysis) for relations to possible forcing functions, leaves much of the variance "unexplained". Techniques such as principal component analysis have been successful in identifying the dominant relationships in multivariate data sets, but significant interpretation of the results is still required and identification of noise effects remains subjective.

Some of this unexplained variance is undoubtedly "noise" arising from depositional processes such as snow drifting; however, evidence reviewed below suggests that much of this complexity records the important climatic processes, related to the El Niño-Southern Oscillation (ENSO), position of the Amundsen Sea Low, etc., that these projects seek to interpret. Extracting the signal from the noise is thus central to the success of U.S. ITASE and WAISCORES, and will require analytical tools in addition to those used in previously successful projects such as GISP2.

## **3. Why West Antarctica is of Interest**

### **3.1 The Importance of West Antarctica**

Antarctica plays a vital role in dynamic linkages connecting the complex components of the global climate system (e.g., atmosphere, cryosphere, hydrosphere) (U.S. ITASE Steering Committee 1996). West Antarctica, in particular, may be the most climatologically and glaciologically dynamic area of the continent (WAIS Committee 1995). This sector receives about 40% of the moisture transported into the continent (Bromwich 1988) and has the Antarctic's highest interannual variability, possibly due to an El Niño-Southern Oscillation (ENSO) connection (Bromwich and Rogers 2000; Bromwich et al. 2000; Cullather et al. 1996; Genthon and Krinner 1998). Satellite observations indicate that meridional moisture transport is primarily poleward through the Bellingshausen and Amundsen Sea sectors and equatorward in the Weddell Sea sector (Slonaker and Van Woert 1999). Yet the scarcity of climate records keeps this region relatively poorly understood.

Evidence from instrumental records indicates that different parts of the continent are affected by separate components of the atmospheric circulation (U.S. ITASE Steering Committee 1996). The high interior plateau is largely influenced by vertical transport from the upper troposphere and stratosphere. The remainder of the continent is connected more to lower tropospheric transport, such as the cyclonic systems around Antarctica that often move southward over the ice sheet. Central West Antarctica, in particular, is strongly influenced by warm air advecting southward and upslope onto the polar plateau bringing higher concentrations of marine aerosols and a significant amount of the moisture transported to this region (Bromwich 1988; Hogan 1997).

### **3.2 Meteorology/Climatology Highlights**

Thorough introductions to Antarctic meteorology and climatology already include Schwerdtfeger (1984) and King and Turner (1997). Bromwich and Stearns (1993) provides a summary of automatic weather station-based research and an example of the utility of AWS data for short-term forecasting has recently been documented in Holmes et al. (2000). Here a brief overview of some of the more compelling recent results from climate models, from studies of numerical reanalysis data sets (e.g., the European Centre for Medium-Range Weather Forecasts (ECMWF)), and from AWS data sets demonstrates the

importance of West Antarctica in the global climate.

Evidence of links to lower latitudes has been discovered in the correlation found between ENSO and moisture convergence in a sector (120° W to 180°, 75° to 90° S) of West Antarctica (Cullather et al. 1996). A study of ECMWF data showed that moisture convergence correlates well with the Southern Oscillation Index (SOI), particularly for the period 1980-90. The nature of this teleconnection to tropical latitudes is unclear and its existence is still debated (Bromwich and Rogers 2000; Bromwich et al. 2000; Genthon and Krinner 1998; Rogers et al. 1999). It may relate to changes in the Amundsen Sea Low as well as other changes in atmospheric circulation over the Antarctic plateau. The SOI also correlates well with deuterium isotopes at Siple Dome (Bromwich et al. 2000). Links such as these help to interpret the ENSO signals being found in Antarctic proxy records (e.g., Legrand and Feniet-Saigne 1991) as well as aid in regional seasonal weather forecasting (Carleton 2000). Another link between the Amundsen Sea Low and West Antarctic climatology appears in glaciochemical records from Siple Dome. In this case, variability in the strength of the low was found to correlate with variability in seasalt concentrations (Kreutz et al. 1999). A link from south to north is seen in the effect atmospheric circulation over Antarctica has on lower latitudes through dramatic seasonal changes in mass balance of the atmosphere (Parish and Bromwich 1997). Variability in the high-pressure system over the plateau results in atmospheric mass transfers over the entire continent with resulting influences on meridional circulation in the southern hemisphere.

### **3.3 High Spatial Variability**

The spatial variability of West Antarctic climate as seen through indicators such as the major ion chemistry and accumulation rates measured in ice cores is high (Reusch et al. 1999). Basic tools such as visual comparisons and linear correlations tell us only that the time series vary widely between sites only ~50 km apart. Higher order tools, such as principal component analysis (PCA), can bring out patterns of coherent overall behavior of species such as seasalt and nssSO<sub>4</sub>, but they only give an outline of the complete picture at best. A gap remains between the direct record in the ice, which is highly spatially variable, and the PCA results (Reusch et al. 1999). To bridge this gap and to go beyond climatological approaches (e.g., 40 year averages) requires new tools to be developed. Such tools will be essential to

extracting all available information from the WAISCORES inland deep core and the U.S. ITASE traverse cores over the coming years.

## **4. Improving the proxy calibrations**

Our ongoing research into improving the calibration of ice-core-based proxies to climate involves two different applications of artificial neural networks (ANNs), one in progress, one planned. ANNs are a powerful nonlinear tool used in, for example, pattern recognition and time series prediction. Numerous sources exist for further information, such as Gardner and Dorling (1998) and Haykin (1999).

### **4.1 Automatic Weather Station Records**

The ANN-based project currently underway (using variants of the multi-layer feed-forward ANN) is attempting to improve the existing database of automatic weather station (AWS) records in West Antarctica. AWS currently provide the only year-round, continuous direct measurements of weather on the ice sheet. As the spatial coverage of the network has expanded year to year, so has our meteorological database. Unfortunately, many of the records are relatively short (less than 10 years) and/or incomplete (to varying degrees) due to the vagaries of the harsh environment. This reduces the usefulness of these data sets, though much has been learned using the AWS data despite these shortcomings (e.g., Bromwich and Stearns 1993; Holmes et al. 2000; Shuman and Stearns 2001). Climate downscaling results from work in temperate latitudes (e.g., Cavazos 1999; Crane and Hewitson 1998; Hastenrath et al. 1995) suggest it is possible to use GCM-scale meteorological data sets (e.g., ECMWF reanalysis products) with ANNs to both fill gaps in the AWS records and extend them back in time to create a uniform and complete database of West Antarctic surface meteorology (at AWS sites). Such records are highly relevant to the improved interpretation of the expanding library of snow-pit and ice-core data sets.

The focus to date has been on Ferrell AWS (77.91° S, 170.82° E), in part because it has one of the longest available records. We use one year of available AWS observations to train an ANN to predict the AWS near-surface temperature and pressure from nearby ECMWF grid point variables (e.g., 500 mbar geopotential height). This intrayear prediction (of observations in the training year) has been very successful (e.g., RMS errors < 2 mbar for pressure). Inter-year prediction (of observations from years not in the training set) remains a work-in-progress (e.g., RMS errors are 4-5 mbar).



Figure 1 shows a preliminary reconstruction of Ferrell pressure for the ECMWF period (1979-1993). ANN predictions have been merged with AWS observations to produce a 15-year record. Error bars derive from RMS errors from predictions against available observations. Two full years have been added at the beginning and numerous gaps (some quite long) have been filled. Temperature predictions have not been as successful so far, likely due to the greater complexity of controls on this variable (and higher spatial variability).

Three different ANN architectures have produced similar predictive skill suggesting that

Ferrell pressure for the ECMWF period (1979-our approach is valid but our training methodology needs refinement. Many possibilities exist, among them exploring different predictors, adding time lags, and using features extracted from the GCM data as predictors instead of the data itself (e.g., using principal component analysis results). Additionally, improved GCM- and meso-scale models (thanks, in part, to more extensive data on local and regional meteorology), should also provide improved predictors for further ANN-based prediction.

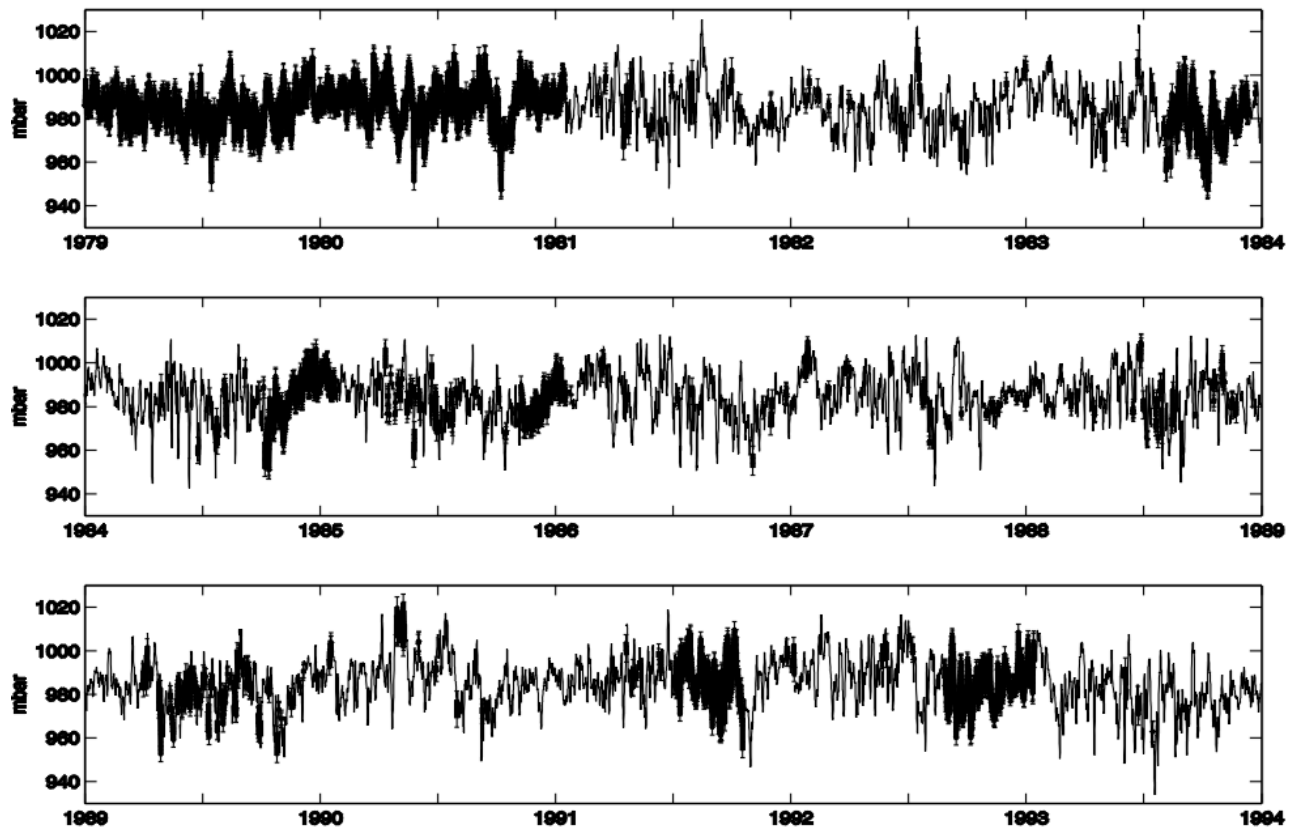


Fig. 1. Preliminary reconstructed surface pressure at Ferrell AWS for 1979-1993 (original observations as thin line, ANN-modeled values as thick lines). The ANN was trained with 1987 data. ECMWF data were used to fill gaps and extend the record back to 1979. Ferrell AWS was installed on the Ross Ice Shelf (77.91 S, 170.82 E) in December, 1980.

#### 4.2 Circulation Feature Extraction

The second ANN-based project, expected to begin soon, will use self-organizing maps (SOMs) (Kohonen 1990; Kohonen 1995) to extract features of the general regional circulation that can be compared to the recent ice core record. SOM analysis has been called a nonlinear analog of

traditional cluster analysis in that the process can identify (physically) related subsets of the data with the advantage of being an unsupervised process requiring no prior specification of categories. (However, this is an imperfect analogy.) Further information on SOMs and their applications in meteorology may be found in Cavazos (2000).

## 5. Summary

Increasing our knowledge of present-day weather and climate in West Antarctica will bring benefits to both the meteorological and the paleoclimate communities. A deepened observational data set will provide more ground truth for proxy calibrations and will help to improve our forecasting models. Better models, in turn, will provide higher confidence data for those times and places where observational data remain unavailable. ANN-based predictions of missing AWS observations will also advance with better model-derived predictors.

There is no doubt that we have learned a great deal from ice-core-based paleoclimate proxies. There is also little doubt that our interpretations would improve with a better understanding of present-day weather and climate in West Antarctica.

## References

- Bergin, M. H., C. I. Davidson, et al., 1995: A Simple Model to Estimate Atmospheric Concentrations Of Aerosol Chemical Species Based On Snow Core Chemistry At Summit, Greenland. *Geophysical Research Letters*, **22**, 3517-3520.
- Bromwich, D. H., 1988: Snowfall in high southern latitudes. *Reviews of Geophysics*, **26**, 149-168.
- Bromwich, D. H. and C. R. Stearns, Eds., 1993: *Antarctic Meteorology and Climatology: Studies Based on Automatic Weather Stations*. Vol. 61. *Antarctic Research Series*, American Geophysical Union, 207 pp.
- Bromwich, D. H. and A. N. Rogers, 2000: The El Niño-Southern Oscillation Modulation of West Antarctic Precipitation. *The West Antarctic Ice Sheet: Behavior and Environment*, R. B. Alley and R. Bindshadler, Eds., AGU.
- Bromwich, D. H., A. N. Rogers, et al., 2000: ECMWF Analyses and Reanalyses Depiction of ENSO Signal in Antarctic Precipitation. *Journal of Climate*, **13**, 1406-1420.
- Carleton, A. M., 2000: ENSO Teleconnections with Antarctica. *Antarctic Weather Forecasting Workshop*, Columbus, OH, Byrd Polar Research Center, The Ohio State University, 79-82.
- Cavazos, T., 1999: Large-scale circulation anomalies conducive to extreme events and simulation of daily rainfall in northeastern Mexico and southeastern Texas. *Journal of Climate*, **12**, 1506-1523.
- , 2000: Using self-organizing maps to investigate extreme climate events: An application to wintertime precipitation in the Balkans. *Journal of Climate*, **13**, 1718-1732.
- Crane, R. G. and B. C. Hewitson, 1998: Doubled CO<sub>2</sub> precipitation changes for the Susquehanna basin: Down-scaling from the GENESIS general circulation model. *International Journal of Climatology*, **18**, 65-76.
- Cullather, R. I., D. H. Bromwich, et al., 1996: Interannual variations in Antarctic precipitation related to El Niño-Southern Oscillation. *Journal of Geophysical Research*, **101**, 19,109-19,118.
- Dibb, J. E. and J. L. Jaffrezo, 1997: Air-Snow Exchange Investigations At Summit, Greenland - an Overview. *Journal of Geophysical Research*, **102**, 26795-26807.
- Duplessy, J. C. and J. Overpeck: The PAGES/CLIVAR Intersection. [Available online from <http://www.ngdc.noaa.gov/paleo/reports/interx/intersect.html>.]
- Gardner, M. W. and S. R. Dorling, 1998: Artificial neural networks (the multilayer perceptron) - A review of applications in the atmospheric sciences. *Atmospheric Environment*, **32**, 2627-2636.
- Genthon, C. and G. Krinner, 1998: Convergence and Disposal of Energy and Moisture on the Antarctic Polar Cap from ECMWF Reanalyses and Forecasts. *Journal of Climate*, **11**, 1703-1716.
- Hastenrath, S., L. Greischar, et al., 1995: Prediction of the Summer Rainfall over South Africa. *Journal of Climate*, **8**, 1511-1518.
- Haykin, S. S., 1999: *Neural networks : a comprehensive foundation*. 2nd ed. Prentice Hall, 842 pp.
- Hogan, A., 1997: A synthesis of warm air advection to the South Polar Plateau. *Journal of Geophysical Research*, **102**, 14,009-14,020.
- Holdsworth, G., K. Higuchi, et al., 1996: Historical Biomass Burning - Late 19th Century Pioneer Agriculture Revolution In Northern Hemisphere Ice Core Data and Its Atmospheric Interpretation. *Journal of Geophysical Research*, **101**, 23317-23334.
- Holmes, R. E., C. R. Stearns, et al., 2000: Utilization of automatic weather station for forecasting high wind speeds at Pegasus Runway, Antarctica. *Weather and Forecasting*, **15**, 137-151.
- Ice Core Working Group, 1998: Ice Core Contributions to Global Change Research: Past Successes and Future Directions.
- King, J. C. and J. Turner, 1997: *Antarctic Meteorology and Climatology*. Cambridge

- Atmospheric and Space Science Series*, Cambridge University, 409 pp.
- Kohonen, T., 1990: The Self Organizing Map. *Proceedings of the IEEE*, **78**, 1464-1480.
- , 1995: *Self-Organizing Maps*. Vol. 30, *Springer Series in Information Sciences*, Springer-Verlag, 362 pp.
- Kreutz, K. J. and P. A. Mayewski, 1998: A basis for reconstructing paleo-atmospheric circulation using West Antarctic glaciochemical records. *Antarctic Science*, in press.
- Kreutz, K. J., P. A. Mayewski, et al., 1997: Bipolar Changes in Atmospheric Circulation During the Little Ice Age. *Science*, **277**, 1294-1296.
- , 1999: Sea-level pressure variability in the Amundsen Sea region recorded in a West Antarctic glaciochemical record. *Journal of Geophysical Research-Atmospheres*, **105**, 4047-4059.
- Legrand, M. and C. Feniet-Saigne, 1991: Methanesulfonic Acid in South Polar Snow Layers: A Record of Strong El Niño? *Geophysical Research Letters*, **18**, 187-190.
- Mayewski, P. A., L. D. Meeker, et al., 1997: Major features and forcing of high-latitude northern hemisphere atmospheric circulation using a 110,000-year-long glaciochemical series. *Journal of Geophysical Research*, **102**, 26345-26366.
- Minikin, A., M. Legrand, et al., 1998: Sulfur-containing species (sulfate and methanesulfonate) in coastal Antarctic aerosol and precipitation. *Journal of Geophysical Research*, **103**, 10,975-10,990.
- O'Brien, S. R., P. A. Mayewski, et al., 1995: Complexity of Holocene climate as reconstructed from a Greenland ice core. *Science*, **270**, 1962-1964.
- Parish, T. R. and D. H. Bromwich, 1997: On the forcing of seasonal changes in surface pressure over Antarctica. *Journal of Geophysical Research*, **102**, 13,785-13,792.
- Peixoto, J. P. and A. H. Oort, 1992: *Physics of Climate*. Am. Inst. of Phys., 520 pp.
- Reusch, D. B., P. A. Mayewski, et al., 1999: Spatial Variability of Climate and Past Atmospheric Circulation Patterns from Central West Antarctic Glaciochemistry. *Journal of Geophysical Research*, **104**, 5985-6001.
- Rogers, A. N., D. H. Bromwich, et al., cited 2000: ENSO variability in West Antarctic precipitation: ECMWF Operational Analyses versus ERA-15. [Available online from <http://www.ecmwf.int/pressroom/conf/abstracts/extended-abstracts/Bromwich2/final.htm>.]
- Schwerdtfeger, W., 1984: *Weather and Climate of the Antarctic*. Elsevier, 261 pp.
- Sherrell, R. M., E. A. Boyle, et al., 2000: Temporal variability of Cd, Pb, and Pb isotope deposition in central Greenland snow. *Geochemistry, Geophysics, Geosystems*, **1**, Paper number 1999GC000007.
- Shuman, C. A. and C. R. Stearns, 2001: Decadal-length composite inland West Antarctic temperature records. *Journal of Climate*, **14**, 1977-1988.
- Slonaker, R. L. and M. L. Van Woert, 1999: Atmospheric moisture transport across the Southern Ocean via satellite observations. *Journal of Geophysical Research*, **104**, 9229-9249.
- Sommer, S., D. Wagenbach, et al., 2000: Glaciochemical study spanning the past 2 kyr on three ice cores from Dronning Maud Land, Antarctica 2. Seasonally resolved chemical records. *Journal of Geophysical Research-Atmospheres*, **105**, 29423-29433.
- Turner, J., D. H. Bromwich, et al., 1999: Antarctic First Regional Observing Study of the Troposphere. *Weather and Forecasting*, **14**, 809-810.
- U.S. ITASE Steering Committee, 1996: Science and implementation plan for US ITASE: 200 years of past Antarctic climate and environmental change. *US ITASE Workshop*, Baltimore, Md., National Science Foundation.
- Wählin, P., 1996: One Year's Continuous Aerosol Sampling at Summit in Central Greenland. *Chemical Exchange Between the Atmosphere and Polar Snow*, E. W. Wolff and R. C. Bales, Eds., Springer-Verlag, 131-143.
- WAIS Committee, 1995: WAIS: The West Antarctic Ice Sheet initiative, WAIS Science and Implementation Plan.

# MM5 WINTERTIME SIMULATIONS OF THE ANTARCTIC BOUNDARY-LAYER WIND FORCING

Thomas R. Parish \*

Department of Atmospheric Science, University of Wyoming, Laramie WY 82071

## 1. Introduction

One remarkable characteristic of the Antarctic surface wind regime is its high directional persistence. Directional constancy, a ratio of the vector wind magnitude over the mean wind speed, is typically 0.9 or greater. This indicates that the winds in the lower atmosphere are essentially unidirectional. The constancy displayed by the surface wind regime is among the highest on earth, rivaling even the trade winds. Unlike the case in the middle latitudes where the wind constancy increases with height and is a maximum in the upper troposphere, winds over the Antarctic continent are typically greatest at the surface and decrease upward. Lettau and Schwerdtfeger (1967) first noted this and referred to the systematic alignment of winds from the upper atmosphere to the surface as a "negative thermal wind" effect. This arises in part due to the presence of radiatively-cooled, negatively-buoyant air lying over sloping terrain, which produces a horizontal temperature gradient and hence a thermal wind. The resulting horizontal pressure gradient force from such a thermal field is responsible for the infamous Antarctic katabatic wind regime. Knowledge of the thermodynamic state of the lower atmosphere is prerequisite to understanding the atmospheric dynamics of the Antarctic surface wind field.

Numerical model simulations of Antarctic surface winds have progressed rapidly in quality during the past decade. Recent results have shown that simulated winds in the lower atmosphere are in good agreement with available observations and generally fit well with the streamlines suggested by Parish and Bromwich (1987). In general, flows at the lowest levels are directed some 20-60° to the left of the fall line, consistent with Coriolis deflection of gravity-driven flows. As noted by Parish and Cassano (2000), however, the fact that there is reasonable agreement between model results and observations is not sufficient to ensure that the

Antarctic atmosphere is being handled in a representative and realistic manner. Parish (2001) has noted that seemingly realistic flow regimes can be generated by a number of different processes since the Antarctic terrain plays such a central role in the shaping of the wind field. In particular, it is difficult to differentiate flows that are katabatic in origin as opposed to those that develop owing to effects of orographic blocking. This can be of significance in a practical sense since secondary fields that are critical to accurate forecasts, such as cloud and precipitation, are highly sensitive to the dynamics of the wind field. Initialization is a critical factor for any modeling system. For Antarctic applications, care must also be taken regarding the low-level wind and temperature fields such that they are formulated in a consistent and physically meaningful process. Failure to do may result in spurious initial accelerations of the low-level wind field that can persist throughout the integration period and contaminate the numerical results.

To infer the importance of the katabatic forcing in producing the Antarctic wind field, a series of numerical simulations have been conducted. The Fifth Generation Penn State/NCAR Mesoscale Model (MM5) Version 3.4 has been used for all model experiments. Details of MM5 can be found in Grell et al. (1994). The forecast period covers the midwinter conditions and consists of daily numerical simulations from 15 June to 15 July 2001. Selection of this time period coincides with the maximum katabatic forcing possible. Simulations were initialized using the 0000 UTC NCEP AVN Global Model grids. Each model run was carried out for a 36-h period. Only the 24- and 36-h times were used in the analyses that follow. The MRF boundary layer (Hong and Pan 1996) and CCM2 radiation (Hack et al. 1993) schemes were used in all simulations. To ensure consistent initial wind and temperature fields, the parameter ISFC in the interpolation subroutine INTERPF was set to 7. This allowed the initial fields of temperature and wind over the sloping Antarctic terrain to be initialized in a manner that is as dynamically consistent as possible.

All simulations to be discussed incorporate a single domain consisting of 127 x 127 grid points

---

\* *Corresponding author address:* Thomas R. Parish, Department of Atmospheric Science, University of Wyoming, Laramie, Wyoming 82071; email: parish@uwyo.edu

with 60-km grid spacing. There are 25 levels in the vertical including seven within the lowest 250-m to resolve details in the low-level flow. For brevity only the 30-day averaged results from the lowest sigma level ( $\sigma = 0.9990$ ), corresponding to a height of approximately 10 m above the continental ice surface, will be discussed.

## 2. Wind Conditions During Winter 2001

Selection of the 60-km grid resolution represents a compromise between large areal coverage and sufficient resolution to depict terrain-induced boundary layer flows. Grid resolution is sufficient to capture the broad scale wind and temperature fields over the continental interior but is unable to resolve fine-scale details of the local terrain such as the complex topography associated with the Transantarctic Mountains. For the simulations conducted, the 24- and 36-h results were averaged for the entire midwinter period 15 June – 15 July 2001. This provides estimates as to the mean thermodynamic and dynamics conditions within the lower atmosphere. Figure 1 illustrates the mean streamlines of the wind at the lowest sigma level. It can be seen that a broad drainage is present off the high plateau of Antarctica extending down to the continental margin. Strong topographic control of the surface wind regime is obvious. Winds over the entire

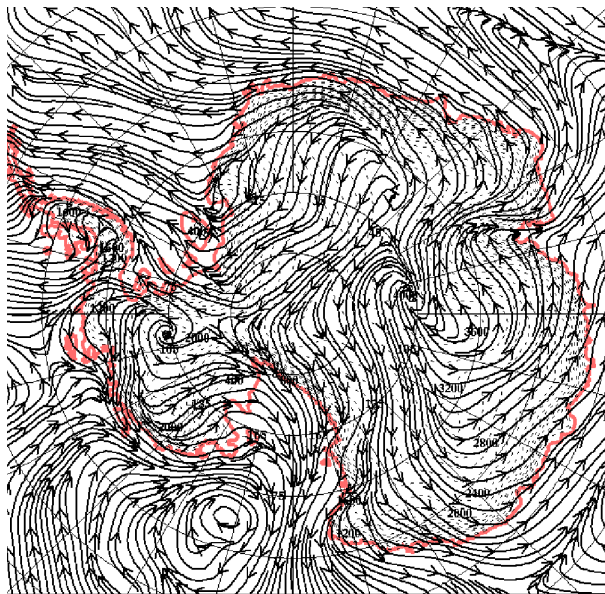


Fig. 1. Mean streamlines at lowest sigma level (10 m agl) from MM5 simulations for midwinter period 15 June – 15 July 2001. Antarctic terrain contour heights (m) represented by dashed lines.

continent are closely aligned with the underlying topography. Circumpolar easterly flow is present to the north of the continent. The wind pattern shown in Fig. 1 is in close agreement with the mean streamlines suggested by Parish and Bromwich (1987). In that simulation, the mean streamlines were representative of katabatic processes. Confluence features of the surface wind similar to Parish and Bromwich (1987) are seen as well in the mean streamlines for the midwinter MM5 simulations.

Mean wind speeds for the midwinter period are also comparable with previous work and available observations. Figure 2 shows the mean wind speeds at the lowest sigma level from the MM5 simulations. In general, the mean midwinter wind speeds are light over the continental interior and increase toward the coast. The strongest wind speeds over the continent are found over the steep coastal terrain where magnitudes of approximately  $15 \text{ m s}^{-1}$  are typical. Some wind speed maxima coincide with the confluence zones seen in the mean streamlines such as Adélie Land, the Siple Coast region of West Antarctica and the Amery Ice Shelf. Both the continental streamline and wind speed patterns are suggestive of a wind regime in which the katabatic component is the dominant forcing mechanism. There exists strong control of the surface wind regime by the underlying terrain. Both patterns of wind speed and wind direction are what would be expected of a purely katabatic wind regime.

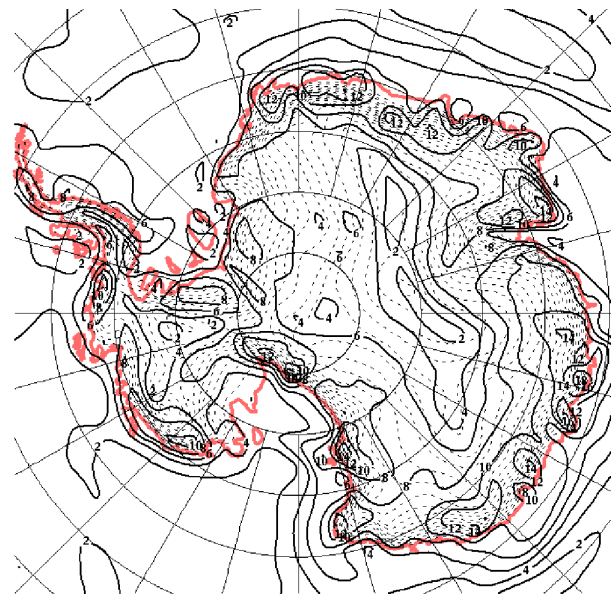


Fig. 2. As in Fig.1, except for mean wind speeds.

To understand the dynamics and thermodynamics of the atmosphere, it is useful to output individual terms within the respective model equations. Parish and Waight (1987) and Cassano (1998) have shown the utility in diagnosing model output when terms in the prognostic equations are known. For the midwinter study, the horizontal pressure gradient force (PGF) from MM5 was output at every sigma level. These values were then averaged over the entire 30-d period to determine the mean PGF at each level for each grid point. Figure 3 illustrates the mean PGF at the lowest sigma level for the midwinter period. Here the vectors are scaled by the Coriolis parameter and thus the magnitudes of the PGF represent geostrophic values. The outstanding feature in Fig. 3 is the direction of the mean PGF over the continent, which is down the direction of the local fall line. The PGF magnitudes are also shaped by the terrain with the largest values over the steepest terrain slopes near the coast. The topographic control of the PGF displayed in Fig. 3 is impressive and is again suggestive of a katabatic-forced wind regime.

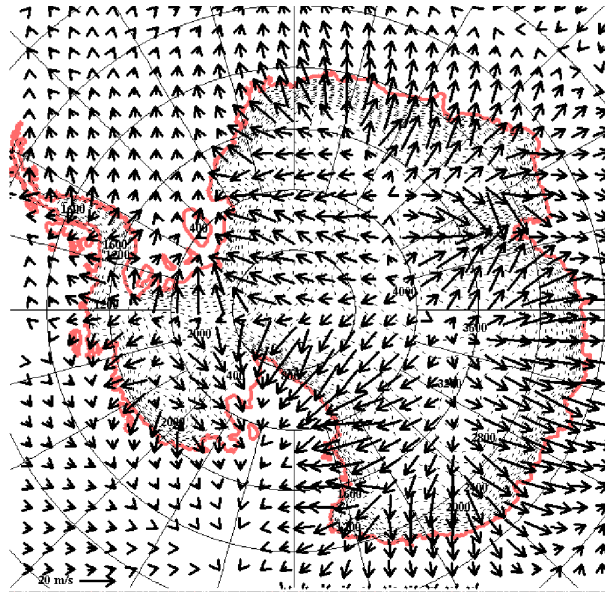


Fig. 3. As in Fig. 1, except for the mean horizontal pressure gradient. Vector magnitude referenced in terms of geostrophic wind speed ( $m s^{-1}$ ).

### 3. Katabatic Forcing of the Midwinter Antarctic Surface Wind Regime

To understand the forcing of the midwinter Antarctic surface winds, the horizontal pressure gradient force must be resolved into components representing katabatic and large-scale ambient processes. The horizontal pressure-gradient,  $F$ , in

the downslope direction can be expressed (Mahrt 1982):

$$F = g \frac{d}{\Theta_o} \sin \alpha - \cos \alpha \frac{g}{\Theta_o} \frac{\partial(\overline{\Theta h})}{\partial s} - \frac{1}{\rho} \frac{\partial p}{\partial s_{amb}} \quad (1)$$

where  $d$  is the potential temperature deficit, the difference in potential temperature at any point in the katabatic layer between the radiatively cooled layer and the ambient atmosphere. The term  $\alpha$  refers to the terrain slope,  $h$  is the height of the diabatically cooled layer,  $\Theta_o$  is a reference potential temperature, and  $s$  refers to a horizontal distance. Other symbols have their usual meteorological meaning. The first term on the right represents the effect of radiatively-cooled air over sloping terrain that is responsible for katabatic winds. It will be referred to as the katabatic component of the PGF. The second term represents the effects of the change in the depth and/or cooling of the katabatic layer in the downslope direction on the acceleration. Ball (1960) notes that this term is generally small for Antarctic winds. The third term represents the component of the PGF in the free atmosphere above the katabatic layer, or also called the ambient PGF.

Cassano (1998) has shown that it is possible to infer each of these terms from numerical model output, and thereby depict the momentum balance of katabatic flows. In this study, a diagnosis of all three terms has been made from the MM5 output fields. The process of determining the katabatic component of the PGF proceeds as follows. A background potential temperature profile at each grid point over the sloping ice terrain is computed by fitting a line to the potential temperatures in a layer between 1000 and 2500 m above the ice surface. This is generally above the katabatic layer and presumably represents the temperature profile in the free atmosphere above the radiatively-cooled layer. The difference between the sigma level potential temperature and the inferred potential temperature in the ambient environment is the potential temperature deficit.

Calculation of the potential temperature deficit for the midwinter conditions from the MM5 simulations was made for each 24- and 36-h time period. These fields were then averaged for the entire 30-d period to arrive at estimates of the mean potential temperature deficit over the continent. Figure 4 illustrates the mean potential temperature deficit at the lowest sigma level for the midwinter period. The largest deficits are found

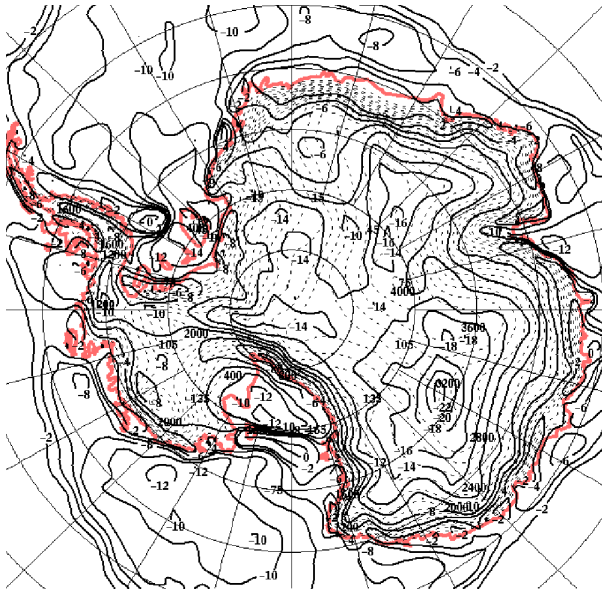


Fig. 4. As in Fig. 1, except for the mean potential temperature deficit (K).

over the high interior of the continent and decrease toward the coast. The greatest deficits are in excess of 20K over the Dome C region. Deficits over the interior generally are in excess of 15K, decreasing to less than 5K right over the steep coastal ice slopes. The pattern of the potential temperature deficits roughly matches that of inversion strength (Schwerdtfeger 1984).

Calculation of the mean midwinter katabatic component of the PGF follows directly from Eq. (1) after the potential temperature deficit field has been calculated. Terrain slopes are computed using the same finite difference form as other variables on cross points (Grell et al. 1994). The resulting vector field of the katabatic component of the PGF is shown in Fig. 5. As in Fig. 3, the vectors are scaled by the Coriolis force and represent geostrophic wind magnitudes. Similar to the PGF in Fig. 3, the vectors are directed down the fall line with the largest magnitudes over the steep coastal margin. It is obvious from Fig. 5 that the katabatic component can only explain a fraction of the total PGF in Fig. 3. Experiments have been conducted to examine the sensitivity of the potential temperature deficit calculations to the choice of parameters for layer thickness and height of the ambient atmosphere. It is clear that the vectors of the katabatic component of the PGF in Fig. 4 are representative. This suggests that the Antarctic topography effectively controls the surface wind field through processes other than simply katabatic forcing.

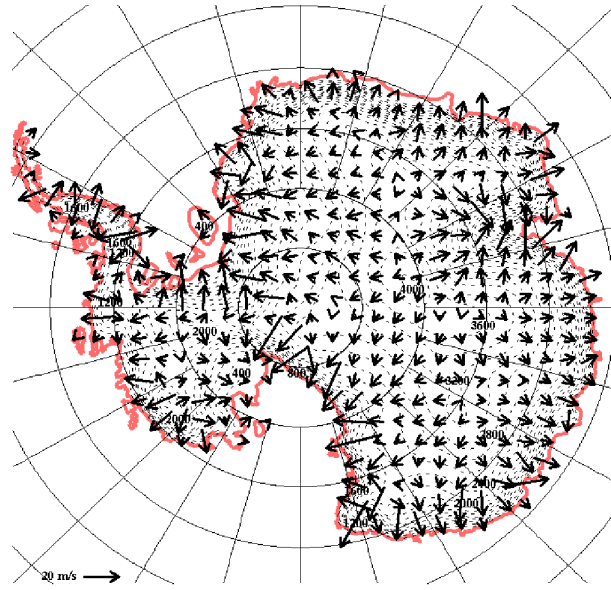


Fig. 5. As in Fig. 1, except for the component of the mean horizontal pressure gradient due to katabatic processes. Vector magnitude referenced in terms of geostrophic wind speed ( $m s^{-1}$ ).

The vector difference between the total PGF and the katabatic component of the PGF should provide an estimate as to the ambient forcing in the lower atmosphere. Fig. 6 illustrates the difference field. It can be seen that the ambient PGF is considerably larger than the inferred katabatic PGF for nearly all grid points. In addition, the mean ambient midwinter PGF retains a close association with the underlying ice terrain. Again, the PGF vectors are directed downslope and the largest magnitudes are found over the steep coastal slopes. This suggests that, regardless of the katabatic forcing, the Antarctic orography forces an adjustment in the horizontal pressure gradient force such that the net forcing mirrors the topographic slopes. Parish and Cassano (2001) and Parish (2001) have noted that such an adjustment is consistent with barrier winds, which take place as stable air is forced against a topographic ridge.

#### 4. Summary

The directional constancy of the Antarctic wind field is the result of the dominant influence of the underlying terrain. A series of daily 36-h numerical simulations using MM5 were conducted over the period 15 June to 15 July. Model results were then averaged to arrive at estimates of midwinter conditions over Antarctica.

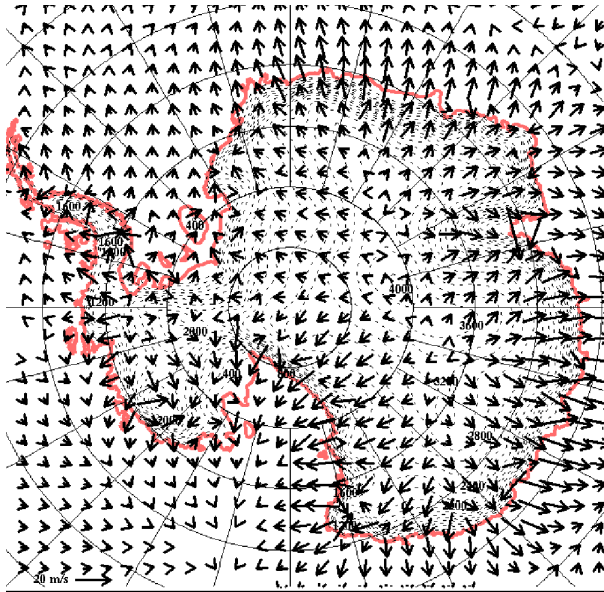


Fig. 6. As in Fig. 1, except for the component of the mean horizontal pressure gradient above the katabatic layer. Vector magnitude referenced in terms of geostrophic wind speed ( $m s^{-1}$ ).

Time-averaged winter winds near the surface are directed along favored topographic pathways similar to what would be expected from katabatic forcing. The mean PGF from MM5 is directed downslope with the largest forcing above the coastal ice slopes. Analyses show, however, that the component of the PGF due to katabatic processes is but a fraction of the total PGF. The mean ambient PGF also reflects strongly the influence of the underlying continental ice terrain. Antarctic orography is responsible for an adjustment of the large-scale pressure field such that the gradients reflect the fall line of the ice slopes to produce a PGF indistinguishable from that forced by katabatic processes. This suggests that even the midwinter wind field is not necessarily dominated by katabatic episodes but rather reflects the adjustment of the ambient pressure field with the Antarctic terrain. This presents a paradigm shift regarding the role of katabatic processes in shaping the surface wind field.

From a practical standpoint, the strong control of the topography on the surface wind field has implications regarding model initialization. Clearly, the initial fields must reflect the underlying model terrain. The PGF at the start of the model integration must reflect dynamics consistent with the terrain-induced forcing such as seen in Fig. 3. The thermodynamic fields must yield a representative field of potential temperature

deficits appropriate for the synoptic situation. Otherwise, anomalous accelerations in the low-level wind field will result.

There are also implications regarding validation of model results based on actual station data. Comparison should take into account differences in the model terrain height, slope and direction. Owing to finite grid representation, significant differences arise between observed terrain heights and slopes and those represented in numerical models. This is, unfortunately, most serious over the steep coastal slopes where the observational database for Antarctica is the most complete. It is inappropriate to compare observations to model results where grid resolution is insufficient to depict actual forcing. Likewise, incorporation of Antarctic data into numerical models must also recognize the need for compatibility between the actual station height and terrain slope with that represented in the model.

## References

- Ball, F. K., 1956: The theory of strong katabatic winds. *Aust. J. Phys.*, **9**, 373-386.
- Cassano, J. J., 1998: The impact of numerical model configuration on simulated Antarctic katabatic winds. Ph.D. Thesis, University of Wyoming, 216 pp.
- Grell, G. A., J. Dudia, and D. R. Stauffer, 1994: A description of the fifth-generation Penn State/NCAR Mesoscale Model (MM5). NCAR Tech. Note NCAR/TN-382+STR, 108 pp.
- Hack, J. J., B. A. Boville, B. P. Briegleb, J. T. Kiehl, P. J. Rasch, and D. L. Williamson, 1993: Description of the NCAR Community Climate Model (CCM2). NCAR Tech. Note NCAR/TN-382+STR, 108 pp.
- Hong, S.-Y., and H.-L. Pan, 1996: Nonlocal boundary layer vertical diffusion in a medium range forecast model. *Mon. Wea. Rev.*, **124**, 2322-2339.
- Lettau, H. H., and W. Schwerdtfeger, 1967: Dynamics of the surface-wind regime over the interior of Antarctica. *Antarct. J. U.S.*, **2**(5), 155-158.
- Mahrt, L., 1982: Momentum balance of gravity flows. *J. Atmos. Sci.*, **39**, 2701-2711.
- Parish, T. R., 2001: Topographic forcing of the Antarctic wind field. Preprints Sixth Conference of Polar Meteorology and Oceanography, San Diego, 355-358.
- Parish, T. R., and D. H. Bromwich, 1987: The surface windfield over the Antarctic ice sheets. *Nature*, **328**, 51-54.



- Parish, T. R., and J. J. Cassano, 2001: Forcing of the wintertime Antarctic boundary layer winds from the NCEP/NCAR Global Reanalysis. *J. Applied Meteor.*, **40**, 810-821.
- Parish, T. R., and K. T. Waight, 1987: The forcing of Antarctic katabatic winds. *Mon. Wea. Rev.*, **115**, 2214-2226.
- Schwerdtfeger, W., 1984: *Weather and Climate of the Antarctic*. Elsevier, 261 pp.

# Satellite Remote Sensing of Antarctic Cloud Properties

Dan Lubin and Joannes Berque

Scripps Institution of Oceanography, University of California, San Diego  
La Jolla, California, 92093

## 1. Introduction

Multispectral satellite imagery from the Advanced Very High Resolution Radiometer (AVHRR) can be used to estimate the ice water path and effective particle radius of clouds over Antarctica. With validation from surface observations from a field program, satellite retrieval techniques can extrapolate field observations to larger geographic areas and longer time scales. With support from the National Science Foundation, satellite tracking antennas have been maintained at McMurdo and Palmer Stations in Antarctica since 1988 and 1990, respectively. The data from this satellite tracking effort have been archived at the Scripps Institution of Oceanography's Arctic and Antarctic Research Center (AARC) and at the University of Wisconsin's Antarctic Meteorological Research Center (AMRC). A large database therefore exists for using satellite data to study seasonal and interannual variability in cloud properties as they relate to atmospheric dynamics and thermodynamics.

## 2. Retrieval Algorithms

We developed and tested our retrieval algorithms using NOAA-12 AVHRR data from 1992. During 1992, ground-based Fourier Transform Infrared (FTIR) retrievals of cloud optical properties over the South Pole were available for intercomparison (Mahesh et al., 2001). To retrieve cloud optical properties over the Antarctic Plateau, we use AVHRR-measured radiances in the infrared channels 3, 4, and 5 (3.7, 11, and 12  $\mu\text{m}$  center wavelengths, respectively). With these three radiances, we can estimate the effective cloud temperature, ice water path, and effective particle radius using a discrete ordinates radiative transfer model (Stamnes et al., 1988). The radiative transfer model is set up with a vertically inhomogeneous atmosphere coupled to a model snowpack. The snowpack is modeled as an optically thick scattering and absorbing layer, with radiative parameters (single scattering albedo, volume extinction, asymmetry factor) estimated using Mie theory (Wiscombe, 1980).

The radiative parameters are calculated for the snow grains using equivalent spheres (Grenfell and Warren, 1999). It is necessary to include a rigorous model for the snowpack to simulate the surface albedo at 3.7  $\mu\text{m}$ , which is small (of order 3 - 5%) but non-negligible. Over clear-sky scenarios, the coupled snow-atmosphere radiative transfer model is used to estimate an effective snow grain size. For most of the clear-sky AVHRR images covering the South Pole during 1992, the satellite-measured radiances are consistent with snow grain sizes larger than 75  $\mu\text{m}$ . We can therefore specify the snow grain size with confidence, as a lower boundary condition, when applying the radiative transfer model to cloudy conditions.

To estimate cloud optical properties, a Henyey-Greenstein phase function is used, and the cloud layer's radiative parameters are calculated for ice crystal size distributions using Mie theory and equivalent spheres (Grenfell and Warren, 1999). Of the cloudy sky AVHRR images available during 1992, seven were contemporaneous with the FTIR measurements of Mahesh et al. (2001). The satellite-based and ground-based retrievals are consistent with each other. From the satellite-based retrievals, the effective particle radius for these seven test cases ranged from 7.8 - 27.3  $\mu\text{m}$ . The ice water path ranged from 2.1 - 8.4  $\text{g m}^{-1}$ . We therefore see that over the Antarctic Plateau, satellite-measured radiances are consistent with optically thin clouds with relatively small effective particle size. Recent field observations (Professor Von Walden, University of Idaho, personal communication) indicate that some clouds over the South Pole may contain liquid rather than ice water. If we estimate the cloud optical properties using Mie theory for liquid water droplets, the retrieved effective radius increases by approximately ten  $\mu\text{m}$ . This is related to the difference in refractive index between liquid water and ice. Research is underway to determine if cloud phase discrimination is possible in Antarctic AVHRR data, as it appears to be for Arctic AVHRR data (Key and Intrieri, 2000).

### 3. Applications

This retrieval method is limited to the sunlit part of the year, because the solar backscattered radiance at 3.7  $\mu\text{m}$  is required. However, this is the time of most interest for weather forecasting at McMurdo Station. By analyzing several years of AVHRR data, in conjunction with meteorological data (automatic weather station or reanalyses), we should gain insight into the processes that govern the formation and persistence of cloud cover over the Antarctic continent, the Ross Ice Shelf, and the Ross Sea. This retrieval algorithm can be readily adapted to Moderate Imaging Spectroradiometer (MODIS) data, as well as AVHRR data.

### References

- Grenfell, T. C., and S. G. Warren, 1999: Representation of a nonspherical ice particle by a collection of independent spheres for scattering and absorption of radiation, *J. Geophys. Res.*, **104**, 31,697-31,709.
- Key, J., and J. Intrieri, 2000: Cloud particle phase determination with the AVHRR, *J. Appl. Meteorol.*, **39**, 1797-1805.
- Mahesh, A., V. P. Walden, and S. G. Warren, 2001: Ground-based infrared remote sensing of cloud properties over the Antarctic Plateau, part II: cloud optical depths and particle sizes, *J. Appl. Meteorol.*, **40**, 1279-1294.
- Stamnes, K., S.-C. Tsay, W. Wiscombe, and K. Jayaweera, 1988: Numerically stable algorithm for discrete-ordinate-method radiative transfer in multiple scattering and emitting layered media, *Appl. Opt.*, **27**, 2502-2508.
- Wiscombe, W., 1980: Improved Mie scattering algorithms, *Appl. Opt.*, **19**, 1505-1509.

# THE ANTARCTIC MESOSCALE PREDICTION SYSTEM (AMPS): POTENTIAL APPLICATIONS FOR RIME

Ying-Hwa Kuo, Jordan Powers, and James F. Bresch  
National Center for Atmospheric Research  
Boulder, Colorado

David H. Bromwich  
Byrd Polar Research Center, The Ohio State University  
Columbus, Ohio

John J. Cassano  
CIRES, University of Colorado  
Boulder, Colorado

## 1. Introduction

In October 2000, the National Center for Atmospheric Research (NCAR) and the Byrd Polar Research Center at the Ohio State University jointly developed an Antarctic Mesoscale Prediction System (AMPS). Since then, AMPS has been providing twice-daily numerical guidance for both the Antarctic and the McMurdo Station area. The forecast products are posted on the internet (<http://www.mmm.ucar.edu/rt/mm5/amps/>) and are being used by field forecasters, research planners, and polar meteorologists at McMurdo and elsewhere. AMPS was developed in response to the recognized needs for improved forecast guidance from high-resolution mesoscale numerical weather prediction models (Bromwich and Cassano 2000) over the Antarctic. The goals of AMPS are:

- To provide real-time mesoscale and synoptic forecast products for Antarctica, tailored to the needs of field forecasters at McMurdo Station;
- To improve and incorporate physical parameterizations suitable for high latitudes;
- To improve the science of mesoscale numerical weather prediction over the Antarctic through a close collaboration between forecasters, numerical modelers, and polar research scientists.

The project has completed its first field season, and the system has been used effectively by the forecasting contingent in McMurdo (see the presentation by Cayette et al. from this workshop). In addition, the AMPS system has been used to support the rescue of Dr. Shemenski from South Pole in April 2001 and the GLOBEC field experiment.

In this paper, we will describe the AMPS system, and suggest ways that AMPS can be used to support the Ross Island Meteorological Experiment (RIME).

## 2. A Description of AMPS

The forecasting component of AMPS is a modified version of the Fifth Generation Pennsylvania State University /NCAR Mesoscale Model – MM5 (Grell et al. 1995). The MM5 is configured with three domains with horizontal grid sizes of 90-km, 30-km, and 10-km (Figs. 1 and 2). The 90-km grid includes New Zealand, as Christchurch is the origin of flights to McMurdo. The 30-km grid covers the entire Antarctic continent. This provides mesoscale prediction over the entire continent at a resolution higher than available from other operational models. The 10-km grid is centered over the McMurdo Station area, with an objective to resolve local topographic features and provide improved mesoscale prediction that is important for aviation forecasting. The three model domains are integrated forward using the two-way interactive grid-nesting approach. Each domain has 29 levels in the vertical.

The initial condition for AMPS is based on the National Centers for Environmental Prediction (NCEP) Aviation global analysis (AVN), which is subsequently enhanced through objective analysis

---

Corresponding author address: Ying-Hwa Kuo,  
MMM Division, NCAR, P.O. Box 3000,  
Boulder, CO 80207.  
Email: kuo@ucar.edu

of available observations. The observed data in the Antarctic region include reports from manned surface stations, surface automatic weather stations (AWSs), and upper-air stations over the continent; some satellite-derived wind measurements are also available. Both the 90-km and 30-km grids are initialized at 0000 and 1200 UTC, and are integrated for 48 hours. The 10-km mesh is activated 6 h into the forecast of the 30-km grid (interpolated from the 30-km grid), and is then integrated forward for 24 h. The lateral boundary condition for AMPS is obtained from the AVN global forecasts.

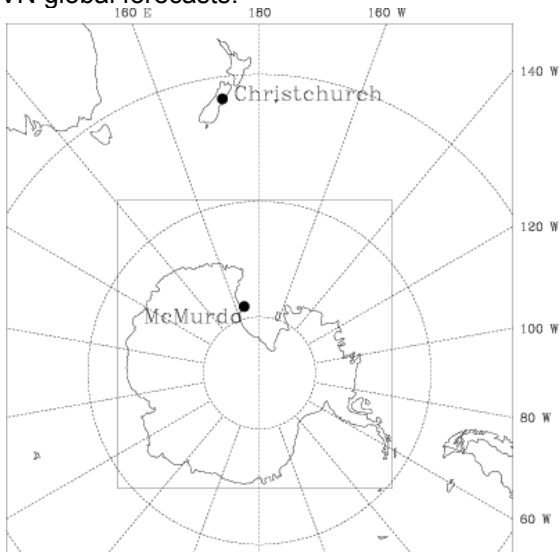


Fig. 1. The 90-km and 30-km AMPS domains. Inner box shows the domain of the 30-km grid. The loci of Christchurch, New Zealand and McMurdo stations are marked on the figure.

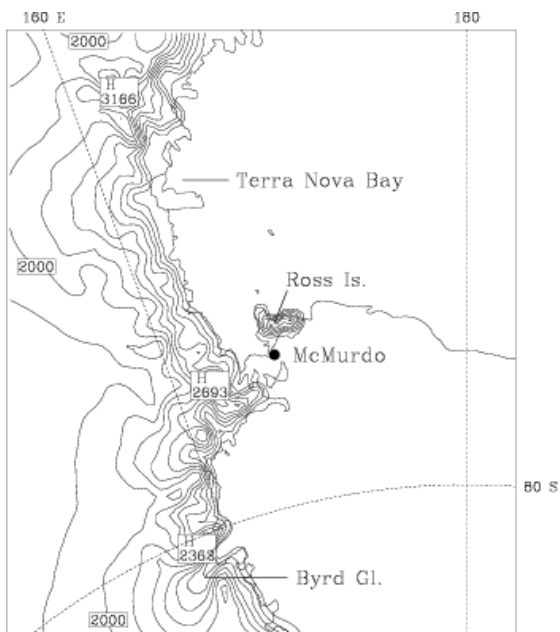


Fig. 2. The 10-km AMPS domain.

Over the past five years, the Ohio State University (OSU) has adapted and tested several physical parameterization schemes suitable for applications over high latitudes. They have incorporated these physical parameterizations into a version of MM5, which is called the Polar MM5. Through collaboration between NCAR and OSU, we have incorporated these physics improvement into the AMPS forecast component (which is based on MM5 Version 3.4). First, to avoid the over prediction of cold clouds (see, e.g., Hines et al. 1997), the Fletcher ice nuclei concentration curve has been replaced with that of Cooper (1986). Second, the thermal properties of the permanent ice and snow types have been adjusted to better reflect the observed values. Third, the most suitable planetary boundary layer (PBL) scheme determined for use in the persistent stable boundary layer over the Antarctic ice sheet, the ETA model PBL scheme (see Bromwich et al. 2001a) is employed in AMPS. Fourth, the NCAR Community Climate Model Version 2 (CCM2) radiation scheme is modified to include the radiative properties of clouds as determined from the microphysical species. Other scheme tunings have also been implemented.

### 3. Potential Applications for RIME

An important goal of RIME is to improve weather forecasting support for U.S. operations at Ross Island. It is obvious that AMPS can potentially serve as a “test-bed” for process-oriented research as well as mesoscale modeling research for RIME. Moreover, AMPS can be enhanced to provide forecasting support for the field operation of the RIME. As such, we propose the following AMPS research be carried out in support of RIME:

#### a. Detailed verification of AMPS forecasts

We need to perform a careful verification of AMPS on both the synoptic scale and mesoscale on a routine basis. This would allow us to identify systematic model biases and deficiencies. Results from such verification studies would provide direction for future model development, as well as guidance on the type of process-oriented research that needs to be carried out in RIME.

#### b. Development of an operational regional data assimilation and analysis system

Bromwich et al. (2001b) examined the performance of AMPS for an event of mesoscale cyclogenesis in the western Ross Sea during 13-

17 January 2001. They found that the performance of AMPS strongly depends on the quality of the NCEP AVN global analysis which is used in the AMPS model initialization. It would be desirable to develop a regional data assimilation system using the variational approach (i.e., 3DVAR) that can effectively incorporate all available surface (i.e., AWS), upper-air observations, and satellite-derived measurements and products (i.e., GPS radio occultation soundings). The operation of such a regional data assimilation system would greatly improve the performance of AMPS.

#### **c. Potential enhancement of AMPS**

The execution of RIME will undoubtedly require additional forecasting support on top of routine operational forecasting at the McMurdo Station. For example, guidance needs to be provided on: (a) what meteorological systems to be studied; (b) when and where to take special measurements; and (c) the operations of research aircraft (if one is involved). This will require accurate forecasting at high resolution in time and space. Depending on the availability of computing resources, several potential enhancements can be implemented for AMPS in support of the field operation of RIME. This includes: (1) extending the forecast duration of the forecast from 48 hours to 72 hours for the 90-km/30-km grids, and from 24 hours to 36 hours for the 10-km grid; (2) expanding the 10-km domain to fully cover the experimental domain of RIME; and (3) adding a 3.3-km mesh within the 10-km mesh to provide enhanced prediction of small scale circulation systems.

#### **d. Interactive display system**

A suite of pre-determined AMPS forecast products are currently available on the web. While this is very useful for routine operational forecasting at McMurdo, this may not be sufficient for RIME. For field operation, it would be desirable to examine the structure of a forecasted weather system of interest, and to evaluate different measurement strategies (e.g., planning for the flight route for an instrumented research aircraft). The field operation planning of RIME would greatly benefit from an interactive graphic display system that make use of the full model grid fields (both in time and space) and can display the user requested plots on the fly. Such a system has been found to be highly valuable for mesoscale field experiments in the past.

## **References**

- Bromwich, D. H., and J. J. Cassano, 2001: Meeting Summary: Antarctic Weather Forecasting Workshop. *Bull. Amer. Meteor. Soc.*, **82**, 1409-1413.
- Bromwich, D.H., J.J. Cassano, T. Klein, G. Heinemann, K.M. Hines, and K. Steffen, 2001a: Mesoscale modeling of katabatic winds over Greenland. Part I: Verification of the polar MM5 and comparison with NORLAM. *Mon. Wea. Rev.*, in press.
- Bromwich, D. H., A.J. Monaghan, J.G. Powers, J.J. Cassano, H.-L. Wei, Y.-H. Kuo, and A. Pellegrini, 2001b: Antarctic mesoscale prediction system (AMPS): A case study from the 2000/2001 field season. *Mon. Wea. Rev.*, conditionally accepted.
- Cooper, W.A., 1986: Ice initiation in natural clouds. *AMS Meteor. Monograph*, **21**, [R.G. Braham, Jr., Ed.], Amer. Meteor. Soc., Boston, 29-32.
- Grell, G.A., J. Dudhia, and D.R. Stauffer, 1995: A Description of the Fifth-Generation Penn State/NCAR Mesoscale Model (MM5), NCAR Tech. Note TN-398+STR, 122 pp. [Available from UCAR Communications, P.O. Box 3000, Boulder, CO 80307.]
- Hines, K.M., D.H. Bromwich, and Z. Liu, 1997: Combined global climate model and mesoscale model simulations of the Antarctic climate. *J. Geophys. Res.*, **102**, 13747-13760.

# RIME: IMPROVING MULTISCALE FORECASTING OF ANTARCTIC METEOROLOGY

David P. Bacon\*, Thomas R. Parish<sup>1</sup>, Kenneth T. Waight III<sup>2</sup>  
Center for Atmospheric Physics, Science Applications International Corporation,  
McLean, VA

<sup>1</sup> Dept. of Atmospheric Science, University of Wyoming, Laramie, WY

<sup>2</sup> Mesoscale and Environmental Simulations and Operations, Inc., Raleigh, NC

## 1. Introduction

Weather forecasting in and around Antarctica is notoriously difficult. This arises in part because of the failure of current models to include the important orographic and coastal features of the continent and problems with basic surface and boundary layer physics and cloud processes. The uncertainty in model forecasts presents logistical problems for the United States Antarctic Program (USAP), including cancelled and aborted flight operations. It has also contributed to an increased risk for USAP personnel both in deployment phase and in the ability to mount rapid recovery operations in an emergency.

The Ross Island Meteorology Experiment is proposed to improve our basic understanding of the meteorology of the Ross Sea region. The Ross Sea area is considered to be a representative region for studies of physical processes and of moisture, momentum, and energy fluxes, hence the knowledge gained on RIME will improve our modeling for the entire continent of Antarctica.

A model is the instantiation of our understanding of the physical processes of the system the model purports to represent. To the extent that a model agrees with observations, it represents a confirmation of the physical understanding and the techniques used to simulate the physical processes encapsulated in the model. To the extent that a model disagrees with observations, it represents evidence that either the physical understanding is lacking or the techniques used to simulate the physical processes are inappropriate or both. In the case of Antarctica, it is easy to document that the techniques used to date are not sufficient to the task; it is also quite evident that our physical understanding is incomplete.

The weather of Antarctica is dominated by

three processes: (1) the polar high and the baroclinic waves that circumnavigate the continent leading to incursions into the continental landmass; (2) terrain forcing as the synoptic circulation interacts with the steep terrain and coastal and ice boundaries; and (3) katabatic processes that arise from strong radiative cooling of the surface and the downslope acceleration of the flow. These processes then couple with the moisture and surface features leading to rapid degradation in ceiling and visibility and high wind situations that preclude air operations. This has a severe impact on the science mission of the USAP due to the cancellation of flight operations, or worse the aborting of an operation in process.

Weather forecasting, however, involves a system of systems, each of which must be considered in order to improve forecast skill. The system of systems includes: (1) data acquisition; (2) data ingest, quality control, and assimilation; (3) physical modeling; (4) visualization; and (5) results dissemination. Only via a balanced approach will it be possible to improve forecasting for operations in Antarctica.

Several groups are proposing new observation systems (ATOVS, COSMIC) that will add much needed data to the system, but this new data must be ingested, quality controlled, and assimilated into the forecasting systems. RIME has the potential not only to add to our understanding of the basic physical processes but to also provide ground truth to verify some of the remotely sensed data that is soon to be collected.

Finally, RIME could serve as a testbed for testing new operational forecasting concepts. This could include a distributed modeling concept in which local computing resources are used to provide operational numerical weather prediction and / or high bandwidth communications channels could be used to provide a reach-back capability to enable remote resources to provide support.

This paper discusses the physical modeling aspects of RIME (surface properties, air-surface fluxes, multiscale dynamics, thermodynamics, and microphysics), on the required datasets for model

---

\*Corresponding author address: David P. Bacon, Center for Atmospheric Physics, Science Applications International Corporation, 1710 SAIC Dr., McLean, VA 22102; e-mail: david.p.bacon@saic.com

development and evaluation, and on the potential operational concepts that could be explored during the course of the experiment.

## **2. Antarctic Meteorology**

Circulations such as baroclinic waves and gravity waves can lead to flow instabilities (e.g. Kelvin-Helmholtz instabilities) due to the associated wind shear. These instabilities occur over scales of tens to tens of thousands of meters increasing the turbulence intensity levels leading to increased gusts that are important for air operations. Furthermore, wind shear and/or buoyancy play an important role in generation of atmospheric boundary layer turbulence. At night, the formation of a nocturnal surface inversion due to longwave radiation cooling decouples the nocturnal boundary layer from the remainder of the well-mixed daytime planetary boundary layer. The resulting changes in the wind direction and speed may result in moisture at different levels being advected at different speeds (speed shear) or directions (directional shear). In the morning, the unstable daytime boundary layer begins to grow, the shear-distorted moisture mixes vertically potentially leading to ceiling and/or visibility problems.

Perhaps one of the most important mesoscale circulations generated from the interaction of the Antarctic surface with the atmosphere is the terrain forced (Schwerdtfeger, 1975) and katabatic (Parish, 1981) winds. Due to the diurnal heating and cooling of mountain slopes, thermal circulations often develop along these slopes. During the day, solar radiation warms the mountain slopes or valley walls, which in turn warm the air in contact with them. Due to convective mixing, air gets heated up to several hundred meters above the sloping surface. This heated air, being less dense than the air at the same elevation above valley floor, rises as an upslope wind. During the night, mountain slopes cool more quickly by outgoing radiation than the valley floor. The air in contact with the slopes and up to a depth of several tens of meters cools through conduction and turbulent mixing. This cooler dense air flows down the slope. These winds are sensitive to the local and regional topographic slope and diurnally varying temperature. They are observed in many mountainous regions of the world, particularly in Alaska, Greenland, Antarctica, Alps, Himalayas, and Rockies. Wind speeds of more than 90 m/s in Antarctica and 50 m/s in the mountain regions of Europe have been observed in some of these flows.

Intrinsic in the formation of katabatic flow is the exchange of heat and moisture between the surface and the lower layers of the atmosphere. This exchange is governed by the surface properties, which for the Antarctic involves a dynamic snow/ice condition. Fresh fallen snow has a low density, high ventilation factor, significant forward scattering component and hence different albedo and heat transfer coefficients than snow that has been compressed and glazed or completely melted to form an ice sheet. Blue ice has entirely different properties. Atmospheric radiation transport is an important factor in the melting of the snow surface and hence in the aging of the snow. Once the energy and moisture is in the lowest layer of the atmosphere, the boundary layer circulations and microphysics become important processes in determining the vertical energy and moisture distribution. A better understanding of the energy and moisture exchange will lead to better simulation of the katabatic circulation and also to the low level moisture which is important for visibility and ceiling prediction. Another factor important for visibility is blowing snow.

The discussion above shows how the atmospheric energy is distributed over a variety of flow modes, including thermally and internally generated global and local circulations and their eddies in an inherently multi-scale environment. The weather in Antarctica is significantly affected by this wide range of flow scales through variations in the mean transport wind, differential advection of moisture due to vertical and horizontal wind shear, and vertical mixing. When these complex flow modes and winds associated with them are generated, they can lead to ceiling and/or visibility restrictions on air operations. Therefore, these space-time flow scales and their interaction with each other and the moisture should be represented accurately in any study of Antarctic weather.

## **3. Numerical Weather Prediction for Antarctica**

The earliest numerical simulations of Antarctic meteorology were conducted at the University of Wyoming (Parish, 1981) and research has since been conducted into terrain forcing (Parish, 1983) and katabatic winds (Waight, 1987; Gallée and Schayes, 1992). While these simulations were informative, the ability to forecast using these techniques was limited due to the resolution of the models. To study these processes numerically, it is essential that five conditions be met: (1) horizontal resolution sufficient to resolve the



important variations in surface properties including elevation, land/water fraction, ice/snow coverage, and albedo; (2) vertical resolution sufficient to resolve the near surface stability and moisture profiles; (3) surface properties at a resolution sufficient to drive the relevant physics; (4) a physical formulation that is consistent and contains all of the relevant physics; and (5) a numerical method that is appropriate for the solution of the equation set that encapsulates the physical formulation. The current state-of-the-art does not satisfy any of these criteria.

To demonstrate the resolution requirement for Antarctica visually, it is only necessary to consider the topography of the continent. Figure 1 shows the recent RADARSAT data obtained by the Canadian Space Agency and analyzed by The Ohio State University (Liu *et al.*, 1999). Clearly visible are the steep elevation changes along much of the coastline as well as the long gradual sloping regions from the continental plateau towards the coastal regions. This terrain data, especially the local variation in slope, is critical to accurate forecasting of the weather.

Most weather forecasting systems put the bulk of their resources in the middle troposphere. This is a natural result of the fact that the mid-latitude weather is most variable in terms of the precipitation, of which the governing cloud microphysical processes typically occur in the middle troposphere. In Antarctica (and in the Arctic), the lack of a liquid phase means that most of the important microphysical processes occur in the planetary boundary layer (PBL). This is the reason for the statement above that vertical resolution is required, and also the explanation for why most operational forecast systems are not designed for this problem.

The surface of Antarctica is not homogeneous; the physical properties of snow and ice of various ages are different in ways important to understanding the surface heating and the flux of moisture, momentum, and heat to the atmosphere. This is one of the fundamental areas of RIME – measuring these critical fluxes and documenting the variability.

The measurements conducted by RIME may represent the best hope for completing a physical understanding of the processes that drive Antarctic meteorology and hence allowing us to create an accurate model for simulation and forecasting of the atmospheric environment of the region. Because of the wide range of scales of motion, it is important that simulations and forecasts at many scales be performed. Flow simulations ranging from local katabatic wind

systems to large scale cyclones should be studied. This will help explore the interaction of baroclinic systems with the topography of Antarctica and the resulting terrain forced circulation. It will also examine the development of katabatic flow in the near-coastal regions.

#### 4. OMEGA

A number of numerical weather prediction models have potential application to Antarctic forecasting and should be considered as part of the modeling component of RIME. COAMPS, ETA, and MM5 are all used operationally and could be extended to this region. MM5 has already been extended with the development of the Polar MM5 version (Cassano *et al.*, 2001). COAMPS, ETA, and MM5, however, all use a conventional nested grid methodology with essentially the same equation set and hence proof of concept with one of the models is a strong indication that similar modifications to the others will yield similar improvement in skill.

Over the past eight years, the Center for Atmospheric Physics (CAP) of SAIC has developed the Operational Multiscale Environment model with Grid Adaptivity (OMEGA), a high resolution, high fidelity, operational weather forecasting system (Bacon *et al.*, 2000). OMEGA, a non-hydrostatic multiscale forecast system developed originally for atmospheric dispersion issues, has been used to forecast extreme or severe meteorological events from global scale to local scale as well as point and large area dispersion phenomena.

While the bulk of the applications of OMEGA to date have been at the mesoscale and below, its

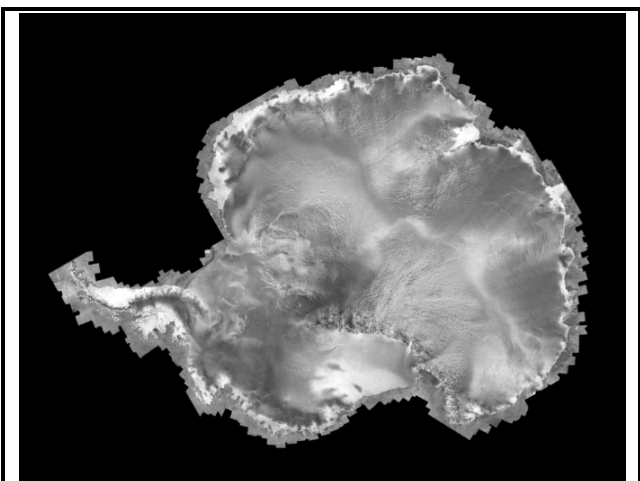


Fig. 1. Digital elevation model of Antarctic obtained from RADARSAT data. (RADARSAT image provided by Dr. Ken Jezek of The Ohio State University.)

unstructured grid provides a powerful advantage in problems that involve a spectrum of scales from global to local. (Figure 2 shows a global OMEGA grid that was constructed to test the concept of multiscale forecasting for Washington, DC.) This is important for Antarctica where the circumpolar circulation and its interaction with the complex terrain of the continent are important contributors to the weather.

A fairly complete description of OMEGA can be found in Bacon et al. (2000). OMEGA is a complete, operational, atmospheric simulation system. It includes the OMEGA model, static world-wide surface datasets required to define the necessary surface properties (elevation, land/water fraction, albedo, vegetation, etc.), data preprocessors to assimilate meteorological data, automated routines to download data from various operational data centers, as well as post-processors to analyze and visualize the simulation results. The kernel of the system is the OMEGA model – a three-dimensional, time-dependent, non-hydrostatic model of the atmosphere. It is built upon an unstructured triangular grid, which can adapt to a variety of static user-defined fields as well as dynamically during the simulation to the evolving weather. The triangular unstructured grid makes it possible to represent the underlying terrain with great accuracy. The dynamic adaptation increases the spatial resolution only where it is needed, (such as in the region of weather systems or steep terrain), automatically during runtime, thus optimizing the use of the computational resources.

The variable resolution and adaptive nature of the OMEGA grid structure give it a unique advantage in simulating the Antarctic atmospheric circulations. For example, the OMEGA grid can adapt to the terrain and/or initial sea ice concentration, thus resolving the large-scale dynamics as well as the local scale circulations associated with fine scale representation of the terrain features. This means that OMEGA can simultaneously resolve the meso- $\alpha$  scale ( $O(100\text{ km})$ ), meso- $\beta$  scale ( $O(10\text{ km})$ ), and meso- $\gamma$  scale ( $O(1\text{ km})$ ) forcing that drives the local scale wind field without the need to place high resolution everywhere and without human interaction.

OMEGA includes an embedded Atmospheric Dispersion Model. This capability is useful in the Antarctic in terms of monitoring the potential path of an effluent plume and hence to the study of a number of air quality issues in Antarctica. The meteorological and dispersion capabilities of OMEGA have been the subjects of several model evaluation and verification studies, the most recent

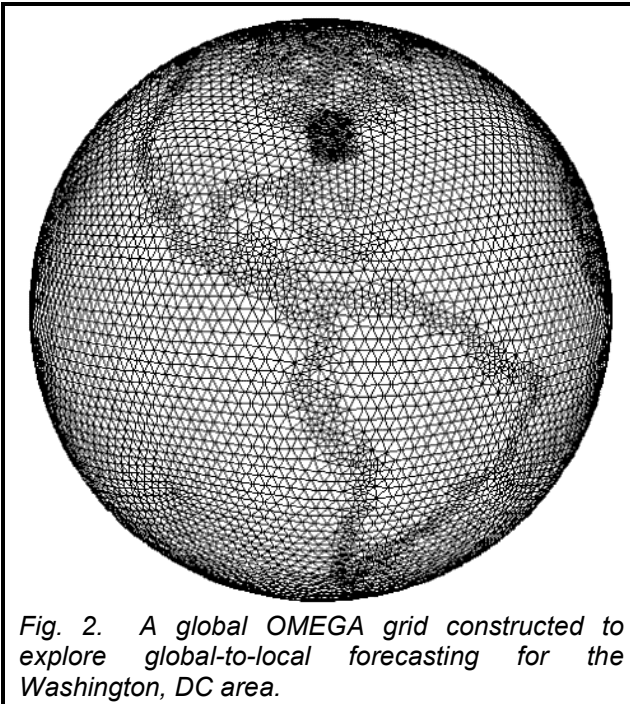


Fig. 2. A global OMEGA grid constructed to explore global-to-local forecasting for the Washington, DC area.

of which was evaluation against data from the ETEX experiment (Boybeyi et al., 2001).

## 5. Benefits of Static and Dynamic Adaptation

The unique capabilities of OMEGA have shown the benefits of static and dynamic adaptation. Figure 3 shows a static grid that was constructed for a regional simulation of the Antarctic Peninsula. This grid had horizontal resolution ranging from 30 to 75 km. The OMEGA simulation clearly showed flow blocking caused by the geography of the peninsula.

Figure 4 shows how dynamic adaptation can maintain resolution in those regions required by physical processes. This simulation of a severe tornadic outbreak in 1979 used a dynamic adaptation criteria of low-level moisture concentration. The grid was able to maintain high resolution automatically in those regions where the physical processes produced severe convection and tornados.

## 6. Conclusions

RIME is intended to advance our understanding of the meteorology of Antarctica and its potential impact on the weather and climate of the rest of the world. As such, the knowledge gathered in RIME *must* be transferred to models to allow us to extend our knowledge and to test it under varying assumptions. This is justification enough to have multiple modeling efforts participating in order to form a critical mass.

OMEGA represents a unique atmospheric modeling and forecasting system. The adaptive grid permits the easy gridding of the complex terrain of Antarctica and the dynamic adaptation should allow us to explore the interaction of weather systems with the complex topography of the Antarctic coast – including the area surrounding the Ross Sea.

Finally, OMEGA in its global mode, may prove useful in understanding the global impact of Antarctic weather.

### References

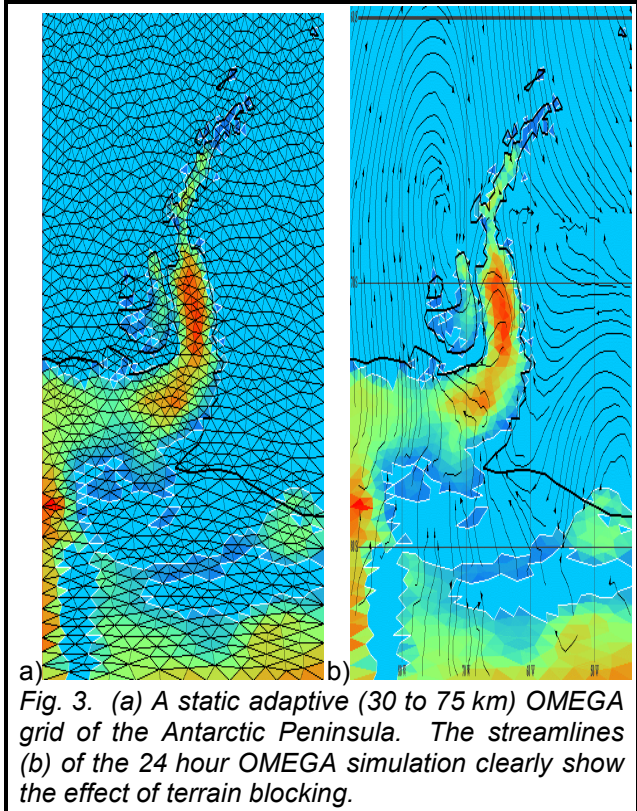
Bacon, D. P., N. N. Ahmad, Z. Boybeyi, T. J. Dunn, M. S. Hall, P. C-S. Lee, R. A. Sarma, M. D. Turner, K. T. Waight, S. H. Young, J. W. Zack, 2000: A Dynamically Adapting Weather and Dispersion Model: The Operational Multiscale Environment model with Grid Adaptivity (OMEGA). *Mon. Wea. Rev.*, **128**, 2044-2076.

Boybeyi, Z., N. N. Ahmad, D. P. Bacon, T. J. Dunn, M. S. Hall, P. C. S. Lee, R. A. Sarma, and T. R. Wait, 2001: Evaluation of the Operational Multiscale Environment Model with Grid Adaptivity against the European Tracer Experiment. *J. Appl. Met.* **40**, 1541–1558.

Cassano, J. J., J. E. Box, D. H. Bromwich, L. Li, and K. Steffen, 2001: Verification of Polar MM5 simulations of Greenland’s atmospheric circulation. *J. Geophys. Res.*, in press.

Liu, H., K. C. Jezek, and B. Li, 1999: Development of an Antarctic digital elevation model by integrating cartographic and remotely sensed data: A geographic information system based approach. *J. Geophys. Res.*, **104**, 23199-.

Parish, T. R., 1981: The katabatic winds of Cape



Denison and Port Martin. *Polar Rec.*, **20**, 525-532.

Schwerdtfeger, W., 1975: The effect of the Antarctic Peninsula on the temperature regime of the Weddell Sea. *Mon. Wea. Rev.*, **103**, 41-51.

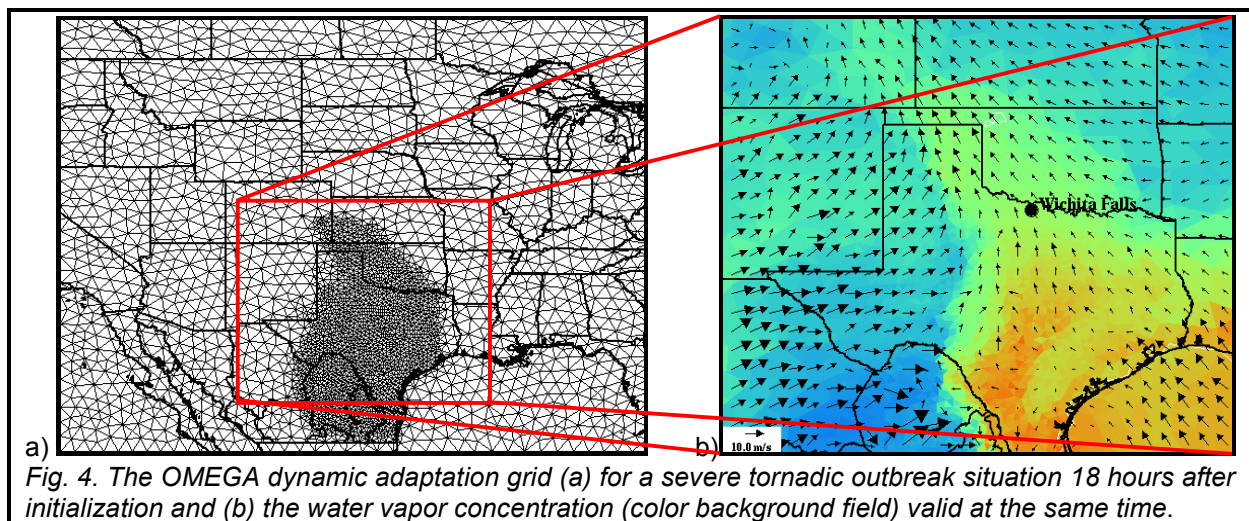


Fig. 4. The OMEGA dynamic adaptation grid (a) for a severe tornadic outbreak situation 18 hours after initialization and (b) the water vapor concentration (color background field) valid at the same time.

## AMPS Operational Utility

Arthur M. Cayette, Chester V. Clogston and James E. Frodge  
SPAWAR Systems Center, Charleston, SC

### 1. Introduction

Since the inception of the Antarctic Mesoscale Prediction System (AMPS) a unique combination of research and numerical modeling development has provided a robust experimental model for the Antarctic. This model has been evaluated in the operational field at McMurdo Station. Operational forecasters have viewed the output twice daily, finding great value in the strengths identifying weaknesses in various situations. Although it is an experimental model, the fine resolution and increased prognosis reliability has made this the model of choice for the U.S. Antarctic Program weather operations personnel.

Weaknesses have been discovered in the placement of moisture, and temperatures within the inversion layer. Strengths have been found in wind patterns, coastal thickness values, elevated inversions, and projections of low level moisture when initial validation correlates.

The operational stem of this partnership is one of direct contribution for direct benefit. The information technology era has provided the capability to collect and distribute information that in previous years was only available to a select few. Technology has also assisted in providing Automatic Weather Station (AWS) data and optical instrumentation, aiding weather observations taken from inexperienced field observers. Operations benefit from this joint alliance to increase accuracy in a highly volatile location where forecasting accuracy balances between mission success and the safety of life.

### 2. Environmental Concerns

The location of Ross Island does not provide an easy environment to conduct air operations. From the beginning of Antarctic aviation a suitable alternative to the McMurdo area was explored. The Metcalf and Eddy engineering team from Boston, MA presented a potential hardened runway plan at Marble Point in May 1958. This area presented not only a large area to build a hardened runway but better weather to conduct aviation operations (Metcalf and Eddy, 1958).

Three contrasting boundary layer environments with unique surface conditions are joined in the McMurdo region. The Plateau offers an elevated area with prevailing winds to support

and maintain an arid environment. Inflections from this region will typically provide dry katabatic winds and produce fair weather at McMurdo.

The Ross Sea provides a huge moisture source with a warm surface creating instability. Moisture can be derived from this region even during the dark of winter with sublimation driven by relatively thin and warm sea ice, polynas, and leads. A major change in McMurdo area weather can be noticed when the Ross Sea opens and the availability of moisture maximizes. Other changes in the local weather can occur, produced by the location of open water in relation to McMurdo. When strong southerly winds are driven through the McMurdo Sound, a reciprocating northerly flow will typically produce snow and reduced cloud bases driven by the newly opened water. Strong winds to the east of Ross Island force ice packs into the McMurdo Sound and decrease instability and available moisture in the area providing an improved condition over the norm.

The third unique environment within the area is the Ross Ice Shelf. This region is a dynamic modification of the two previously mentioned air masses placed over the coldest surface provided. If left standing, the potential temperature will be reduced to the lowest value in comparison. When intrusions from the Ross Sea progress over this cold surface, the natural surface based inversion is enhanced and moisture is typically condensed and trapped at low levels.

It is for these reasons that a thorough knowledge of the area, geographic effects, and an advanced understanding of atmospheric dynamics are required to successfully forecast weather conditions.

### 3. Forecasting Tools

Interpreting satellite information has been the backbone of short-term weather forecasting. This process is used worldwide, but higher levels of dependency have been placed on this tool where there is limited support from computer generated numerical models. Numerical modeling faces many of the same challenges as the forecaster in resolving the unique terrain features and convergence of multiple variables. At the May 2000 Antarctic Weather Forecasting Workshop, many of these physics and modeling obstacles

were outlined. Regardless, an initial effort was made to develop a numerical tool that best reflects the polar environment - AMPS.

#### 4. AMPS Strengths

AMPS has provided a robust year of operations for the United States Antarctic Program. During this year of utilizing the tool in a secondary operational role, it has provided valuable insight into features that assist in the forecast development process.

The primary strength is the projection of wind patterns around Ross Island. The wind direction and velocity fields are used frequently with a high degree of confidence in most situations. Wind depictions above 1,000 ft (300 m) are most accurate; below 1,000 ft the direction is generally fair and the velocity bias will vary depending on the situation. Generally the bias is high in conditions that promote southerly winds to 25 kts (13 m/s), and low in situations where observed winds are greater than 30 kts (15 m/s).

Situations where low clouds or fog has formed in close proximity and under light wind regimes are most difficult to forecast due to variability in wind directions based on local observed weather and satellite imagery. AMPS has offered precision in this area, indicating weak shifts in wind that may advect low level moisture or dry air into the region when fog or low clouds exist. In the example provided, a photo indicates fog to the south of McMurdo (Fig. 1). In Fig. 2, the AMPS 16-h forecast indicates fog to the south of McMurdo. (over Williams Field), which retreated as the wind shifted from the north as indicated.



Fig. 1. View of fog bank extending from the Windless Bight. View is to the south.

This same run shows the accuracy of moisture values. This element is both a strength and weakness of the system. When the moisture is properly located in the analysis the accuracy of the

wind directions assist in advection. Development and dissipation of moisture is generally represented well.

The resulting wind shift from the north as projected on the on the 22hr forecast drives a layer of elevated moisture from Lewis Bay which further develops in the McMurdo Sound and is photographed showing the low cloud cover moving over the station (Figs. 3 and 4).

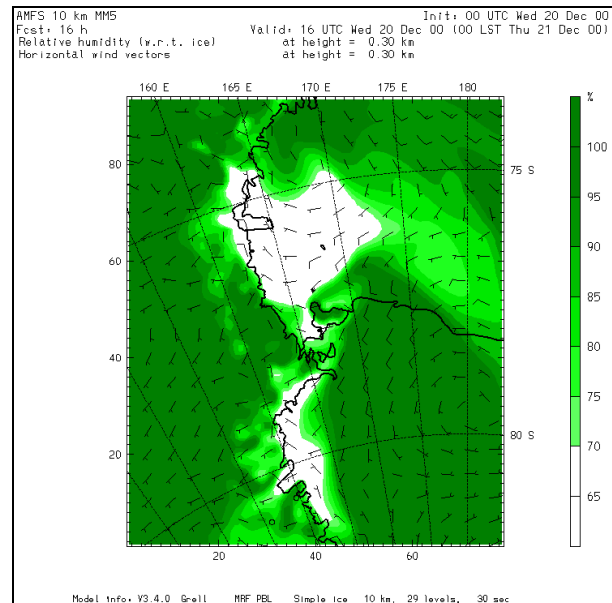


Fig. 2. AMPS 16hr forecast.

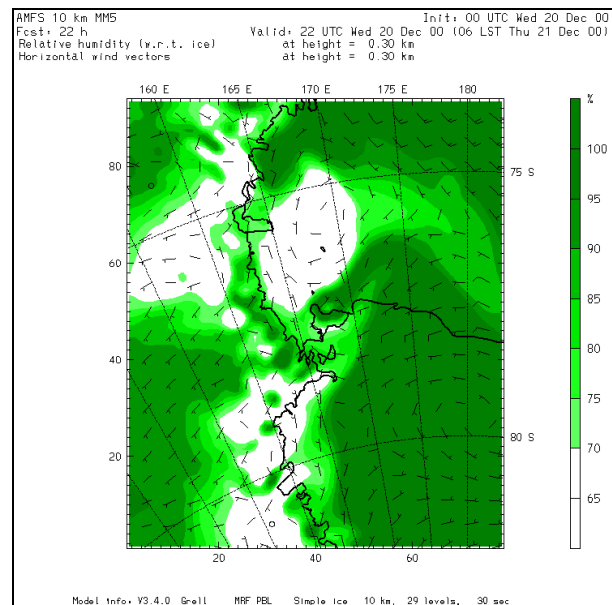


Fig. 3. AMPS 1K RH 22hr forecast



Fig. 4. View of retreating fog and advancing cloud deck from the north.

### 5. AMPS Weaknesses

Although AMPS has provided a valued tool there are areas of improvement that are needed. Accurate representation is not depicted for the immense terrain that is offered in the area. Hut Point Peninsula is absent on the 10-km scale. This obstacle provides a major adjustment to wind directions and produces converging winds causing acceleration in the area of the active airfields that is not represented because of the absence of this feature. As depicted in figure 5 (Seefelt, 1996), a developed runway crosswind was captured as a result of deflected super katabatic wind flows. This feature would not be detected without the depiction of Hut Point Peninsula causing the redirection.

The second element of concern is the representation of surface temperatures. The modeled temperature patterns over a 24hour period will not have a similar cycle when compared to the daily observations. This weakness was observed repeatedly through out the season. A main contributor to this error could be unveiled by the performance of the surface temperatures over this last month (August 2001). With the majority of the Ross Sea covered with ice, a more consistent surface is now offered to the environment. The actual may now be more closely related to the model's representation. Surface temperatures over this period fall within a few degrees and frequently mirror the general trend (figure 6).

The temperature errors extend upward though the surface based inversion. AMPS frequently produces a weaker inversion that breaks easier with surface temperature fluctuations. It should be stated that elevated inversions are regularly captured at or near the observed level.



Fig. 5. Wind pattern from a 3km grid model provided by Mark Seefelt

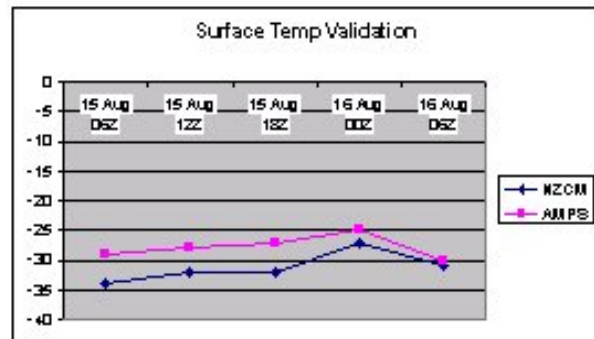


Fig. 6.. AMPS 24hr temperature validation 16 Aug, 2001

### 6. Summary

The MM5 product has provided the first real forecasting tool since the introduction of the Automated Weather Sensors and the High Resolution Picture Transmission satellite receiver. It produces many tools to extend forecasting and the forecaster's confidence beyond observations and satellite interpretation.

If surface based temperatures can be more accurately depicted and forecasted, increased accuracy can be readily obtained in the forecasting of fog. This element is highly dependent on the cooling temperature trends.

Greater confidence and accuracy in mid-range forecasting will assist in optimizing mission scheduling and accomplishment. Increased conventional and non-conventional data sets will

be required to increase the accuracy of initial parameters. Polar physics modifications are being studied and implemented. The addition of this joint effort to improve weather forecasting capabilities leads to the inflection of an accurate polar environment and refinement of the global depiction.

The combination of improved observational tools, computers and numerical models has led to substantial improvements in the accuracy of forecasts (Polger et al., 1994). It is the priority of Aviation Technical Services personnel to follow this same path and overcome the limitations that Antarctica presents.

## References

- Metcalf and Eddy Engineers, 1958: Report on Study of Feasibility of Construction of an Airfield in the Gnesiss Point - Marble Point Area. *Bureau of yards and Docks, Department of the Navy.*
- Seefelt, M.W., 1996: Wind flow in the Ross Island region Antarctica based on the UW-NMS model, *University of Wisconsin Master of Science Thesis.*
- Polger, P.D., B.S. Goldsmith, R.C. Przywarty, and J.R. Bocchieri., 1994: National Weather Service warning performance based on WSR-88D. *Bulletin of the American Meteorological Society* , **75**, 203-214.

## Improvements in Data Source Collection in Antarctica

James E. Frodge, Chester V. Clogston and Arthur M. Cayette  
SPAWAR Systems Center, Charleston, SC

### 1. Introduction

It is a goal of Aviation Technical Services (ATS) to use all available resources to improve short term forecasting to nearly 100% mission accuracy level and to improve mid-range forecasting for an improved mission planning capability. In addition, we are also working toward a better understanding of cyclic patterns, which would allow the National Science Foundation a reasonable representation of the number of years required for extended planning purposes. All this is incumbent upon increasing the amount of data, the ability to access data, and the utilization of data in the forecast process. There is more data available than currently utilized for a host of reasons, such as poor communications from sites or lack of awareness that other groups or agencies may be collecting it. Technological improvements need to be made to ensure quality data is collected and distributed in real-time to have the greatest impact in research and operations.

### 2. Improvements

ATS continues to move forward with infrastructure improvement. We've gone from a weather office with a single 100-MHz personal computer with a 9600-baud modem to a series of Windows NT based workstations networked to an undedicated T-1 line. The Internet capability has allowed McMurdo Weather (Mac Weather) to significantly increase the amount of data flow into and out of the office. Access to multiple models, observations collected and transmitted to the Global Telecommunications System (GTS), and the ability to communicate to other forecasters/modelers have all contributed to increased accuracy of forecasts.

Other impacts have been the launch of the National Oceanic and Atmospheric Administration NOAA-16 polar orbiting satellite, which has brought us back to the point we were before NOAA-14 went astray. A coverage blackout that was nearly 7 hours in duration is now back to just under 5 hours. This outage continues to be during the middle of flight operations. We also installed a simple receiver with a limited use omni-directional antenna. It was hoped that this would fill the gap during the operational day between the NOAA and Defense Meteorological Satellite Program (DMSP) passes by capturing automatic picture

transmission imagery from passes of the Russian polar orbiting satellite constellation (METEOR). A grid system installation has improved the use of this tool. This aging system was shut down during the 2000-01 season. Japan's Geostationary Meteorological Satellite (GMS-5) assists with intercontinental flights, vapor winds, and construction of composite images. This system's coverage is decreasing with age.

We have improved our resources in the data acquisition area as well. We've gone from 2 automated surface observing systems (ASOS), and 1 AIR radar wind sounding (RAWIN) system to 2 ASOS, 13 automatic weather stations (AWS), 2 Portable ASOS (PASOS) and 1 global positioning system (GPS) RAWIN system. In addition, we have procured new meteorological (MET) Kits to improve camp observations. How this has made an impact is:

- a) GPS RAWIN has decreased the wind failure rate to 5% from a high of 25% with the AIR RAWIN system.
- b) 2 PASOS, one on each Tower at the active airfields, modified to meet synoptic and outside continental United States (OCONUS) reporting requirements.
- c) Aging ASOS remaining on site to support Pegasus runway and provide extended data collection.
- d) AWS network area expansion with the addition of 13 AWS sites placed to provide advanced indications of weather events (Fig. 1).
- e) Provision of new MET Kits to include a ceilometer and visibility sensor for larger camp operations to increase the accuracy of these important observations.

Three initiatives for this season are a direct link to the AWS on Odell Glacier, collection and transmission of continental aircraft report (AIREP) data, and the collection and distribution of extended Terra Nova Bay (TNB) data. The weather data link to Odell Glacier will provide greater frequency of weather data and easier access to information at this emergency landing field. The second initiative for this coming season is receiving TNB weather data. The Italians have up to 11 AWS sites (Fig. 2) and take an upper air



sounding as well. We are working with them to collect as much data as possible and put it into the GTS. The benefit of the TNB data will greatly improve our ability to quantify systems approaching from the north and most importantly, making the data available for research and assimilation into the global and mesoscale models.

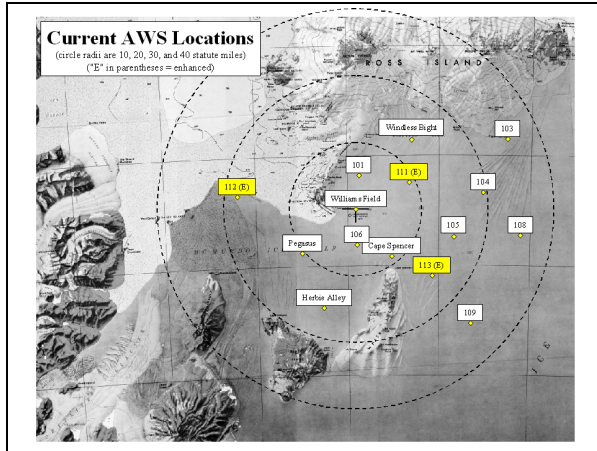


Fig. 1. Current AWS Locations.

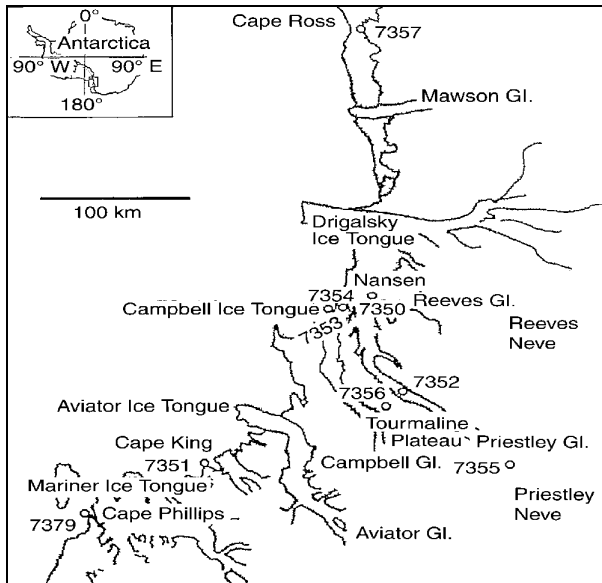


Fig. 2. Italian AWS Locations near TNB (Midpoint AWS, further inland, not shown).

### 3. Computer Modeling

As forecasters we can't begin to measure the impact computer modeling has had over the recent years to the improvement of accuracy in forecasting. This is especially true for forecasting in McMurdo. In the past we relied on one global model, the Navy Operational Global Atmospheric Prediction System (NOGAPS) from the Navy's

Fleet Numerical Meteorology and Oceanography Center (FNMOC), which provided an 81km grid. Since the improvement in our connectivity we now are able to utilize products from not only FNMOC and their NOGAPS model, but the Air Force Weather Information Network (AFWIN) standard version of the the Pennsylvania State University / National Center for Atmospheric Research (NCAR) Fifth Generation Mesoscale Model (MM5), the National Centers for Environmental Prediction (NCEP) Aviation model (AVN), and most recently an experimental model, the Antarctic Mesoscale Prediction System (AMPS) from NCAR, which employs a version of the MM5 with polar modifications developed by the Polar Meteorology Group at the Byrd Polar Research Center (BPRC). The AMPS model was implemented as a result of the May 2000 Antarctic Weather Forecasting Workshop, held at BPRC. The availability of all of these models to the forecaster has drastically improved the ability to provide an accurate forecast. A brief synopsis of the models and what they provide us are:

- a) AFWIN MM5
  1. 45-km MM5 covering continent
  2. 15-km for Ross Island which is being activated for the full period this operating season
  3. Agreement to implement polar modification when validated
- b) FNMOC support with the Optimum Path Aircraft Routing System (OPARS) and NOGAPS.
- c) AMPS MM5 (non-operational)
  1. 90-km MM5 covering most of Southern Hemisphere
  2. 30-km MM5 covering continent
  3. 10-km over Ross Island
  4. Very receptive to improvements and modifications
- d) NCEP's AVN long range trend support with 14 day outlook

### 4. Future potential improvements

As far forward as we have come in the last few seasons, it's a small step in the direction we need to go. The only way to continue to improve is to look into and plan for future improvements. Currently Mac weather has proposed initiatives, for the near future, that will continue are movement down the right path. Some of these are:

- a) Weather camera installations at the active runway and a potential to extend to remote locations

- b) Weather radar. We are currently looking into a small system for testing at McMurdo
- c) Extended data distribution using NOAA Port and a potential addition of a Local Data Manager (LDM) server to use Unidata's Internet Data Distribution (IDD) system. We are working with the University Corporation for Atmospheric Research (UCAR) and NOAA to distribute as much data as possible
- d) Move several current AWS sites to better utilize their capability in areas void of data (Fig. 3)
- e) Improved portable MET Kits for all field operations
- f) MET Kits with communications capabilities (i.e. HF or Iridium e-mail)
- g) A direct link of all observations to the server for transmission to the GTS. This would limit the amount of time personnel would have to transfer data from one system to another
- h) Improve the display of all observations (ASOS, PASOS, AWS, human, etc.) graphically on one display system.
- i) Improved visualization using specialized software (VIS5D) with overlays of satellite and analysis (Fig. 4)
- j) Better coverage of upper air data through the Constellation Observing System for Meteorology, Ionosphere, and Climate (COSMIC) and soundings utilizing sounders and light detection and ranging instruments (lidars).
- k) Continued improvement to MM5 capabilities and global depiction through RIME efforts
- l) Look for ways to close the gap in satellite coverage during operational hours

## 5. Summary

Conventional data sources for Antarctica are sparse and will continue to be so in the future. Such is the case with all hostile environments. But the continuing efforts through technology and research will gradually erode the gaps in this area. Where conventional means become an obstacle technology assists in form of AWS, ATOVS (Advanced Tiros Operational Vertical Sounder), and COSMIC to name a few. As improvements are made in data collection technology it will assuredly have an impact on research and numerical predictions.

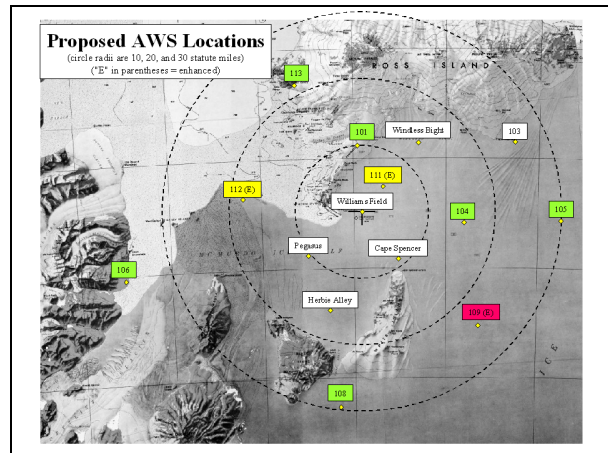


Fig. 3. Proposed AWS Locations.

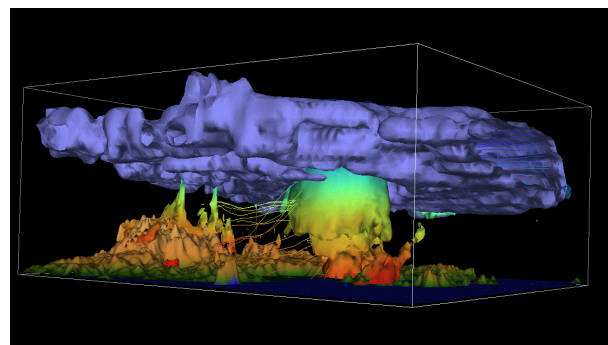


Fig. 4. VIS5D with overlays of satellite and analysis.

# PERFORMANCE OF POLAR MM5 IN SIMULATING ANTARCTIC ATMOSPHERIC CIRCULATION

Zhichang Guo\*, David H. Bromwich, and John J. Cassano

Polar Meteorology Group, Byrd Polar Research Center, The Ohio State University,  
Columbus, Ohio

## 1. Introduction

Verification of a complete annual cycle of 72h nonhydrostatic mesoscale model simulations of the Antarctic atmospheric circulation is presented. The simulations are generated with the Pennsylvania State University (PSU)-National Center for Atmospheric Research (NCAR) Fifth-generation Mesoscale Model (MM5), which is modified for polar applications, and is referred to as the Polar MM5. With a horizontal resolution of 60km, the Polar MM5 has been run for the period of January 1993 through December 1993 in a year-long series of short-term forecasts from initial and boundary conditions provided by the operational analyses of the European Centre for Medium-Range Weather Forecasts (ECMWF). For every short-term forecast the model is integrated for 72 hours with the first 24 hours being discarded for spin-up purposes. The simulations to be analyzed are compiled from the series of remaining 48 hour forecasts.

It is found that proper treatment of the upper boundary condition is very important to the performance of MM5 in simulating Antarctic atmospheric circulation. With a different upper boundary condition and top pressure level, another complete annual cycle of 36h simulations of the Antarctic atmospheric circulation is generated for the period of January 1998 through December 1998. The preliminary results of the new simulations, though not discussed here, will be presented at this workshop, and published at a later date.

A brief description of Polar MM5 is presented in section 2. The model performance primarily in relation to observations from automatic weather station (AWS) sites, manned stations and climatological maps, is evaluated in section 3 on annual, seasonal, synoptic and diurnal time scales. Concluding remarks on the model performance are given in Section 4.

## 2. Polar MM5

The Polar MM5 model is based on version 2 of the PSU / NCAR MM5, which includes three-dimensional prognostic equations for the horizontal and vertical components of the wind, temperature, and pressure perturbations in its nonhydrostatic version. Additional three-dimensional prognostic equations for the water vapor, cloud water (ice) and rain water (snow) mixing ratios are also part of the model equations. Parameterizations for moist physics, radiative transfer, and turbulence are included in the model, with multiple options available for the representation of many of these processes. A detailed discussion of the modifications made to the standard version of MM5 for use over polar regions has been described in Bromwich et al. (2001) and Cassano et al. (2001). A brief description of Polar MM5 and its configuration for simulations over Antarctica is presented in this section.

In moist physics of the Polar MM5 the Reisner explicit microphysics parameterization is used to represent the resolvable scale cloud and precipitation processes, and the Grell parameterization is used to represent the sub-grid scale cloud processes. Results from MM5 sensitivity simulations show that excessive cloud cover was a problem over the Antarctic and the use of the Fletcher (1962) equation in the parameterization scheme is the major reason for this bias. In order to eliminate this cloudy bias in simulations the equation for ice nuclei concentration from Meyers et al. (1992) was used in Polar MM5 to replace the Fletcher (1962) equation in the explicit microphysics parameterization.

The radiative transfer of shortwave and longwave radiation through the atmosphere is predicated with a modified version of the NCAR community climate model, version 2, (CCM2) radiation parameterization, in which the predicted cloud water and ice mixing ratios are used to determinate radiative properties of the modeled cloud cover. The modified radiation scheme allows for a consistent treatment of the radiative and

---

\* Corresponding author: Zhichang Guo, Polar Meteorology Group, Byrd Polar Research Center, e-mail: guo@polarmet1.mps.ohio-state.edu

microphysical properties of the clouds and for the separate treatment of the radiative properties of liquid and ice phase cloud particles,

Turbulent fluxes in the atmosphere are parameterized using the 1.5 order turbulence closure parameterization used in the National Centers for Environmental Prediction Eta model. Heat transfer through the model substrate is predicted using a multi-layer "soil" model. The thermal properties used in the "soil" model for snow and ice surface types are modified following Yen (1981), and two additional substrate levels have been included in Polar MM5 to increase the substrate depth. Also, a sea ice surface type is added to the 13 surface types available in the standard version of MM5 (Hines et al., 1997). The sea ice surface type allows for fractional sea ice cover in any oceanic grid point, with surface fluxes within the sea ice grid points calculated separately for the open water and sea ice portions of the grid point. These fluxes are then averaged before interacting with the overlying atmosphere.

The model domain used in this study consists of  $120 \times 120$  grid points, centered at the South Pole, with a horizontal resolution of 60 km. The pressure at the model top is set at a constant pressure of 100 hPa, and a total of 28 vertical sigma levels are used, of which seven are located within the lowest 400 m of the atmosphere. The lowest sigma level is located at a nominal height of 11 m above ground level (AGL). This relatively high resolution near the surface is required to accurately represent the evolution of the shallow katabatic layer over the Antarctic ice sheet.

The model topography data over the Antarctic continent are interpolated from a 5 km resolution digital elevation model of Antarctica. The areas for Filchner-Ronne Ice Shelf and Ross Ice Shelf are manually identified from the climatic maps. The  $2.5^\circ$  horizontal resolution ECMWF surface and upper air operational analyses are used to provide the initial and boundary conditions for the model atmosphere. In addition the  $1.125^\circ$  ECMWF global surface analyses are used to specify the initial surface temperature and deep soil temperature. The daily polar gridded sea ice concentration data with 25-km horizontal resolution derived from the Defense Meteorological Satellite Program's (DMSP) Special Sensor Microwave/Imager (SSM/I) are used to identify the sea ice surface type and its cover fraction over each model grid.

The Polar MM5 is used to produce short duration (72 h length) simulations of the atmospheric state over Antarctica from Jan. 1993 through Dec. 1993. The model is initialized with

the 00 UTC ECMWF analyses for each preceding even day or 31st of the preceding month of each forecast mode, with the 24 – 72 h forecasts used for model verification.

### 3. Verification Results

Model output from the Polar MM5 simulations over the Antarctica is compared to available observational data on annual, seasonal, synoptic, and diurnal time scales in the following sections. The primary data sources used for verification of the Polar MM5 simulations presented in this paper are climatological maps, and observations from the University of Wisconsin automatic weather stations and the manned stations over the Antarctica. The validation is intended to demonstrate the high level of skill present in the Polar MM5 simulations. This analysis also serves to highlight areas requiring additional model improvements.

Annual mean fields from the Polar MM5 simulations are calculated for the surface temperature, near surface temperature inversion, near surface winds, total cloud cover, and accumulated precipitation minus sublimation. The model verification using climatological maps indicates that the Polar MM5 reproduced these fields with a high degree of realism.

Figure 1 shows the mean annual near surface temperature in 1993 simulated by Polar MM5. In comparison with climatological map synthesized by Giovinetto et al. (1990) tremendous fidelity between the simulated and observed temperature fields can be found for both distribution and magnitude. Both maps have the coldest mean annual temperatures  $-60^\circ\text{C}$  which are located near the highest elevation of the ice sheet, in a region of least cloud cover. In addition the temperature gradients along the East Antarctic escarpment are reproduced quite well in the simulated field. There is also a clear representation of the Antarctic Peninsula and West Plateau in the temperature field. As will be shown below, the model reproduces the annual cycle of temperature quite accurately at a large number of AWS and manned sites located on the Antarctic ice sheet, lending further credence to the distribution of the mean annual temperature simulated by the Polar MM5.

The Polar MM5 annual resultant wind vectors from the lowest model level (approximately 11 m AGL) with the model surface elevation are shown in Figure 2. In comparison with a detailed streamline pattern obtained by Parish and Bromwich (1987), PMM5 clearly produces the continent-scale drainage flow over East Antarctica

as cold low-level air flows from the high plateau to the sea. The drainage flow over the ice sheet is directed downslope and to the left of the ice fall line, as expected for katabatic flow in the Southern Hemisphere. The weakest resultant wind speeds are located along the ice divide, with stronger flow located over the steep coastal slopes, where the most persistent katabatic flow is likely to be located.

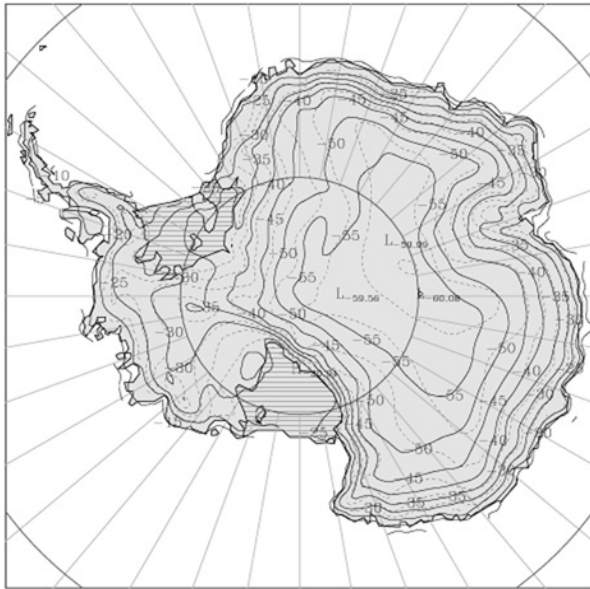


Fig. 1. Annual mean surface air temperature ( $^{\circ}\text{C}$ ) in 1993 simulated by PMM5.

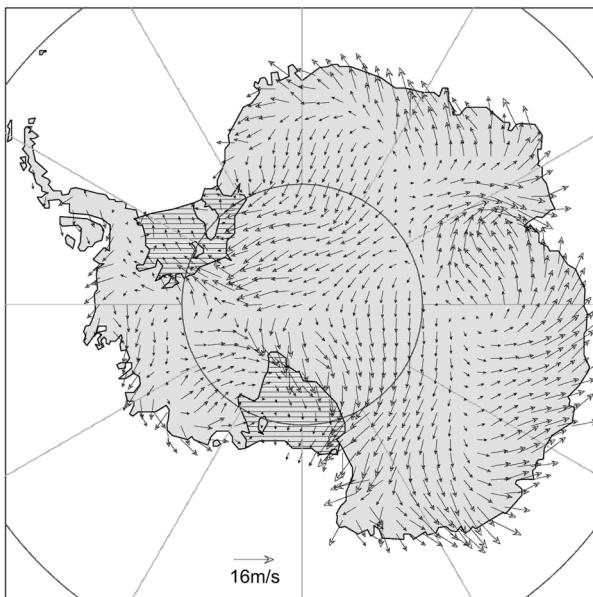


Fig. 2. Annual resultant near surface wind fields in 1993 simulated by PMM5.

The variables air temperature, wind speed, wind direction, and relative humidity, which will be used for model verification, are measured at both the AWS and the Antarctic manned stations. The AWS basic units measure these variables at a nominal height of 3 meters above the surface. The temperature and wind speed predicted by the Polar MM5 is interpolated from the model lowest level (nominal 11 m AGL) to a constant height of 3 m AGL for comparison with the AWS and manned station measurements. This interpolation is done by applying Monin-Obukhov similarity theory to the temperature and wind speed at the lowest model level, the model surface temperature, and the model specified surface roughness length. The model surface pressure has also been adjusted from the model grid point elevation to the elevation of the AWS observation, using the hypsometric equation.

The model verification using observations from the AWS array and manned stations indicates that the Polar MM5 simulates the near surface atmospheric state with a high degree of accuracy.

The monthly mean values of surface pressure, temperature, wind speed, wind direction and water vapor mixing ratio are averaged over four AWS sites (Dome C, Ferrell, Nico, Lynn) and four manned stations (Neumayer, Hally, Davis, Vostok) that had nearly complete records of all variables from Jan. 1993 through Dec. 1993 and the corresponding model grid points in the Polar MM5. These monthly means are plotted in Figure 3. The monthly bias, root mean square error (RMSE), and correlation coefficient from the comparison of the Polar MM5 simulations to the AWS observations are also calculated from the observations and model output (not shown). The bias is defined as the difference between the Polar MM5 monthly mean and the AWS observed monthly mean value of a given variable.

Figure 3 shows that the seasonal cycle in near surface temperature, pressure, wind speed and wind direction is reproduced by the model quite well although persistent biases exist in surface pressure. Comparison of the observed and modeled surface pressure and the model verification statistics reveals a negative bias in the modeled surface pressure that persists throughout the twelve month period. This bias ranges from 2 hPa to 8 hPa when averaged over eight sites. The persistent biases in the pressure are attributed in part to an uncertainty in the station elevation and associated error in the initialization fields. The correlation between the observations and the model forecasts, for the surface pressure, are high

(around 0.8) when averaged over the eight sites, and is indicative of the high level of skill present in the Polar MM5 forecasts.

Similar to the surface pressure, the near surface air temperature is well simulated by the Polar MM5. The monthly mean bias averaged over the eight sites ranges from  $-3.2^{\circ}\text{C}$  to  $-1.7^{\circ}\text{C}$ . The negative bias in the near surface air temperature corresponds to the negative pressure bias over entire 12 months. This anticorrelated variation in the temperature and pressure biases is consistent with the hydrostatically expected variations in the model pressure (i.e., colder temperatures lead to increased surface pressures). The correlation between the observed and modeled near surface temperature is not as large as that for the surface pressure, but is still moderately large (around 0.65) when they are averaged over the eight sites. The RMSE averaged over the eight sites varies from  $3^{\circ}\text{C}$  to  $8^{\circ}\text{C}$ . It is at a minimum during the summer months, when synoptic forcing is weakest and the diurnal variability is dominant, and is at a maximum during the more synoptically active winter months.

The seasonal cycle of modeled wind speed and wind direction is similar to the observations when averaged over the eight sites. The model verification statistics reveals a relatively high correlation (around 0.68) and a small bias between the observed and

the Polar MM5 simulation (dotted lines) and from the AWS and manned station observations (solid lines) for January through December 1993. The monthly mean values have been averaged over eight sites (and model grid points) as described in the text.

modeled wind direction. Among five variables shown in Figure 3 the correlation between the observed and modeled wind speed is the lowest, with little seasonal variation. It is believed that the errors in the ECMWF initialization, coarse spatial resolution (smoothing of topography), and cold biases in near surface temperature, which have important effects on the predicted katabatic flow, are main causes in biases of wind speeds. Although the correlation of wind speed is poor there is a good agreement between the monthly mean values of observed and modeled wind speed, and the model captures trends in the monthly mean wind speed with a reasonable degree of skill.

The model also reproduces seasonal variations of the mixing ratio accurately. The correlation between the modeled and observed water vapor mixing ratio is qualitatively similar to that for the temperature, but is slightly lower for the mixing ratio than the temperature.

The synoptical variability in the model simulations is evaluated by considering time series of the daily running mean and 3-hourly observations and the Polar MM5 output.

Figures 4 and 5 show time series of daily running mean AWS (dotted lines) and Polar MM5 (solid lines) data at Dome C AWS for the winter (Jun., Jul., Aug.) and summer (Jan. Feb. Mar.) 1993 respectively. A positive bias is evident in the surface pressure at Dome C as it is found and discussed in monthly mean pressure biases averaged over eight sites. The monthly mean wind speeds are generally well represented, however, the model tends to underestimate the wind speed variance such that periods of higher wind speeds are not well forecast. Despite these biases, most of the variability of surface pressure, temperature, wind speed, and wind direction at Dome C site is well represented by Polar MM5 for both winter and summer time. The good agreement between the modeled and observed time series is consistent with the high monthly correlation of the modeled and observed values.

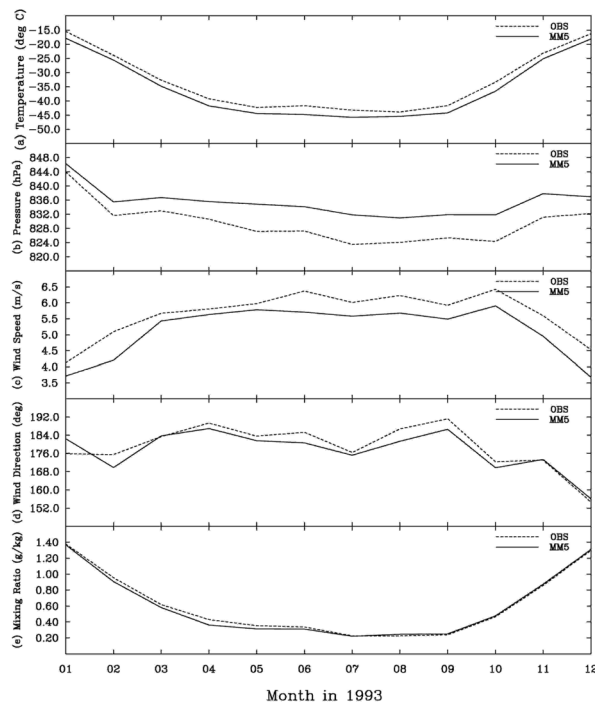


Fig. 3. Monthly mean values of air temperature at 3 m (a), pressure (b), wind speed at 3 m (c), wind direction (d), and mixing ratio (e) calculated from

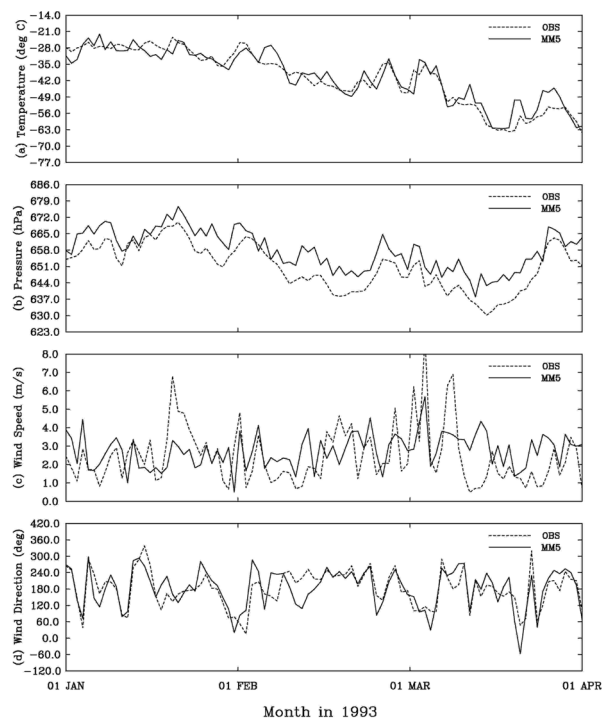


Fig. 4. Time series of daily running mean AWS (dotted lines) and Polar MM5 (solid lines) data at Dome C AWS for Jan. Feb. and Mar. 1993.

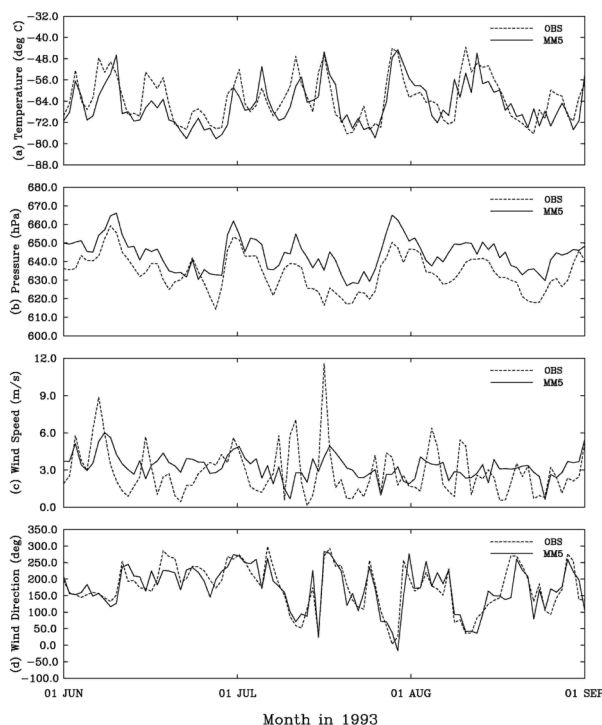


Fig. 5. Time series of daily running mean AWS (dotted lines) and Polar MM5 (solid lines) data at Dome C AWS for Jun. Jul. and Aug. 1993.

#### 4. Summary

The performance of the Polar MM5 has been evaluated over Antarctica for the time scales from annual to diurnal. A comparison of a yearlong series of short-term forecast of atmospheric state with observations from AWS and manned stations and climatological maps shows that simulations from Polar MM5 accurately capture both the large and regional scale circulation features with minimal bias in the modeled variables. Over all time scales the Polar MM5 is most skillful in the prediction of the surface pressure, temperature, wind direction, and water vapor mixing ratio, with slight less skillful predictions of wind speeds.

#### 5. Acknowledgments

This research was funded by National Science Foundation grants OPP-9725730 to D.H. Bromwich.

#### References

- Bromwich, D.H., J.J. Cassano, T. Klein, G. Heinemann, K.M. Hines, K. Steffen, and J.E. Box, 2001: Mesoscale modeling of katabatic winds over Greenland with the Polar MM5. *Mon. Wea. Rev.*, in press.
- Cassano, J.J., J.E. Box, D.H. Bromwich, L. Li, and K. Steffen, 2001: Verification of Polar MM5 simulations of Greenland's atmospheric circulation. *J. Geophys. Res.*, Special Issue on the PARCA (Program for Arctic Regional Climate Assessment), in press..
- Fletcher, N.H., 1962: *Physics of Rain Clouds*. Cambridge University Press.
- Giovinetto, M.B., N.M. Waters, and C.R. Bentley, 1990: Dependence of Antarctic surface mass balance on temperature, elevation and distance to open ocean. *J. Geophys. Res.*, **95**, 3517-3531.
- Hines, K.M., D.H. Bromwich, and Z. Liu, 1997: Combined global climate model and mesoscale model simulations of Antarctic climate. *J. Geophys. Res.*, **102**, 13747-13760.
- Meyers, M.P., P.J. DeMott, and W.R. Cotton, 1992: New primary ice-nucleation parameterizations in an explicit cloud model, *J. Appl. Meteor.*, **31**, 708-721.
- Parish, T.R., and D.H. Bromwich, 1987: The surface wind field over the Antarctic ice sheets. *Nature*, **328**, 51-54.
- Yen, Y.C., *Review of thermal properties of snow, ice and sea ice*. CRREL Rep. 81-10, 1981.

# PERFORMANCE OF FORECAST MODELS IN THE RESCUE OF DR SHEMENSKI FROM SOUTH POLE IN APRIL 2001

Andrew J. Monaghan\* and David H. Bromwich

Polar Meteorology Group, Byrd Polar Research Center, the Ohio State University, Columbus, OH

## 1. Introduction

Over the past decade, numerical weather prediction over polar regions has made significant progress. This is in part due to the implementation of physical parameterizations that are well suited to polar phenomena. The Polar MM5, for example, is a version of the Fifth Generation Pennsylvania State University / National Center for Atmospheric Research (NCAR) Mesoscale Model (MM5) which has been modified for use over extensive ice sheets (Cassano et al. 2001). As a result of the May 2000 Antarctic Weather Forecasting Workshop the Antarctic Mesoscale Prediction System (AMPS), which employs the Polar MM5, was implemented in the 2000-2001 field season. AMPS is an experimental program which employs a suite of models run at NCAR and dedicated to numerical weather prediction in Antarctica. AMPS is run for 3 domains at various resolutions covering most of the Southern Hemisphere from 40 S, with the finest grid focussing on the United States Antarctic Program's base of operations, McMurdo.

In the Antarctic, the importance of operational forecasting has become apparent in recent years. One reason is the effort to lengthen the field season, requiring flights in early spring and late autumn, when the entire continent is subject to extremely cold temperatures, strong winds, and the polar night. In addition, there is the occasional need to perform emergency evacuations of injured or ill personnel.

In late April 2001, a DeHaviland Twin Otter aircraft made an unprecedented late-season flight from Rothera to Amundsen-Scott South Pole Station (Fig. 1) in the evacuation of Dr. Ronald Shemenski, a medical doctor seriously ill with pancreatitis. The operation was complicated by near 24-hour darkness over interior Antarctica and extreme cold temperatures at the South Pole – below the minus 55°C operating limits of the commonly used LC-130 military aircraft. Frequent

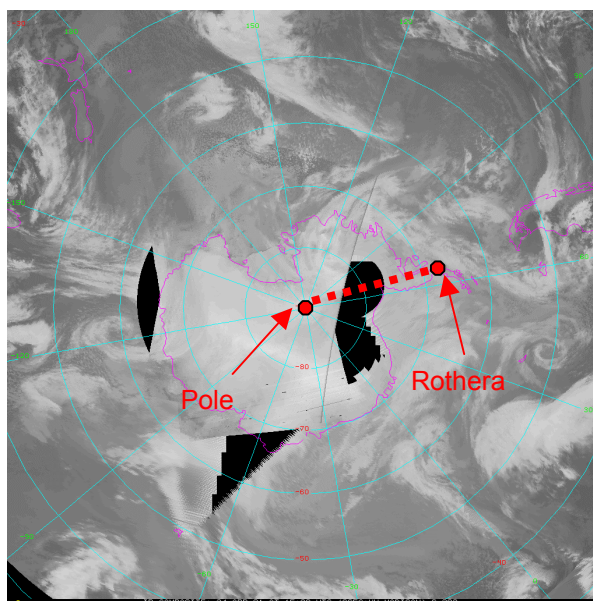


Fig. 1. Approximate flight path from Rothera to Pole, superimposed on a satellite composite showing conditions during the flight (courtesy, Antarctic Meteorological Research Center).

blowing snow conditions and the lack of a lighted runway or control tower made landing the aircraft at the South Pole a hazardous proposition. Throughout the operation, pilots relied on weather forecasters in the Falkland Islands and McMurdo to predict weather conditions accurately for the 10-hr flight. Due to the sparse observational network, forecasters relied heavily on numerical weather prediction models to aid in their analyses.

We are currently analyzing the performance of several of the numerical weather prediction models that aided meteorologists in forecasting weather throughout the operation. Specifically, there were 3 key forecast objectives:

1. Predicting when the winds would subside at the Pole for flight in.
2. If and when a low-pressure center near Marie Byrd Land would bring inclement weather to the Pole before the plane landed.

\* Corresponding author address: A. Monaghan, Byrd Polar Research Center, 1090 Carmack Rd., Columbus, OH 43210; email: monaghan@polarmet1.mps.ohio-state.edu



- If and when a low-pressure center in the Bellingshausen Sea would bring inclement weather to Rothera upon the return flight.

Perhaps the most important of these was the need to accurately depict the winds at Pole, as the blowing snow poses the greatest danger to the pilots. For this reason, and in the interest of brevity, we will focus only on this objective. In the near future, the comprehensive results of this work, covering all of the forecast objectives (and in greater detail), will be submitted to a journal for publication.

Table 1. Models Used in Study

| Agency | Model          | Domain     | Resolution (approximate) |
|--------|----------------|------------|--------------------------|
| ECMWF  | ECMWF Forecast | Global     | 55-km                    |
| NCEP   | AVN            | Global     | 110-km                   |
| NCAR   | Global MM5     | Global     | 120-km                   |
| NCAR   | AMPS MM5       | Antarctica | 30-km                    |
| BPRC   | Polar MM5      | Antarctica | 60-km                    |

Acronyms: European Centre for Medium Range Weather Forecasts (ECMWF), National Centers for Environmental Prediction (NCEP), Aviation Model (AVN), Byrd Polar Research Center (BPRC).

## 2. Models and Data

Table 1 gives a summary of each model used in the study. It is noteworthy that there are some models not included in the analysis. We have tried to include the primary models used by the U.S. forecasters. This excludes, for example, the United Kingdom Meteorological Office forecast model (UKMET). In addition, archived data could not be obtained for one of the primary models used in aid of the U.S. forecasting effort - the Air Force Weather Agency's standard version of the MM5.

The models were compared against data from Automatic Weather Stations (AWSs) and rawinsondes in all possible cases. ECMWF Tropical Ocean Global Atmosphere (TOGA) Operational Analysis data was used to analyze the upper-level model performance, and to fill in gaps in time series data. The ECMWF/TOGA data was quality checked using rawinsondes, and by extrapolating AWS data to the 700 hPa level using the technique of Phillpot (1997), and found to be in good agreement with the observations. Satellite data was also used where possible, and is hoped to provide more insight when BPRC obtains the high-resolution data from McMurdo (currently being shipped).

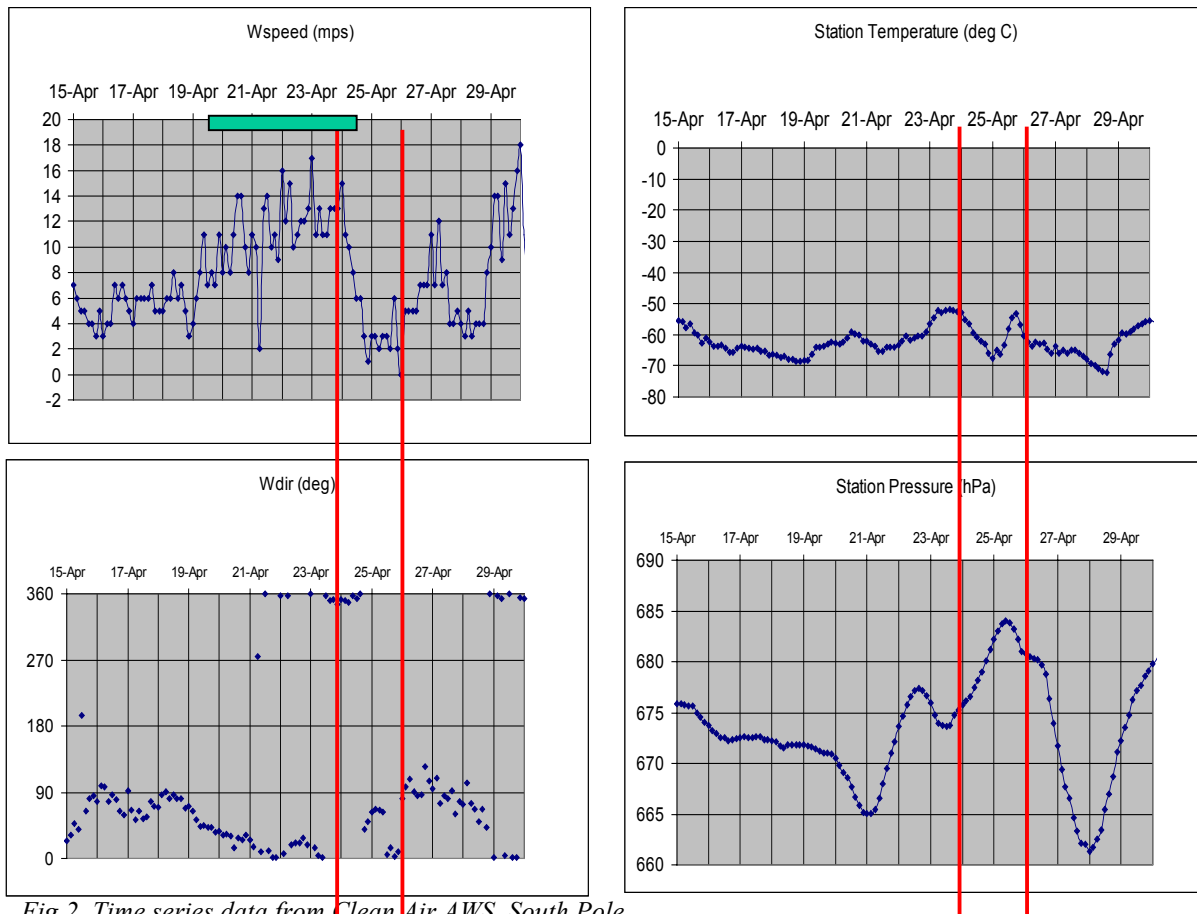


Fig.2. Time series data from Clean Air AWS, South Pole.

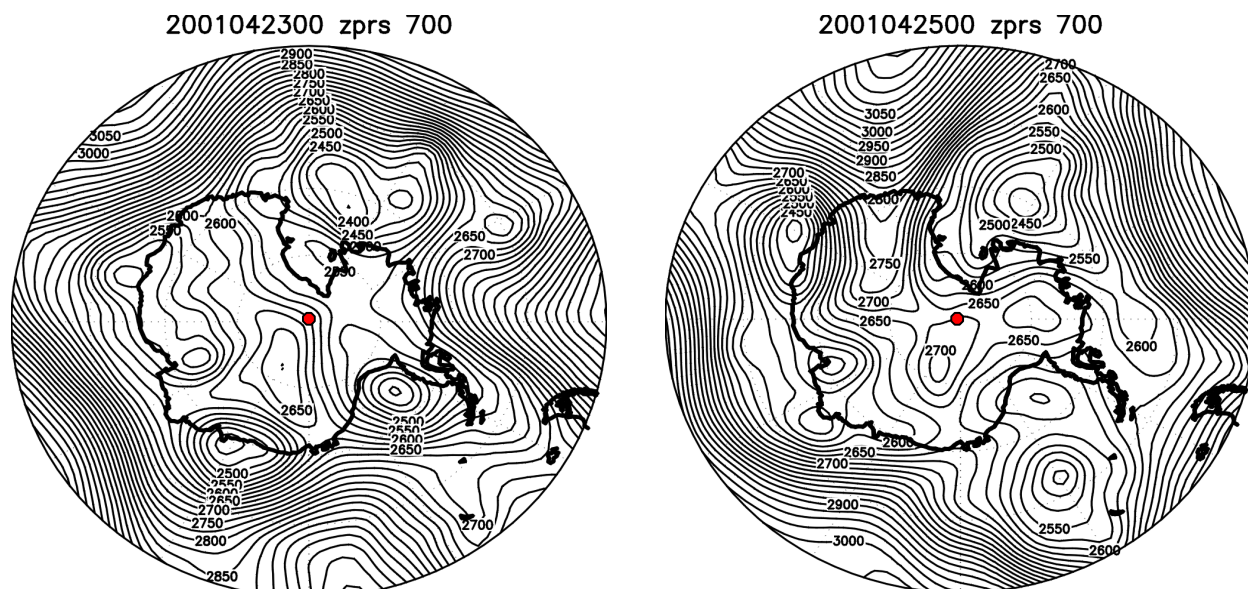


Fig. 3. ECMWF/TOGA Operational Analysis, 700 hPa geopotential height fields (a.) during the strong winds and (b.) after the winds subside.

### 3. Model Performance

Figure 2 shows the time series data at Clean Air AWS (-90.00 S, 00.00 E), located at the South Pole. The area between the red lines indicates the flight window to and from the Pole, which coincides with the winds subsiding. The green bar indicates times when blowing snow was reported. We are still investigating what caused the winds, and subsequently, why they subsided. However, it appears to be related to the poleward movement of a high pressure center initially located over East Antarctica. This is shown in Fig. 3, which shows the 700 hPa fields during (a.) and after (b.) the wind event. The movement of the system in relation to the winds subsiding, and its relation to nearby centers of low pressure (e.g., in the Amundsen Sea), suggest slackening in the pressure gradient. It is noteworthy that at the Pole, the 700 hPa surface is actually below the ground surface. However, the surface pressure at Pole is generally very close to 700 hPa (Fig. 2), and it can be argued that it is representative of the surface conditions. Comparing the South Pole 700 hPa winds from the ECMWF/TOGA data to the Clean Air AWS winds, it is seen that they are in good agreement (Fig. 4), justifying the use of the 700 hPa fields to depict the general surface synoptic conditions.

Figure 5 shows the surface wind speed forecasts for each of the models in late April 2001. It is immediately seen that all of the models underpredict the wind intensity during the period of blowing snow from 20-24 April. For the critical time period when the winds subside (indicated by

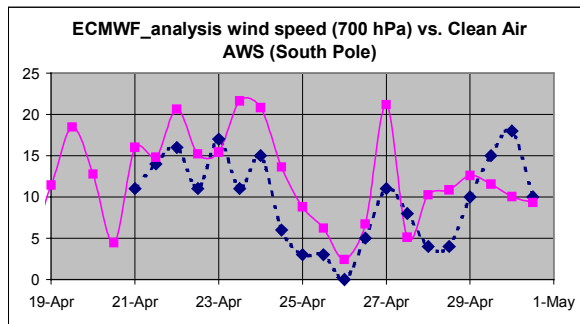


Fig. 4. ECMWF/TOGA Operational Analysis 700 hPa wind speed (solid) vs. Clean Air AWS surface (2m) wind speed, South Pole (dashed).

the violet bar showing the flight duration), the models perform with varying skill. Table 2 summarizes the skill of each model in predicting wind speed and direction, with respect to Clean Air AWS for all model initializations between 21-25 April 2001. Note that the average difference does not discriminate between positive and negative differences, while the average departure considers the absolute value of the difference. This makes a significant difference when considering the skill of the Global MM5, whose average is dampened because it does not predict the winds to subside from 24-26 April. The lack of the winds subsiding in the Global MM5 forecast may be related to a discrepancy at the pole in the outdated surface topography, which created a “hole” (this anomaly has since been adjusted to reflect the accurate topography).

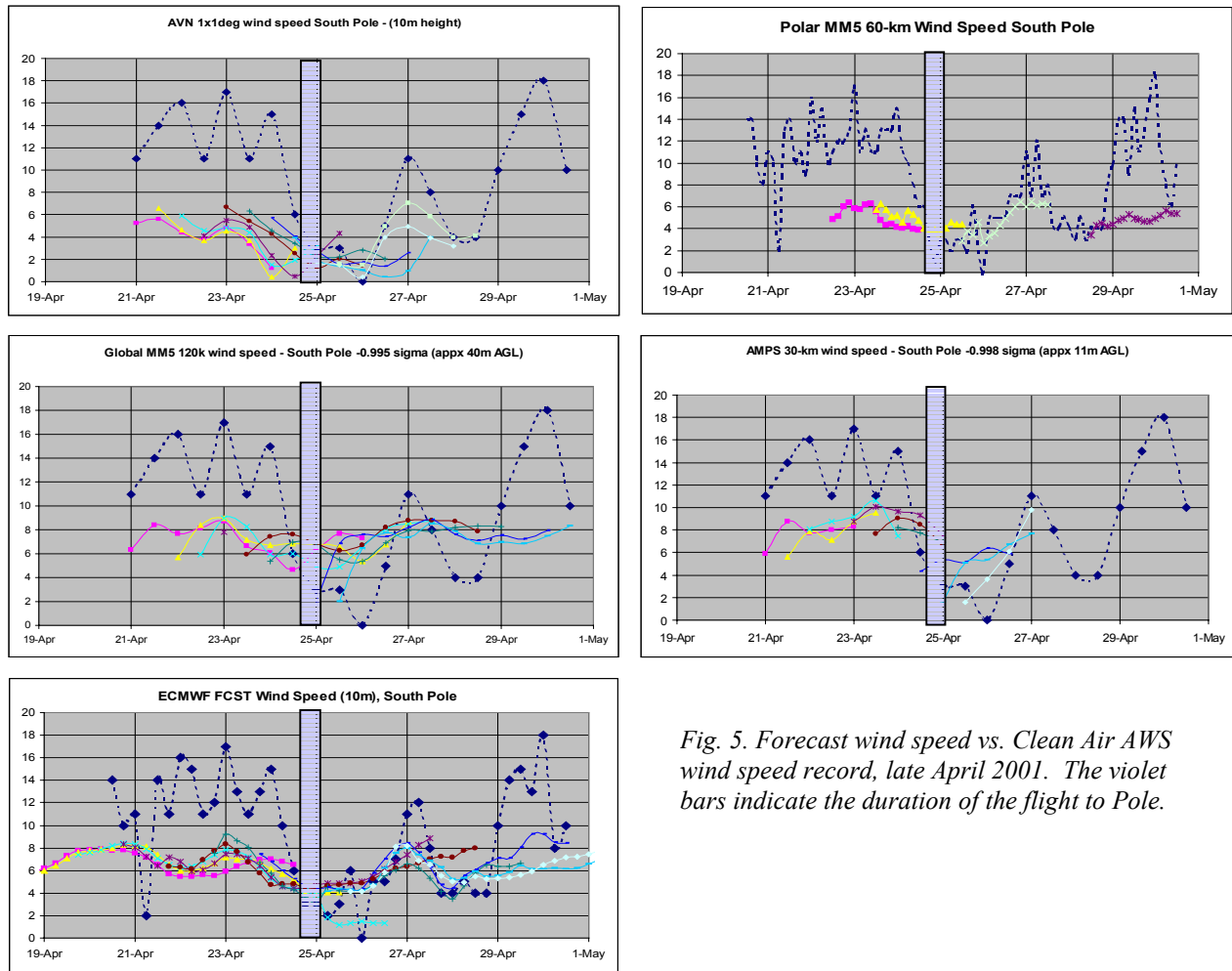


Fig. 5. Forecast wind speed vs. Clean Air AWS wind speed record, late April 2001. The violet bars indicate the duration of the flight to Pole.

Table 2. Model Results for South Pole winds. Averages are calculated for all model initializations between 21-25 April 2001. Due to a lack of archived data, one extra forecast was included for the 60-km Polar MM5 calculations (12 UTC 27 April).

| Model              | Wind Speed      |                | Wind Direction | # points | Time Res |
|--------------------|-----------------|----------------|----------------|----------|----------|
|                    | Avg. Difference | Avg. Departure | Avg. Departure |          |          |
| ECMWF_Fcst_0.5_deg | -2.0            | 3.7            | 23.4           | 64       | 12       |
| AMPS_MM5_30k       | -2.0            | 4.2            | 29.1           | 41       | 12       |
| Global_MM5_120k    | -0.8            | 4.3            | 36.8           | 78       | 12       |
| AVN_1_deg          | -4.9            | 5.2            | 57.5           | 70       | 12       |
| Polar MM5_60k      | -3.9            | 4.5            | 66.1           | 68       | 3        |

#### 4. Summary

Analysis and investigation into the performance of each of the models in predicting the winds at Pole, as well as all other forecast aspects of the rescue of Dr. Shemenski, is ongoing. The conclusions here are based on what has been analyzed thus far, and must be considered tentative. In general, it appears that

the models that are of highest spatial resolution near the Pole predict the wind speed and direction most accurately (ECMWF Forecast and AMPS 30-km). Observing the close relation between the accuracy of the wind direction and the accuracy of the wind speed (i.e., good wind speed predictions correspond to good wind direction predictions), one could conclude that an accurate depiction of the topographic forcing is integral to good model skill. Finally, observing the magnitude and fluctuation of the AMPS predicted wind speeds (and other variables, not discussed here), it appears that in addition to high spatial resolution, model skill is also aided by the integration of polar physics parameterizations.

#### 4. Acknowledgments

This research is sponsored by the National Science Foundation, Office of Polar Programs.

## References

- Cassano, J. J., J. E. Box, D. H. Bromwich, L. Li, and K. Steffen, 2001: Verification of Polar MM5 Simulations of Greenland's Atmospheric Circulation, *J. Geophys. Res., Special Issue on the PARCA (Program for Arctic Regional Climate Assessment)*, in press.
- Philpott, H.R., 1997: Some observationally-identified meteorological features of East Antarctica. Meteorological Study No. 42, Bureau of Meteorology, Australian, 275 pp.

# USE OF GPS RADIO OCCULTATION DATA IN RIME

Ying-Hwa Kuo, Tae-Kwon Wee, and William Schreiner  
National Center for Atmospheric Research  
Boulder, Colorado

David H. Bromwich  
Byrd Polar Research Center, The Ohio State University  
Columbus, Ohio

## 1. Introduction

In a workshop held at Byrd Polar Research Center in May 2000 (Bromwich and Cassano 2001), it was concluded that numerical weather prediction for Antarctic latitudes has advanced to the stage where useful forecasts can be made for several days in advance for most parts of the Antarctic continent. However, in comparison with populated areas of the Northern Hemisphere the forecast skill is deficient. In particular, it was recognized that: "*The current state of modeling in Antarctica does not properly represent the environment and is limited in its capability to ingest data.*" A major source of the problem is the fact that Antarctica is a data sparse region of the world. There are a total of 12 radiosonde stations over the entire continent. With the exception of the South Pole station, all the radiosonde stations are located on the periphery of the continent. The lack of data over the Antarctic and Southern Oceans greatly contributes to the uncertainties of global and regional weather analysis over the area, which in turn, limits the skill of weather prediction models. An important goal for RIME is to improve the quality of regional numerical weather prediction models for U.S. Antarctic operation. To achieve this goal, we must identify new data sources for the Antarctic and Southern Oceans, and make optimal use of all available observations to improve the quality of regional analysis.

## 2. GPS Radio Occultation Soundings

An emerging technology in remote sensing is the atmospheric limb sounding technique using the radio signals transmitted by the Global Positioning System (GPS) (Ware et al. 1996). Rocken et al. (1997) have shown that the quality of GPS radio occultation is compatible with that of radiosonde from the surface up to about 40 km. A major GPS/Meteorology project, known as COSMIC – Constellation Observing System for Meteorology, Ionosphere, and Climate, is scheduled for launch in 2005. COSMIC includes a constellation of six

micro-satellites each carrying an advanced GPS receiver and will provide ~3,000 radio occultation soundings that are distributed uniformly around the globe. This data set will be of tremendous value for weather prediction and climate analysis (Anthes et al. 2000).

As discussed by Kuo et al (2000) the raw measurements of the COSMIC system are phase and amplitudes of GPS radio signals. By making use of local spherical assumptions, these raw measurements can be converted to bending angles and refractivity. These are not traditional meteorological observations (such as temperature, water vapor, or pressure). In order to make optimal use of the radio occultation data, advanced data assimilation systems (such as three-dimensional or four-dimensional variational data assimilation – 3DVAR/4DVAR) must be used.

Although COSMIC will not be launched until 2005, several ongoing NASA-sponsored missions (e.g., CHAMP, SAC-C, and GRACE) are equipped with GPS occultation receivers, and will soon be providing high-quality radio occultation soundings. In fact, both CHAMP and SAC-C have already been launched, and will soon (expected in the fall of 2001) be providing up to 750 radio occultation soundings per day. The GRACE mission will be launched later this year and will provide an additional 500 soundings per day. Figure 1 shows the combined total of typical daily GPS radio occultation soundings from CHAMP, SAC-C, and GRACE missions. As compared with the available radiosonde observations, this represents a significant increase in upper-air measurements. It is expected that the CHAMP, SAC-C, and GRACE satellites will be operating during the first field phase of RIME. There is also a high likelihood that GRACE will be operating during the second field phase of RIME (2005-2006). Although data from these will not be available in real-time, they will be very valuable for post analysis and research.

### 3. Preliminary Results from Observing System Simulation Experiments (OSSES)

In an effort to assess the potential impact of GPS/MET radio occultation data on the regional analysis and prediction over the Antarctic and Southern Oceans, we conducted a series of observing system simulation experiments. We first performed a 72-h, 30-km MM5 (Fifth Generation Pennsylvania State University / National Center for Atmospheric Research Mesoscale Model) forecast initialized at 0000 UTC 13 October 1995 with a mesh size of 361 x 361 and 50 vertical levels – the “nature” run. The nature run was initialized with the European Centre for Medium Range Weather Forecasts (ECMWF) global analysis. The model forecast fields during the period of 0000 UTC 14 and 1200 UTC 14 October 1995 were used to simulate a set of refractivity soundings, with distribution in time and space similar to what would be available from the COSMIC mission. Another version of MM5 with 120-km grid resolution, a mesh size of 67 x 67 and 18 vertical levels was used to assimilate the simulated GPS radio refractivity observations, using the 4DVAR technique (Zou et al. 1995). Four experiments were conducted, using MM5 at 120-km grid resolution. All the experiments were started at 0600 UTC 14 October. The first is the NO4D experiment. This represents an experiment with no 4DVAR assimilation. The initial condition of NO4D was obtained from the 12-h forecast of a 120-km MM5 initialized with the NCEP initial condition. The quality of the initial condition is representative of that of the current operational global analysis. The second experiment is the PERF experiment, in which we assume a perfect initial condition (obtained from the natural run) is available for the forecast model at 120-km grid resolution. This represents the best possible performance of a forecast model. Two data assimilation experiments were performed. In 4DVAR1, we performed a 6-h assimilation of the simulated GPS refractivity data during the period of 0600 UTC to 1200 UTC 14 October. In 4DVAR2, two update cycles were used. We first performed a 6-h assimilation of the simulated GPS refractivity data during the period of 0000 UTC to 0600 UTC 14 October. The 6-h forecast from the first assimilation cycle (valid at 0600 UTC) was then used as the first guess for the second assimilation cycle that started at 0600 UTC.

Figure 2 shows the vertical profiles of (a) temperature, (b) specific humidity, (c) pressure, and (d) wind averaged over the period of 1800 UTC 14 and 0600 UTC 15 October 1995. The results of the 4DVAR1 experiment show that the

Occultation Locations for CHAMP, SAC-C, and GRACE, 24 Hrs

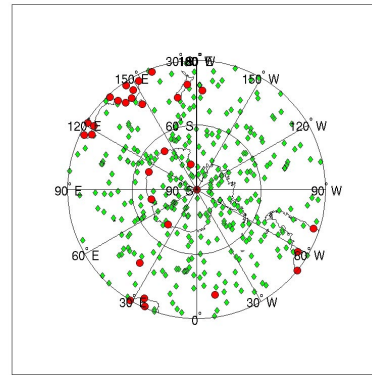


*Fig. 1. Green dots represent typical daily occultation soundings from CHAMP, SAC-C, and GRACE. Red dots are radiosonde stations.*

assimilation of GPS radio occultation soundings from a satellite similar to COSMIC will have significant positive impact on all variables (including winds) throughout the troposphere. More importantly, the improved regional analysis due to GPS radio occultation assimilation has a significant impact on the forecast skill of model. The 4DVAR2 experiment indicates that through the continuous assimilation-update cycle, we can expect even greater impact from the assimilation of GPS radio occultation data. In an operational environment, this type of update cycle can be repeated continuously. The results show that GPS radio occultation data will have a significant impact on meteorological analysis and prediction over the Antarctic and Southern Oceans.

### 4. Suggested Activities for RIME

#### a. Verification of GPS radio occultation soundings

The location and time of each GPS radio occultation can be predicted with high accuracy about one week in advance. RIME provides an unique opportunity to verify the accuracy of GPS radio occultation soundings in the Antarctic environment. We propose to take special soundings (i.e., supplementary radiosondes, dropsondes, or aircraft descent or ascent soundings) at the time and location of GPS radio occultation soundings that take place within the RIME experimental area. These special soundings can then be used to provide independent verification for the retrieved profiles of temperature, moisture and refractivity derived from the GPS radio occultation soundings.

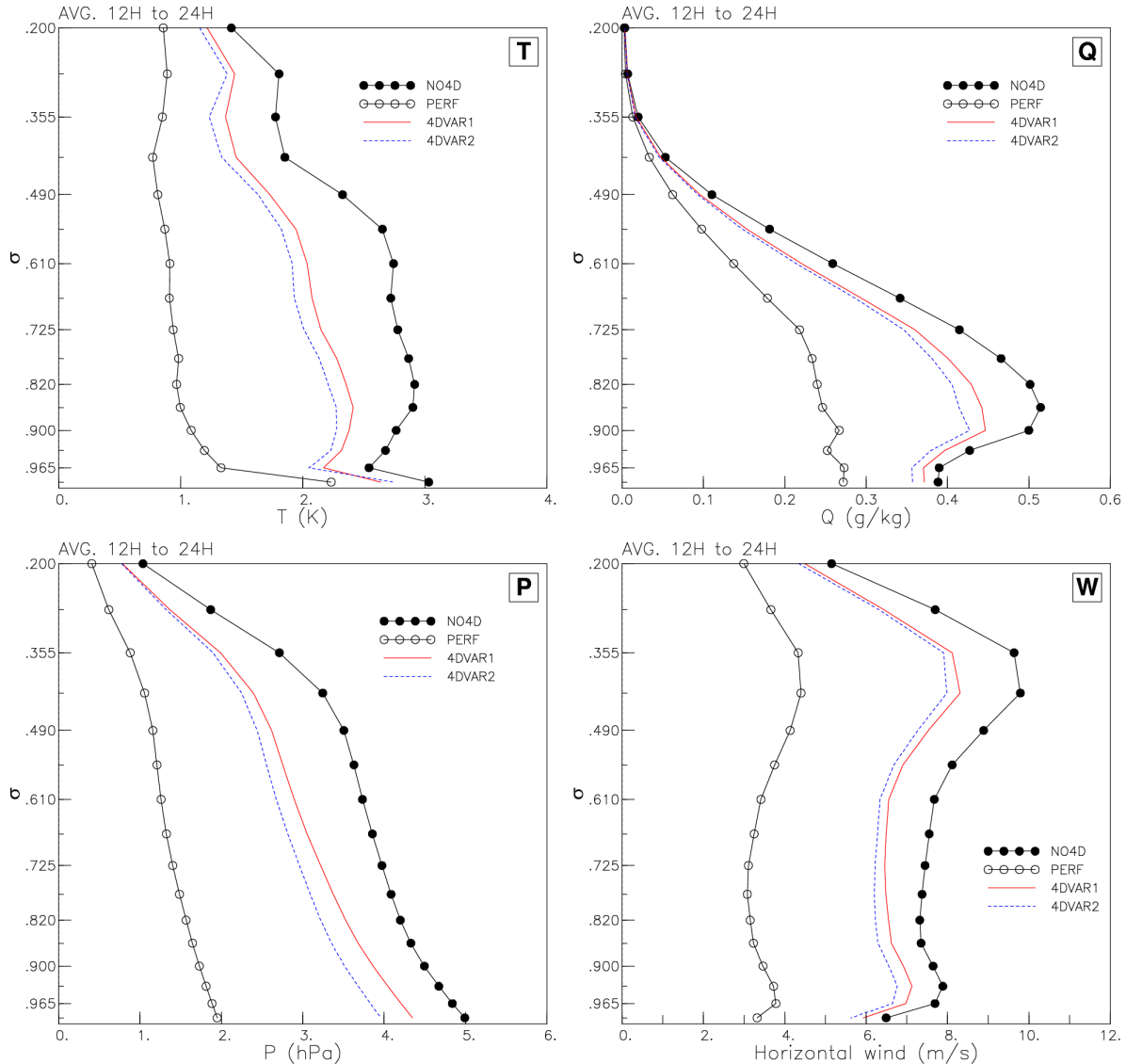


Fig. 2. Vertical profiles of rms errors (as compared with the natural run) for temperature, specific humidity, pressure, and wind fields for experiments NO4D (no data assimilation), PERF (perfect initial condition), 4DVAR1 (one cycle of 4DVAR assimilation), and 4DVAR2 (two cycles of 4DVAR assimilation).

**b. Perform post field-phase RIME analysis**

For many research applications, it would be desirable to have a high-quality grid-point analysis that makes use of all available observations taken during RIME. As mentioned earlier, during the first field phase of RIME, CHAMP, SAC-C, and GRACE will all be operating, and will provide about 1,250 non-real-time GPS radio occultation soundings per day. It would be very important to assimilate these GPS radio occultation soundings together with other satellite, upper-air, and surface observations, and to produce dynamically consistent data sets at a resolution much higher than currently available from the operational global analysis.

**c. Opportunities in the early phase of COSMIC deployment**

The six COSMIC micro-satellites will be launched by one single rocket. These will be deployed over a one year period through differential precession. During the early stage of deployment, these satellites are located within one single orbit. As a result, the GPS radio occultation soundings will not be distributed uniformly around the globe. Rather, they would be “clustered.” This offers the opportunity of high-density (in space) GPS radio occultation soundings locally over the RIME experimental area over certain hours of the day (see Fig. 3). If high-density (in space)

soundings are important for RIME, it might be advantageous to coincide the second RIME field phase with the early deployment of COSMIC.

## References

- Anthes, R. A., C. Rocken, Y.-H. Kuo, 2000: Applications of COSMIC to meteorology and climate. *Terr. Atmos. And Ocean*, **11**, 115-156.
- Bromwich, D. H., and J. J. Cassano, 2001: Meeting Summary: Antarctic Weather Forecasting Workshop. *Bull. Amer. Meteor. Soc.*, **82**, 1409-1413.
- Kuo, Y.-H., S. V. Kokolovskiy, R. A. Anthes, and F. Vandenberghe, 2000: Assimilation of GPS radio occultation data for numerical weather prediction. *Terr. Atmos. And Ocean*, **11**, 157-186.
- Rocken, C., R. Anthes, M. Exner, D. Hunt, S. Sokolovskiy, R. Ware, M. Gorbunov, W. Schreiner, D. Feng, B. Herman, Y.-H. Kuo, and X. Zou, 1997: Analysis and validation of GPS/MET data in the neutral atmosphere. *J. Geophys. Res.*, **102**, 29849-29866.
- Ware, R., M. Exner, D. Feng, M. Gorbunov, K. Hardy, B. Herman, Y.-H. Kuo, T. Meehan, W. Melbourne, C. Rocken, W. Schreiner, S. Sokolovskiy, F. Solheim, X. Zou, R. Anthes, S. Businger, and K. Trenberth, 1996: GPS sounding of the atmosphere from low Earth orbit: Preliminary results. *Bull. Amer. Met. Soc.*, **77**, 19-40.
- Zou, X., Y.-H. Kuo, and Y.-R. Guo, 1995: Assimilation of atmospheric radio refractivity using a nonhydrostatic mesoscale model. *Mon. Wea. Rev.*, **123**, 2229-2249.

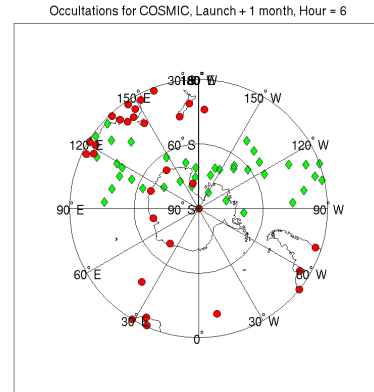


Fig. 3. Hypothetical GPS radio occultation soundings distribution over an one-hour period in the early deployment phase of COSMIC.



# A CASE STUDY OF THE IMPACT OF THE UPPER BOUNDARY CONDITION IN POLAR MM5 SIMULATIONS OVER ANTARCTICA

Helin Wei<sup>1</sup>, David H. Bromwich<sup>1,2</sup>, Le-Sheng Bai<sup>1</sup>, Ying-Hwa Kuo<sup>3</sup>, and Tae Kwon Wee<sup>3</sup>

<sup>1</sup>Polar Meteorology Group, Byrd Polar Research Center, The Ohio State University

<sup>2</sup>Atmospheric Sciences Program, Department of Geography, The Ohio State University

<sup>3</sup>MMM Division, National Center for Atmospheric Research, Boulder, Colorado

## 1. Introduction

In limited area modeling, the upper boundary condition was not addressed extensively until nonhydrostatic models became widely available for numerical weather prediction. Ideally, the boundary condition should be imposed in such way that makes the flow behave as if the boundaries were not there.

In the past, the rigid lid upper boundary condition was utilized because it purportedly eliminated rapidly moving external gravity waves from the solutions, thereby permitting longer time steps. This condition requires  $\omega = \frac{dp}{dt} = 0$  at the

model top. The effectiveness of this approach has been demonstrated when the model top is set far above from the region of interest or the advective effects are dominant in comparison to the vertical propagation of internal gravity wave energy. Otherwise this condition has the undesirable effect of reflecting vertically propagating waves. Reflection does not allow the wave energy to exit the model domain; reflection traps the waves in the domain where they can erroneously interact with other waves.

To overcome this flaw, other kinds of upper boundary conditions have been developed to avoid wave reflection at the upper boundary. Among them, the radiation boundary condition proposed by Klemp and Durran (1983) has been applied to a number of climate models and mesoscale models. This condition permits internal gravity waves to exit the domain, and is more physically based. However there are some constraints when it is applied. First, it must be applied spectrally. It is difficult to employ in more

generally applied numerical models because the vertical wavenumber and frequency of the radiated waves must be specified. Second, it also requires a relatively deep model domain so that the vertical radiation of gravity wave energy is of secondary importance at the model top, otherwise the spurious momentum flux is not negligible (Klemp and Durran, 1983).

Another prominent scheme is the absorbing upper boundary condition. It is designed to damp out the vertically propagating waves within an upper boundary buffer zone before they reach the top boundary by using smoothing, filtering or some other approach, such as adding frictional terms to model momentum equations.

Previous studies show that the radiation and absorbing upper boundary conditions reduce the wave reflection to a great extent, however little work has been done to investigate how they perform over those areas with steep slopes. The Antarctic continent has high and steep terrain. Internal gravity waves induced by topography are stronger than over relatively flat regions. Therefore the model top should be set higher and the absorbing factor should be stronger in order to damp out the strong internal gravity waves. The radiation and absorbing upper boundary conditions are anticipated to have less effect on reducing wave reflection when they are applied to Antarctica without any modification.

For the radiation upper boundary condition, Klemp and Durran (1983) suggested truncation of the radiation condition at the small-wavenumber end. The cutoff wavenumber is determined using a reasonable estimate for  $\omega$ . However, because this radiation condition is derived for pure hydrostatic gravity waves (ignoring the Coriolis forcing), the assumption used in this upper boundary condition may be no longer valid over Antarctica where the internal gravity-inertia waves which propagate upwards are very strong due to

---

<sup>1</sup> Corresponding author address: Helin Wei, Byrd Polar Research Center, 1090 Carmack Rd., Columbus, OH 43210; email: hwei@polarmet1.mps.ohio-state.edu

steep topography and strong Coriolis forcing. Therefore the approach to reduce the cutoff wavenumber cannot fully solve the problems caused by the radiation upper boundary condition.

Raising the model top must be limited as a result of constraints in computer resources. Moreover when the model top is set within the stratosphere, the interaction between troposphere and stratosphere has to be considered in the model physics. This interaction may be important for climate simulation but causes extra complexity for weather prediction. Therefore increasing absorbing factor should be a promising approach to solve the upper boundary condition problem in the Antarctica. However as implied by the results of Morse (1973) increased filtering cannot be applied abruptly at some selected distance from the boundary because erroneous reflection back into the internal model will result. As Pielke (1984) pointed out, both insufficient damping and excessive damping in the absorbing layer will cause reflection. In addition, an absorbing layer whose depth is greater than the vertical wavelength of the mesoscale disturbance is required.

In this study, a new nudging upper boundary is designed. The large-scale forcing is nudged to the model simulation with an exponential function within absorbing upper boundary layers. In this way smoothing and filtering increase more gradually from the bottom absorbing layer to the model top. Considering its baroclinic feature in the tropopause and the lower stratosphere, only the temperature field is applied to this condition, and winds can be adjusted freely according the model physics. A mesoscale model is applied to simulate the synoptic and mesoscale evolution of the atmospheric state over Marie Byrd Land and Siple Coast, West Antarctica, for 9-14 October 1995, using several schemes for upper boundary conditions. Global Positioning System / Meteorology (GPS/Met) soundings are adopted to validate model results.

## **2. Model description and experimental design**

The model used in this study is Polar MM5, Version 2. It is a version of the Fifth Generation Pennsylvania State University/ National Center for Atmospheric Research (PSU/NCAR) Mesoscale Model (MM5) specifically adopted for polar regions (Bromwich et al, 2001). The main modifications in the Polar MM5 allow for a better representation of the cloud cover and radiative fields over extensive ice sheets than the standard MM5. The ice nuclei concentration equation (Meyers et al., 1992) is implemented in the explicit microphysics

parameterization of the Polar MM5. The cloud ice and water content predicted by the explicit microphysics parameterization is now used to determine the radiative properties of clouds in the NCAR Community Climate Model, Version 2 (CCM2) radiation parameterization. Two additional substrate levels (which increase the substrate depth to 1.91 m, compared to 0.47 m in the unmodified version) are added to the multi-layer soil model proposed by Dudhia (1996). A final modification to MM5 is the addition of variable fraction sea ice surface type. This surface type allows a fractional sea ice cover to be specified for each oceanic grid point in the model domain. The surface fluxes for sea ice grid points are calculated separately for the open water and sea ice portions of the grid points and averaged before interacting with the overlying atmosphere.

For the simulations discussed in this extended abstract, the Polar MM5 is used with the nonhydrostatic option. The simulation period is chosen as 9-14 October 1995. During this period a number of synoptic scale low pressure systems crossed the Marie Byrd Land coast and moved inland over West Antarctica. The initial and boundary conditions are generated by ECMWF TOGA data [European Centre for Medium-Range Weather Forecasts (ECMWF) Tropical Ocean-Global Atmosphere (TOGA)]. Figure 1 shows the model domain and topography. It includes 121x121 grid points at the horizontal resolution of 60km. There are 28 full vertical sigma levels.

Eight experiments have been designed for this study, each using a different upper boundary scheme (Table 1). The model top is set to 100 hPa for the first three experiments and 10 hPa for the other five. In standard MM5, the truncated wavenumber for the radiation condition is 6. As mentioned in the first section, in order to eliminate the spurious momentum flux generated at the model top, the wavenumber should be truncated at the small end over the Antarctic. So in Experiment Wave3 the truncated wavenumber for the radiation boundary condition is 3. The procedure that is used in Experiment Asm is a simple (Shapiro) filtering with gradually decreasing strength from complete four-point smoothing at the top to no additional smoothing at level six. The damping is applied to temperature, wind and specific humidity fields. The Rayleigh frictional term is added to the momentum equations in the upper 5 model layers. The frictional coefficient increases with height. In Experiment Nudge, the relaxation lateral boundary condition proposed by Davies and Turner (1977) is revised as a upper

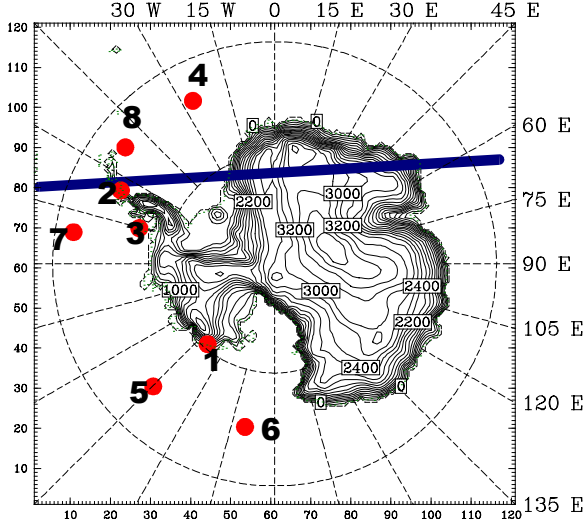


Fig. 1. Model domain and topography (Red Dots are GPS/Met points and the blue line is for cross-section discussed later).

Table 1. Experiments

| Experiment | Upper Boundary Condition | Model Top (hPa) | Description                             |
|------------|--------------------------|-----------------|---|
| Control    | radiation                | 100             | truncated WN=6                          |
| Wave3      | radiation                | 100             | truncated WN=3                          |
| Lid        | rigid lid                | 100             |   |
| Rad10      | radiation                | 10              | truncated WN=6                          |
| Lid10      | rigid lid                | 10              |   |
| Asm        | absorbing                | 10              | smoothing u,v,t,q at up 5 layers        |
| Afri       | absorbing                | 10              | Adding rayleigh friction at up 5 layers |
| Nudge      | nudging                  | 10              | exponential function for top 8 layers   |

boundary condition. The temperature tendency in the upper 8 model layers is given as follows:

$$\left(\frac{\partial \alpha}{\partial t}\right)_n = F(n)F_1(\alpha_{LS} - \alpha_{MC}) - F(n)F_2\Delta_2(\alpha_{LS} - \alpha_{MC}) \quad n=1,2,\dots,8 \quad (1)$$

where  $\alpha_{LS}$  is a large-scale value, and  $\alpha_{MC}$  is a model solution value.  $N=1$  is the model top level. We have changed  $F$  from a linear function to an exponential function so the nudging decreases more gradually from the top boundary to the bottom of the buffer zone:

$$F(n) = e^{-\frac{n+3}{9-n}} \quad n=1,2,\dots,8 \quad (2)$$

where  $F_1$  and  $F_2$  are given by:

$$F_1 = \frac{1}{10\Delta t} \quad (3)$$

$$F_2 = \frac{\Delta s^2}{50\Delta t} \quad (4)$$

where  $\Delta t$  is the time step and  $\Delta s$  is model horizontal resolution.

### 3. Results

#### 3.1 Temperature Sounding

Figure 1 shows eight GPS/Met points whose observed time is just within one hour from our model simulation output times. The first three points are located over the continent and the other points are over the ocean. Point 8 is close to the coast. Figure 2 depicts the vertical temperature soundings for the GPS/Met occultations and the 8 simulation experiments. The values of the model simulation are interpolated to the GPS/Met height coordinate. In general the model simulation has a good agreement with GPS/Met occultations in the lower and middle troposphere. Over those areas far from the coast, where it is nearly impossible for the internal gravity waves to be generated by terrain (such as points 4, 5 and 6), there is less difference among experiments. Even at the model top the various schemes simulate temperature in good agreement with GPS/Met. The largest differences are found at the model tops for those simulations over the continental Antarctic or the ocean close to the coast, where strong internal gravity waves are generated by the topography. Experiments Control and Wave3 produce the worst results, though the latter makes some improvements as a result of the reduced cutoff wavenumber.

When the model top is raised from 100 hPa to 10 hPa, the model generates a more reasonable temperature profile. There is not too much difference between Experiment Lid10 and Experiment Afri, which indicates that the frictional coefficient used in Experiment Afri may be too

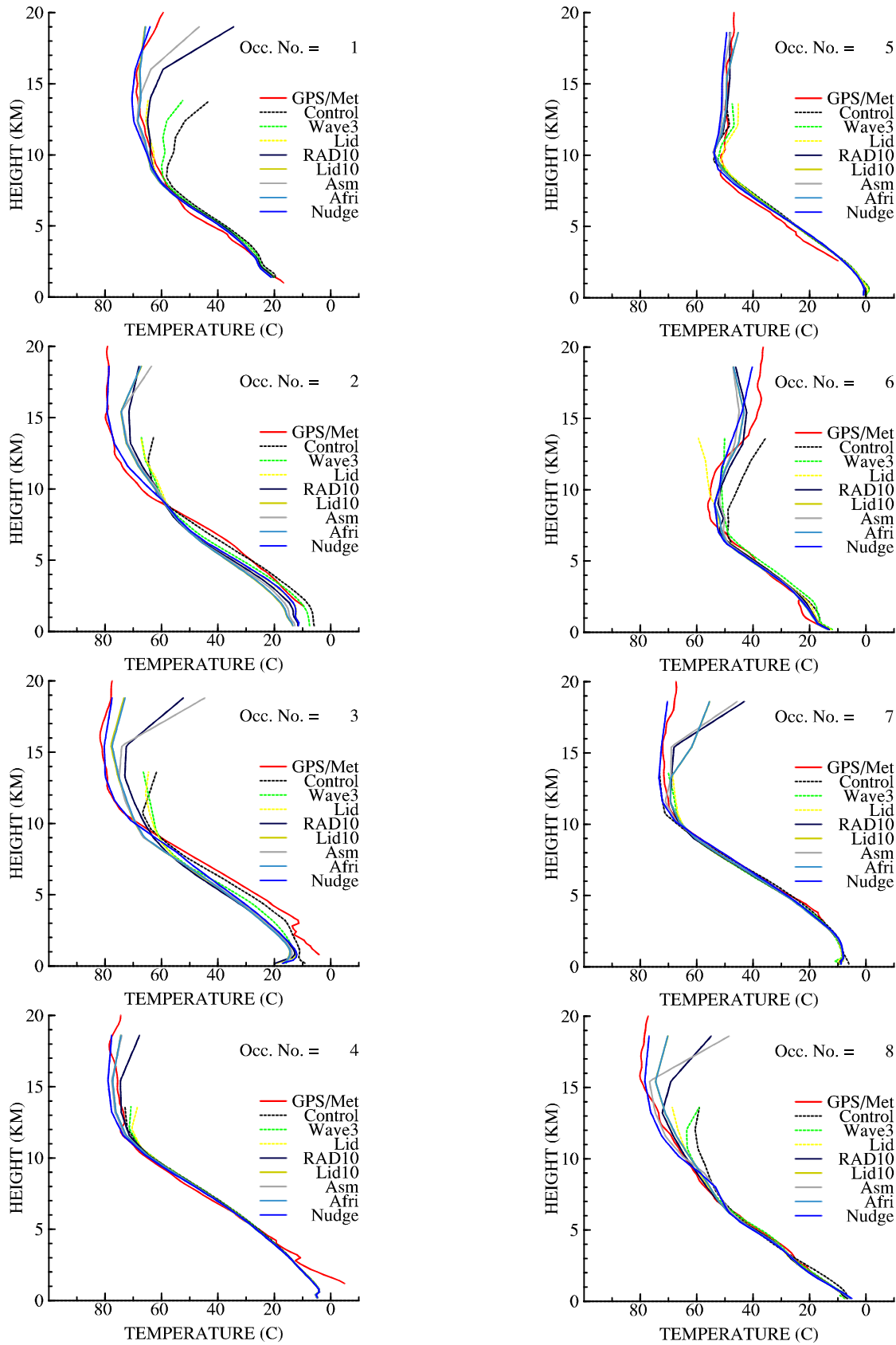


Fig. 2 Temperature Sounding

small. From the profiles over points 3, 7 and 8, the temperature linearly increases with the height for Experiment Asm. This implies that there are some wave reflections from the upper boundary in this case. One of the possible reasons may be that the smoothing coefficient is not used properly in this experiment. It is clear to see that Experiment Nudge produces the best temperature profile for most of the cases.

### **3.2 Sea level pressure**

Figure 3 depicts the difference of sea level pressure between model simulations and ECMWF/TOGA data, averaged over the whole simulation period. The left panel is for the control run (Experiment Control) and the right panel is for Experiment Top10. It is found that raising the model top from 100 hPa to 10 hPa has reduced the biases significantly. Only slight further improvement is found in Experiment Nudge compared with Experiment Top10.

### **3.3 Upper level jet and 500 hPa geopotential height**

The 6-day mean wind velocity at 200 hPa (not shown) implies that the control run underestimates the magnitude of the upper level jet by as much as 10 m/s. The vertical cross sections (along the line shown in Fig. 1) of wind at 00 UTC, 9 October 1995 are presented in Fig. 4. The location of the upper level jet is near 250 hPa in the ECMWF/TOGA data (Fig. 4a), while it is simulated 50 hPa lower in the control run, and the magnitude is 5 to 10 m/s lower than ECMWF/TOGA data. Both Experiment Top10 and Experiment Nudge get the correct location of the jet, but the magnitude in Experiment Nudge is closer to analysis data.

The root mean square difference (RMSD) of geopotential height at 500 hPa between the model simulation and ECMWF/TOGA data is shown in Fig. 5. For the first three experiments, with 100 hPa as model top, the RMSD is larger than the other 5 experiments. Experiment Nudge produces the smallest RMSD.

### **3.4 Wave reflection**

Maddox's (1980b) band-pass filter, based on Barnes's scheme, is applied to the vertical velocity. It is found that that with the radiation boundary condition the large scale waves can pass through the boundary unreflected, however

for the scale of internal gravity-inertia waves (< 1000 km), there are some reflections when they reach the upper boundary. The same reflections are also found for rigid lid and absorbing upper boundary condition schemes, even for longer scale waves. However, less wave reflection has been found in Experiment Nudge when nudging the upper boundary condition with the exponential function.

## **4. Conclusion**

In this study the effects of upper boundary conditions on mesoscale modeling over the Antarctic have been investigated. It is found that:

- 1) Because the Antarctic has high and steep terrain which easily generates internal gravity waves, the model top should be set relatively high so that the model has enough space to damp these waves before they propagate to the upper boundary. Otherwise there are some wave reflections near the upper boundary which can lead to large biases in temperature, wind and sea level pressure.
- 2) Further raising the model top is at the expense of computational resource. The alternative approach to solve the wave reflection at the upper boundary is to find some smoothing and filtering to damp out the internal gravity waves. The strength of damping should be dependent on the strength of the propagating waves. The reflection will be generated if the damping is too strong or too weak. The scheme which nudges the upper boundary with proper damping is demonstrated to be promising for solving the wave reflection problem in the model top over those areas with complex and steep terrain such as Antarctica.
- 3) The current radiation upper boundary in MM5 is derived for pure hydrostatic gravity waves without considering Coriolis forcing. The assumption used in this upper boundary condition may be no longer valid over Antarctica, where the internal gravity-inertia waves propagated upwards are very strong due to steep topography and a strong Coriolis forcing.

## **5. Acknowledgements**

This work was supported by NASA grant NAG5-9518.

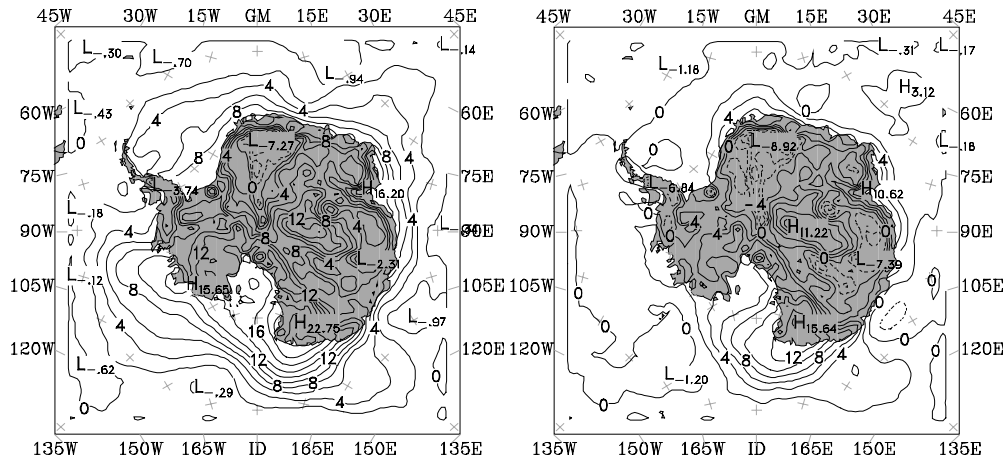


Fig. 3. Sea level pressure difference (hPa) for (a) Experiment Control and (b) Experiment Top10.

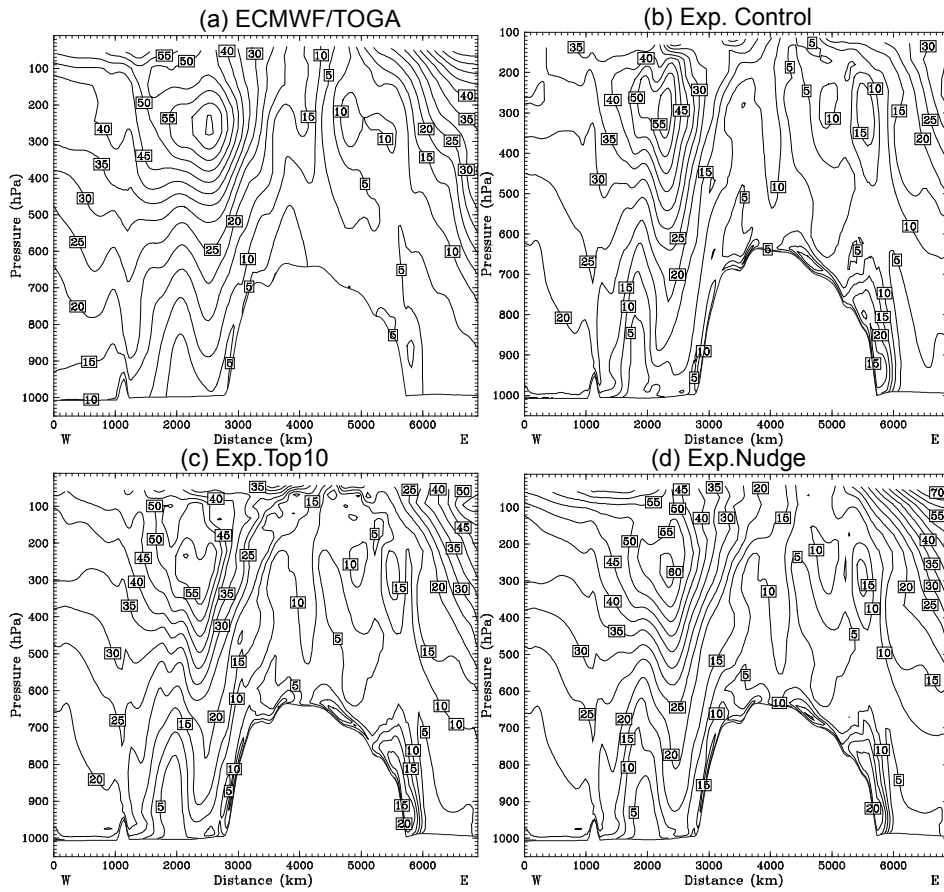


Fig. 4. Vertical cross section of wind

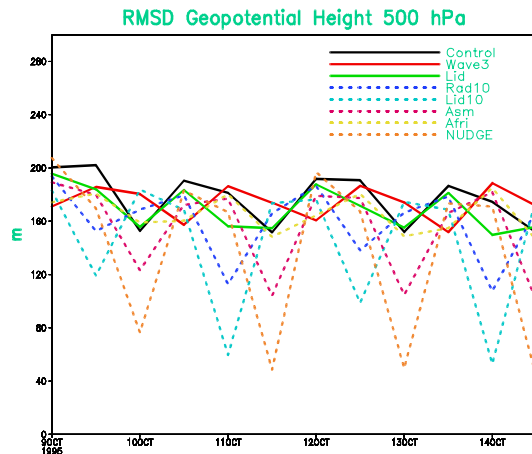


Fig. 5. RMSD of geopt. height at 500 hPa

### References

Bromwich, D.H., J.J. Cassano, T. Klein, G. Heinemann and K. M. Hines, 2001: Mesoscale Modeling of Katabatic Winds over Greenland with the Polar MM5. *Mon. Wea. Rev.*, **129**, 2290–2309.

Davies, H.C., and R.E. Turner, 1977: Updating prediction models by dynamic relaxation: An examination of the technique. *Quart. J. Roy. Metero. Soc.*, **203**, 225-245.

Dudhia J., 1996: A multi-layer soil temperature model for MM5. Preprints, MM5 Users' Workshop, Boulder, Colorado.

Klemp, J.B., and D.R. Durran, 1983: An upper boundary condition permitting internal gravity wave radiation in numerical mesoscale models. *Mon. Wea. Rev.*, **111**, 430-444.

Maddox, R.Z., 1980: An objective technique for separating macroscale and mesoscale features in meteorological data. *Mon. Wea. Rev.*, **108**, 1108-1121.

Mesinger, F., 1997: Dynamics of limited area models: Formulation and numerical methods. *Meteorol. Atmos. Phys.*, **63**, 3-14.

Meyers, M.P., P.J. Demott, and W.R. Cotton, 1992: New primary ice-nucleation parameterization in an explicit cloud model. *J. Appl. Meteor.*, **31**, 708-721.

Morse, B.J., 1973: An Analytical Study of Mesh Refinement Applied to the Wave Equation. NOAA Technical Memorandum WMPO-5, August 1973.

Pielke, R.A., 1984: Mesoscale Meteorological Modeling. Academic Press.

## NOAA/ETL STUDIES IN CONDITIONS RELATED TO THE PROPOSED ROSS ISLAND METEOROLOGY EXPERIMENT (RIME)

P. Ola G. Persson\*

Cooperative Institute for Research in Environmental Sciences/NOAA/ETL, Boulder, CO

### 1. Introduction

The Ross Island Meteorology Experiment (RIME) plans to study the synoptic and mesoscale phenomena along a high-latitude, steep and complex coastline (RIME Workshop Guideline, <http://www-bprc.mps.ohio-state.edu/>). A key component of RIME is model validation and improvement of physical parameterizations. The Ross Island region is impacted by vigorous storms approaching from the northwest, air-sea interaction over the Ross Sea, air-ice interactions over the Ross Ice shelf, topographic forcing near the coastline, and katabatic flow and other influences from the Antarctic interior. In short, the meteorology of the region is complex and affected by a large variety of physical processes ranging from the continent-scale, to the local scale. Some of the phenomena that will be encountered near Ross Island are likely similar to those measured and documented elsewhere in polar or coastal environments.

NOAA's Environmental Technology Laboratory (ETL) has made atmospheric measurements at the South Pole and during several Arctic research programs. The Arctic programs include the Lead Experiment (LeadEx92) in the Beaufort Sea (March –April 1992), the Surface Heat Budget of the Arctic Ocean (SHEBA) project in the Beaufort and Chukchi Seas (Oct. 1997-Oct. 1998; Perovich *et al.* 1999), and the Arctic Ocean Expedition near the North Pole (July - Aug, 2001). Wintertime coastal studies of landfalling storms have been done along the U.S. West Coast in the California Landfalling Jets Experiment (CALJET, 11/97-3/98) and the Pacific Landfalling Jets Experiment (PACJET, Jan-Feb, 2001) (Ralph, *et al.* 2001). Some of the significant physical processes and phenomena observed during these field programs and likely relevant to RIME will be presented in this paper. Lessons learned from the measurement methodology, data analysis, and numerical modeling of the processes and

phenomena will be discussed, including measurement omissions in these programs. The capabilities of various surface-based remote sensors for deployment in polar regions was reviewed by Neff and Gottas (Cassano and Everett 2000).

### 2. SHEBA

The SHEBA field program was conducted on a drifting, multi-year ice floe many hundreds of kilometers from land. The floe was initially well within the Arctic pack ice, but its track and the strong subsequent melt placed it fairly close to the marginal ice zone by the end of the following summer. The conditions at SHEBA are probably most like conditions over the Ross Sea and away from the Antarctic continent. Hence, they might represent upwind conditions for the Ross Island area. The main objectives of SHEBA included measuring all parameters affecting the surface energy budget in a column from the ocean, through the ice/snow and into the atmosphere, and using these to improve global climate model representations of the Arctic environment. These measurements included oceanic turbulent fluxes, snow and ice mass balance measurements, snow and ice macroscale and thermodynamic properties, all surface energy budget terms, atmospheric turbulent fluxes, cloud macroscale and microphysical properties, and the general atmospheric kinematic and thermodynamic structure.

#### 2.1 Cloud measurements

Cloud macrophysical measurements (cloud boundaries, heights, layering, presence of liquid or not) were derived from ETL's K-band cloud radar and DABUL lidar due their complimentary signal properties (Fig. 1). These measurement have provided an annual cycle of observations important for climate studies (Intrieri, *et al.* 2001a), and have also provided valuable data for use in physical process studies. The year-long cloud fractions indicate that clouds were even more prevalent than previous climatologies suggested, and that liquid phase clouds occurred in shallow layers at temperatures below  $-30^{\circ}\text{C}$ . In December

\*Corresponding author address: Dr. Ola Persson, R/ET7, NOAA/ETL, 325 Broadway, Boulder, CO 80305; [ola.persson@noaa.gov](mailto:ola.persson@noaa.gov)



and January, 30% of the clouds contained layers of liquid water, as did 80% of the clouds in August. For the Ross Island region, the detection of layers of supercooled liquid water would be extremely important for 1) nowcasting and forecasting for aircraft operations, and 2) the understanding of cloud formation, precipitation, and radiation processes.

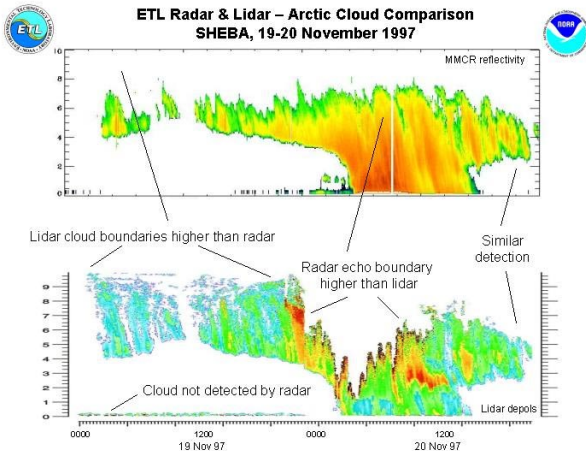


Fig. 1. Time-height sections of a) cloud radar reflectivity and b) lidar depolarization ratio from the SHEBA site. The two instruments yield different measurements and are complimentary (from Intrieri et al, 2001a)

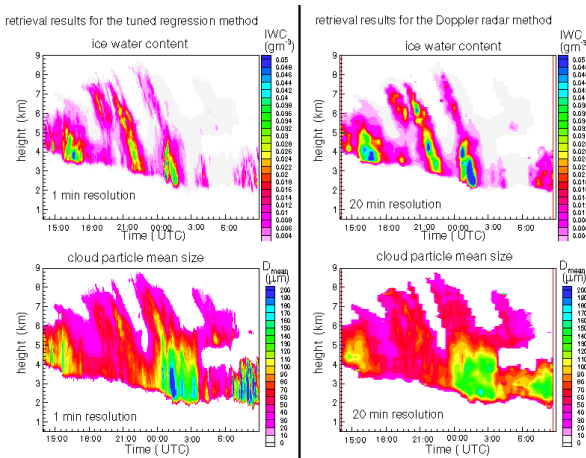


Fig. 2. Ice water content (a, b) and cloud particle mean diameter (c, d) retrieved from a multi-spectral, multi-instrument method (a,c) and from a cloud-radar-only retrieval technique (b,d) (from Matrosov et al 2000).

Cloud microphysical properties have been derived from the cloud radar, lidar, and microwave radiometer measurements. By the use of various multi-spectral, multi-instrument, retrieval techniques, cloud ice water content, liquid water content, and mean particle diameters have been

derived (Fig. 2; Matrosov et al 2001). These retrievals are being validated with aircraft measurements, showing mostly successes of the techniques. The retrievals will be useful for input to radiative transfer models and for validating microphysical parameterizations in mesoscale models.

## 2.2 Surface measurements and physical processes

The Atmospheric Surface Flux Group (ASFG), including ETL, maintained a site at the main SHEBA ice camp. At this site, turbulent fluxes of sensible heat, latent heat and momentum were measured with sonic anemometers at 5 levels on a 20-m tower. Mean winds, temperature, and humidity were also obtained. In addition, measurements of the 4-component broadband, radiative fluxes were made on a smaller mast. Various devices to measure surface temperature, a sodar, two precipitation gauges, and a scintillometer were also deployed. Snow and ice temperature profiles, mass balance measurements, and surface albedo transects were done nearby. The annual cycle of the surface energy budget and the atmospheric surface-layer structure at this site has been documented (Persson et al 2001).

Although SHEBA focused on the annual cycle of the various surface energy budget terms, the analyses have clearly shown the importance of synoptic and mesoscale events for determining the annual cycle and for triggering transitions between major seasonal regimes. As an example, the surface measurements combined with rawinsondes and the cloud observations show the significance of short-term cloud forcing for the near surface environment (Persson et al 1999). Large (6-18°C) wintertime thermal transitions occurred approximately every fourth day, and were due primarily to longwave radiative effects from shallow clouds produced near the top of the Arctic inversion by synoptic or mesoscale disturbances (Fig. 3). Because the radiative flux allows the atmosphere to tap the large thermal gradient of the Arctic inversion, the change in surface temperature with each event is much greater than the change in temperature associated with the disturbance at the top of the inversion. That is, when it becomes cloudy, the surface quickly attains radiative equilibrium with the cloud near the top of the inversion, as seen by the near-zero surface net longwave flux. An important aspect is that the cloud with a temperature of -15 - -25°C, contains layers of liquid water giving it an emissivity near 1.

Each warming event is also associated with a pressure check (not shown), and half of these pressure checks are only a few millibars,

suggesting a significant contribution from mesoscale disturbances. These intermittent warming events force responses in the atmospheric turbulent fluxes and surface conductive fluxes (Fig. 4). The surface sensible heat fluxes were near zero or positive during the warming events or strongly negative during the cold periods. Hence, surface-based mixed layers occurred 25% of the time during the winter. Conductive fluxes produced temperature increases to depths of 1 m in the ice with these events.

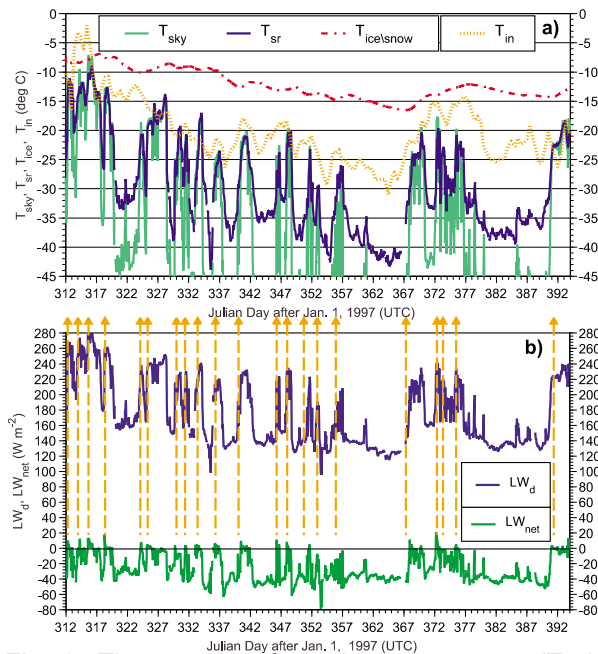


Fig. 3. Time series of a) sky temperature ( $T_{sky}$ ), surface temperature ( $T_{sr}$ ), ice/snow interface temperature ( $T_{ice/snow}$ ) and the air temperature in the upper portion of the Arctic inversion ( $T_{in}$ , and b) the incoming ( $LW_d$ ) and net ( $LW_{net}$ ) longwave radiation at the surface. The vertical dashed arrows mark the warming events.

Using these measurements on a longer time-scale along with a radiative transfer model, the cloud forcing on the terms of the surface heat budget during the course of the SHEBA year was evaluated (Intrieri et al 2001b). The result is that clouds act to warm the ice surface during the entire year, except for a few weeks after the summer solstice. That is, the ability of clouds to trap longwave radiation is more important to the surface energy budget than is their ability to reflect shortwave radiation.

The mean neutral drag coefficient ( $C_D$ ) over all levels at the 20-m tower has been estimated to be  $1.5 \times 10^{-3}$ , but the measurements have revealed vertical and temporal variations (Andreas et al,

2001; Persson, et al, 2001). The vertical variations indicate that the surface roughness of the larger "footprint" of the top level was a factor 2 greater than that of the bottom level. This makes sense, as the tower was sited on a relatively smooth ice floe, but the ice surface became rougher at 1-2 km distance in the predominant wind direction. The year-long series of monthly averages indicates that  $C_D$  increased slowly from  $1.1 \times 10^{-3}$  to  $1.5 \times 10^{-3}$  during the winter, probably due to snow ridging from drifting snow. In May,  $C_D$  increased more rapidly, peaking at a value of  $1.9 \times 10^{-3}$  in August. This summer increase is probably explained by the formation of abrupt edges as leads and meltponds developed.

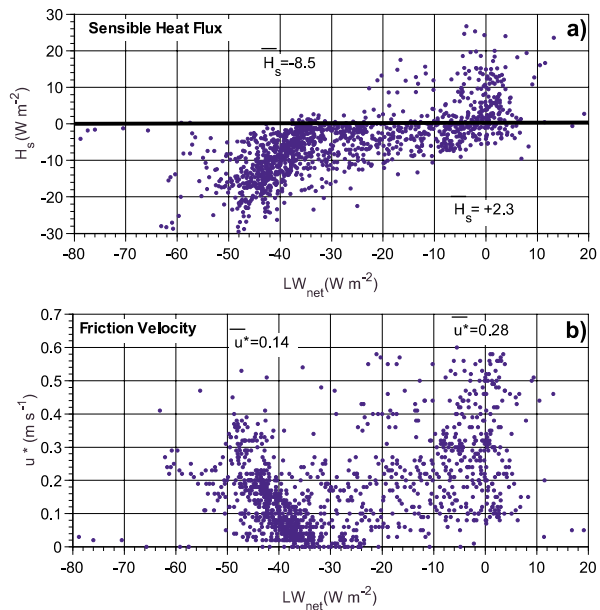


Fig. 4. Scatter plot of hourly  $LW_{net}$  versus a) sensible heat flux ( $H_s$ ) and b) friction velocity ( $u^*$ ) for the Arctic night. The mean values of each for the cold and warm regimes are marked at their corresponding  $LW_{net}$  values of  $-40 \text{ W m}^{-2}$  and  $0 \text{ W m}^{-2}$ , respectively.

The apparent effects of gravity waves on the sonic anemometer cospectra have forced us to reprocess the turbulence data. Instances of spectral peaks occurring at the low-frequency end of the cospectra (periods of 3-13 min) have been noted, with near-zero contributions from the high-frequency portions. Removal of these non-similarity effects tends to remove negative surface stresses under highly stable, weak wind conditions and produce more consistent flux profiles. As a result, we expect that our planned improvement of flux parameterizations will encounter less uncertainty due to data scatter. Future studies

should reveal how prevalent these gravity waves are, if they make an important contribution to the surface fluxes, and, if so, how best to parameterize their effects. These issues may be important for modeling the environment of the Ross Island environment and the Antarctic interior.

The near-surface environment over the Arctic pack ice in SHEBA was observed to be near ice-saturation during nearly the entire year (Andreas, et al 2001). With the use of some simple models, we have suggested that this is due to the moisture flux from open leads combined with the strong radiative cooling over the ice. This fact has direct logistical consequences. Riming on instruments occurs frequently, as do low-level clouds and diamond dust. Additionally, humidity sensors are notoriously inaccurate in a cold, near-saturated environment, often unable to discriminate between unsaturated, saturated, and supersaturated conditions. Sensors should be chosen with care and calibrated carefully. Post-experiment cold chamber tests suggest that our Vaisala HMP235 probes performed best of the sensors deployed, though further tests are needed to determine if they were able to consistently discriminate between saturated and supersaturated conditions. This problem needs to be considered over the Ross Sea.

### 2.3 Relevant modeling results

ETL has begun modeling the pack ice environment at SHEBA using the Penn State/NCAR Mesoscale Model (MM5) with modifications for the Arctic. Because the lack of boundary-layer vertical resolution has been shown to be a problem for operational models in the Arctic (Bretherton et al, 2001) and because the focus of the modeling is on boundary-layer processes, our version uses over 30 levels below 1.5 km. In tests, the RRTM (Mlawer, et al 1997) radiation scheme has been shown to produce better downwelling long wave radiation ( $LW_d$ ) than the Dudhia (1989) scheme (Table 1 and Fig. 5a). Tests are currently being done on the requirements for the boundary-layer scheme. Surface-flux parameterizations are obviously an issue, as is the method for vertical redistribution of the boundary-layer constituents.

It has been found that the treatment of the lower boundary over the pack ice has greater impact on the simulations of the near-surface temperature than does choosing between PBL schemes (Table 1 and Fig. 5b). A surface model consisting of realistic, multi-layer representation of both the ice and the snow is necessary, with a thin (e.g., 5 cm) top snow layer. With thicker surface

Table 1. Longwave radiation, surface model configuration and boundary layer parameterization for five SHEBA wintertime MM5 simulations.

| Exp.      | LWRAD              | SURFACE   | PBL                  |
|-----------|--------------------|---|----------------------|
| HIRES     | Dudhia (1989)      | 5-layer ice, (30 cm each)                               | Blackadar            |
| RRTM      | RRTM (Mlawer 1997) | 5-layer ice, (30 cm each)                               | Blackadar            |
| "2.24e-7" | RRTM               | 5-layer snow, (30 cm each)                              | Blackadar            |
| 3snw      | RRTM               | 3-layer snow (5, 10, 15 cm)<br>2-layer ice (30 cm each) | Blackadar            |
| bt_3snw   | RRTM               | 3-layer snow (5, 10, 15 cm)<br>2-layer ice (30 cm each) | Burk-Thompson (1989) |

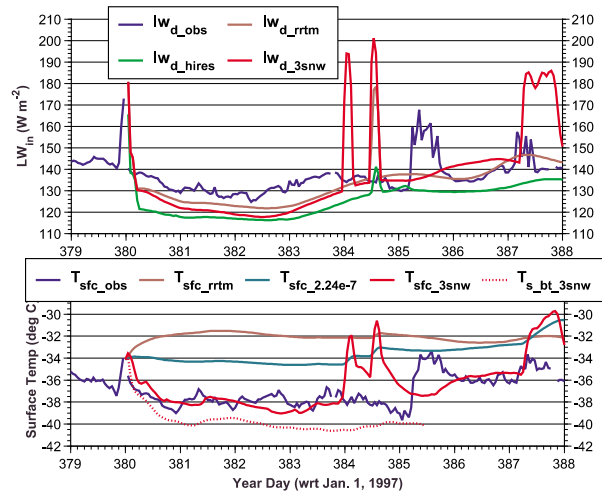


Fig. 5. Observed and modeled a) incoming longwave radiation and b) surface temperature for a January week at the SHEBA site.

layers, the surface and lower atmospheric response to cloud-forcing events, indicated by the spikes in  $LW_d$ , is significantly damped. The errors in timing are due to other problems and should be ignored.

Finally, the modeling work at ETL has shown the value of carefully selecting simple cases to isolate individual parameterizations, and the necessity of validating individual flux terms or processes rather than net fluxes or results of a sequence of processes. For example, obtaining an improved incoming long wave radiation using the RRTM scheme increased the error in the

surface temperature and appeared at first glance to be a deleterious change. However, this error was then corrected by improving the surface snow and ice model.

#### **2.4 Lessons learned**

At least two measurement omissions have caused difficulties in the analyses of SHEBA data. The first is the lack of spatial observations of atmospheric structure. Much of the SHEBA model physics development is being done with single-column models, which require the knowledge of the advective component of a specific parameter. In SHEBA, the advective components were determined from operational ECMWF runs, which were saved for the column over the SHEBA site. Relying on these model-derived advections are causing significant difficulties in validating single-column models because the errors in the ECMWF horizontal advections are often as large or larger than the tendencies from the physical parameterizations in the single-column models (Pinto, et al 2001). In hindsight (which is of course 20-20), an array of rawinsondes centered on the SHEBA site would have made the post-analysis much easier, but was deemed to be too expensive and difficult to deploy and maintain during the SHEBA field program. Such an array would also have provided better synoptic and mesoscale context for the observed local-scale phenomena.

A second omission during SHEBA is the lack of aerosol profile measurements. The radiative transfer models that are being tested with the SHEBA data require an aerosol input. For short wave radiation and even for long wave radiation during the dry Arctic winter, the uncertainties in aerosol concentrations can produce errors of 10's of  $W/m^2$ , comparable to or larger than differences between various radiative transfer models. In addition, the lack of ice condensation nuclei at SHEBA inhibits the understanding of conditions with possible large supersaturations during the winter.

#### **3. LeadEx92 and AOE-2001**

For LeadEx92, the effects of leads on the springtime, pack-ice environment were measured with basic meteorological instrumentation, sonic anemometers, minisodars, and portable sounding units (Ruffieux, et al 1995). The results showed measurable but small temperature effects downwind of a 100-m wide lead, but large sensible heat flux effects. The effects on the surface sensible and latent heat fluxes continued even after ice started forming over the lead. The

enhanced turbulence was noted to 60 m height with the minisodar. Over a multi-year ice floe away from the leads, monthly averages of momentum and sensible heat flux transfer coefficients were obtained. The importance of synoptic events for modulating the surface turbulent fluxes, and the surprisingly large springtime diurnal temperature and stability cycle were also noted during this experiment and reemphasized in the SHEBA analyses.

In the Arctic Ocean Expedition-2001, ETL's main objective was to obtain high temporal resolution measurements (10-min or less) of the late summer Arctic boundary layer structure near the North Pole. These are needed to help interpret observations of large but intermittent changes in aerosol concentrations. Enhancements to the 6-hourly rawinsonde observations were obtained with a 915 MHz wind profiler and two Doppler sodars for wind measurements, a scanning 5-mm microwave radiometer (Westwater, et al 1999) for temperature profiles in the lowest 400 m, and a S-band radar for cloud detection. The University of Colorado also deployed a tethered balloon and kite system to measure the boundary layer thermal and kinematic structure. The deployment of this suite of sensors for boundary-layer measurements in the Arctic is unique. The use of a 915 MHz wind profiler was only justified because of the relatively warm summertime temperatures (higher absolute humidities), as they generally perform poorly in cold conditions [e.g., Neff and Gottas in Cassano and Everett (2000)]. No results are yet available from this field program, as it ended at the end of August, 2001.

#### **4. CALJET and PACJET**

A primary objective of CALJET and PACJET was to study the mesoscale structure of landfalling wintertime storms, documenting their interaction with the steep coastal topography leading to strong winds and heavy coastal precipitation. The studies focused on the low-level jet (LLJ). These programs have an operational component where the observations are disseminated to operational forecast offices for their use and evaluation. The observational platforms include an array of 915 MHz wind profilers along the coast and on offshore islands, the NOAA P-3 aircraft, a mobile sounding unit, and special and operational surface sites, including coastal buoys. A special microphysics array included collocated profilers, ceilometers and S-band Doppler radars at a coastal site and at a site in the downwind coastal

mountains. Two examples of observed phenomena will be presented. The first shows the modulation of frontal structure and precipitation by a barrier jet in the California Bight. The second shows gap flow producing a trapped barrier flow, leading to modulation of the coastal precipitation pattern.

The coastal region of the California Bight has steep orography, especially on its northern end where the Santa Ynez Mountains reach elevations of over 2000 m. As strong southerly winds developed with the approach of cold fronts from the west, significant low-level westward deflection of this flow occurs in the Santa Barbara Channel (Fig. 6). The depth of these barrier winds and the amount of turning can be determined by comparing the windprofiler wind directions at coastal stations along the northern bight with those at an offshore island (Fig. 7). The depth of the turning of the wind is near the minimum coastal mountaintop height of 1.1 km. The magnitude of the vector difference is 6-12 ms<sup>-1</sup> (not shown). This turned, low-level, front-perpendicular flow was observed to perturb the approaching front, producing waves along its length, and retarding its movement at low levels while the upper portion continued moving eastward (Fig. 6). The consequence of this

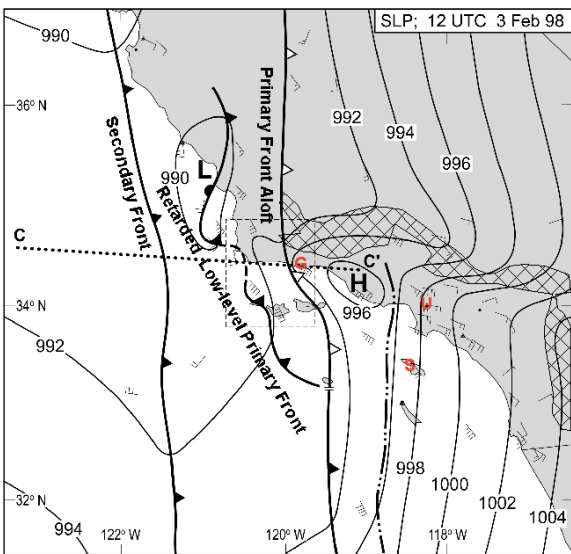


Fig. 6. Mesoscale analysis of sea-level pressure (thin solid) and the three main frontal features present at 12 UTC Feb. 3, 1998 in the California Bight. Surface barbs are shown. The dotted line c-c' shows the location of a cross-section to be presented at the workshop. The location of three profiler sites GLA (G), USC (U), and SCL (S) are shown in red, and the crucial region of terrain higher than 1000 m is cross-hatched.

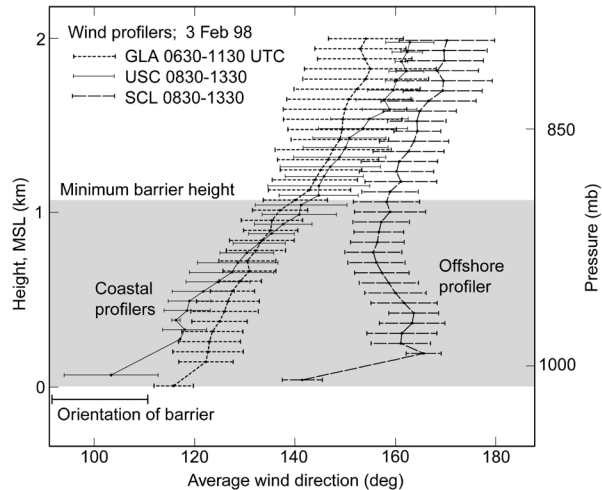


Fig. 7. Six-hour averages of wind direction in the prefrontal environment at the wind profiler sites along the coast (GLA and USC) and on an offshore island (SCL). The locations of these sites are shown in Fig. 6. The shading shows the minimum height of the mountain barriers just to the north of GLA and USC.

decoupling was a destabilization of the air ahead of the retarded low-level primary front because of the cooling behind the primary front aloft. Subsequently, as this air was lifted over the coastal mountains, strong convection with torrential rains was initiated, producing flash flooding. The eastward movement of the low-level jet ahead of the decoupled low-level portion of the front was slowed as well, contributing to the low-level upslope flow. Though deep convection isn't likely in the Ross Island region, similar turning of low-level flow, vertical decoupling, and frontal deformation and retardation are likely.

Along the central California coast north of San Francisco Bay, flow from the California Central Valley through a gap in the coastal mountains produces a region of lower potential temperature that is trapped against the coastal mountains further northwest (Fig. 8). This trapped flow is about 300-700 m deep. With southerly and southwesterly winds associated with landfalling fronts, the coastal lifting begins 50-80 km offshore rather than right at the coast. Hence, when this trapped, cooler, low-level flow is established, lifting is initiated far enough offshore to produce heavy precipitation at the coastal sites as well as in the mountains. When blocked flow isn't present, only the mountain site receives heavy precipitation. With the steep complex coastal orography with significant gaps near Ross Island, similar phenomena should be expected. In fact, the

events near Antarctica are likely to be much more extreme, as the air from the interior will be more stable with larger thermal gradients than that observed in California.

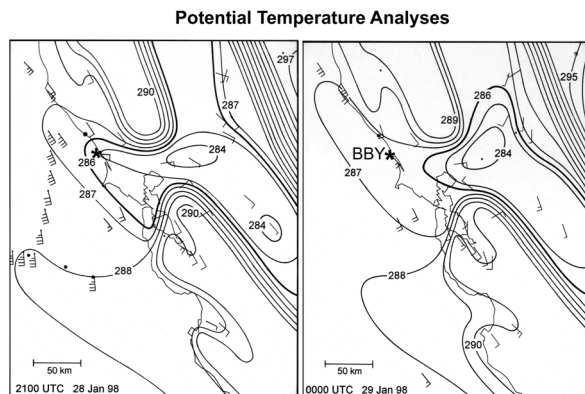


Fig. 8. Surface potential temperature along the central California coast at a) 21 UTC, Jan. 28 and b) 00 UTC Jan. 29, 1998. Also shown are the surface wind barbs at the coastal and buoy sites and, in a), the offshore 65 m winds as measured by the P-3 aircraft.

## 5. Conclusions

The physical process and mesoscale phenomena to be expected for RIME will likely have similarities to those measured by NOAA/ETL in other polar and mid-latitude regions of the world. However, significant differences will undoubtedly be observed. In RIME, the synoptic systems will likely be more vigorous than those seen over the Arctic regions because of the vigorous systems in the "Roaring 50's" of the southern hemisphere. In addition, the pack ice in the Ross Sea may have a different effect on the atmosphere than does the Arctic pack ice because of different ice characteristics. The frontal modification by the terrain was not an issue in the ETL Arctic measurements, and in RIME it will be more extreme than that observed in California because of the greater low-level stability and different scale of the topography. This should lead to different Froude numbers, and probably greater decoupling. Also, because of much greater cooling and altitude in the Antarctic interior, the impact of katabatic flows and gap flows should be at least greater if not different than observed along coastal California.

The determination of instrumentation and measurement strategies must consider both the similarities and differences in program objectives and physical processes between RIME and other

field programs. Hopefully, the examples presented here will be of help.

## Acknowledgements

I would like to express my appreciation to Sergei Matrosov, Taneil Uttal, Paul Neiman, Edgar Andreas, Jian-Wen Bao, and Sara Michelson for their contributions of work and figures used in this paper.

## References

- Andreas, E.L., C.W. Fairall, P.S. Guest, and P.O.G. Persson, 2001: The air-ice drag coefficient measured for a year over Arctic sea ice. *Preprint volume, Conference on Polar Meteorology and Oceanography*, San Diego, CA, 14-18 May 2001, pp. 300-303.
- Andreas, E.L., P. S. Guest, P.O.G. Persson, and C.W. Fairall, 2000: Near-surface water vapor over polar sea ice is always near ice saturation. *J. Geophys. Res.*, submitted.
- Bretherton, C.S., S.R. de Roode, C. Jakob, E.L. Andreas, J. Intrieri, R. E. Moritz, and P. O. G. Persson, 2000: A comparison of the ECMWF forecast model with observations over the annual cycle at SHEBA. *J. Geophys. Res.*, submitted.
- Burk, S.D., and W.T. Thompson, 1989: A vertically nested regional weather prediction model with second-order closure physics. *Mon. Wea. Rev.*, **117**, 2305-2324.
- Cassano, E. N., and L. R. Everett, Eds., 2000: *Antarctic Weather Forecasting Workshop*. Preprint Vol., Byrd Polar Research Center, Miscellaneous Series M-419, The Ohio State University, 108 pp.
- Dudhia, J., 1989: Numerical study of convection observed during the winter monsoon experiment using a mesoscale two-dimensional model. *J. Atmos. Sci.*, **46**, 3077-3107.
- Intrieri, J. M., M. D. Shupe, T. Uttal, and B. J. McCarty, 2001a: An annual cycle of Arctic cloud characteristics observed by radar and lidar at SHEBA. *J. Geophys. Res.*, In press.
- Intrieri, J., C. W. Fairall, M. D. Shupe, P. O. G. Persson, E. L. Andreas, P. S. Guest, and R. E. Moritz, 2001b: Annual cycle of cloud forcing at SHEBA. Submitted to *J. Geophys. Res.*
- Matrosov, S. Y., T. Uttal, A. J. Heymsfield, A. V. Korolev, and G. A. Isaac, 2000: Comparisons of remote and in situ measurements of cloud

- microphysical profiles in Arctic ice clouds. *Abstracts, Fifth International Symposium on Tropospheric Profiling*, Dec. 4-8, 2000, Adelaide, Australia.
- Mlawer, E. J., S. J. Taubman, P. D. Brown, M. J. Iacono, and S. A. Clough, 1997: Radiative transfer for inhomogeneous atmospheres: RRTM, a validated correlated-k model for the longwave. *J. Geophys. Res.*, **102(D14)**, 16,663-16,682.
- Perovich, D., and 22 others, 1999. Year on ice gives climate insights. *Eos, Trans., AGU*, **80** [41], 481-486.
- Persson, P. Ola G., C. W. Fairall, E. Andreas, and P. Guest, 2001b: Measurements near the Atmospheric Surface Flux Group tower at SHEBA Part II: Near-surface conditions and surface energy budget. *J. Geophys. Res.* Submitted.
- Persson, P.O.G., T. Uttal, J. Intrieri, C.W. Fairall, E.L. Andreas, and P.S. Guest, Observations of large thermal transitions during the Arctic night from a suite of sensors at SHEBA. *Preprints, Fifth Conf. On Polar Meteorology and Oceanography*, 10-15 Jan, Dallas, TX, Amer. Meteor. Soc., Boston, 306-309, 1999b.
- Pinto, J., and J. Curry, 2001: Evaluation strategies for conducting single column model experiments for SHEBA. Presentation at the *Conference on Polar Meteorology and Oceanography*, San Diego, CA, 14-18 May 2001.
- Ralph, F. M., D. Reynolds, O. Persson, W. Nuss, D. Kingsmill, Z. Toth, W. Blier, C. Velden, P. Neiman, A. White, J.-W. Bao, D. Miller, D. Jorgensen, J. McFadden, J. Dostalek, and S. Weygandt, 2001. Improving the understanding and prediction of heavy rain in land-falling Pacific winter storms: The CALJET and PACJET Experiments. *Preprints, Conf. on Precipitation Extremes: Prediction, Impacts, and Responses*, 14-19 January, Albuquerque, New Mexico.
- Ruffieux, D. R., P. Ola G. Persson, C. W. Fairall, and Dan E. Wolfe, 1995: Ice pack and lead surface energy budgets during LEADDEX 92. *J. Geophys. Res.*, **100**, C3, 4593-4612.
- Westwater, E., Y. Han, V. G. Irisov, V. Leuskiy, E. N. Kadyrov, and S. A. Viazankin, 1999: Remote sensing of boundary layer temperature profiles by a scanning 5-mm microwave radiometer and RASS: Comparison experiments. *J. Atmos. Ocean. Tech.*, **16**, 805-818.

# The University of Wisconsin Contribution to the Ross Island Meteorology Experiment (RIME)

Matthew Lazzara

Antarctic Meteorological Research Center  
Space Science and Engineering Center  
University of Wisconsin-Madison

## Abstract

With a goal for improving short term to medium range weather forecasting in Antarctica, the Ross Island Meteorology Experiment (RIME) offers an opportunity to demonstrate applications of weather observations from ground and space based platforms. The University of Wisconsin's Automatic Weather Stations (AWS) have served the United States Antarctic Program for over 20 years. This platform will provide critical ground truth, as well as raw observations needed for weather forecasting and experiment activities. As the Earth observing era matures during the next five to ten years, space based platforms will offer forecasters and modelers critical new products and data that maybe the key to improved forecasts. The University of Wisconsin's Antarctic Composite satellite images have offered an unparalleled view of the Southern Hemisphere for nearly nine years. The composites are only the tip of the iceberg for the potential applications of Antarctic satellite observations (e.g. cloud masking, cloud optical properties, etc.). In order to improve numerical weather prediction (NWP) and weather forecasting, it is necessary to ingest these different data streams into a data assimilation system. The inclusion of all weather observations will provide a valuable data set for NWP.

## Outline

### I. Automatic Weather Stations (AWS)

- a) History of AWS
- b) Next Generation AWS network and RIME

### II. Satellites and RIME Data Center and Data Visualization

- a) Historical use of satellite data in the Antarctic
- b) Satellite capabilities:
  - Fluxes, albedo, cloud amount, effective emissivity, cloud top pressure, cloud classification, cloud

masking, precipitable water, cloud drift and water vapor winds, etc.

- c) A RIME Data Center
- d) Data Visualization

### III. Data Assimilation

- a) Impact of data assimilation
- b) Antarctic Data Assimilation System (ADAS):
  - AWS, Raobs, Ship, Buoy, Synoptics, Satellite (ATOVS, MODIS/AIRS, COSMIC, etc.)
  - MM5, WARF, CRAS, RAMS (UW-NMS), etc.
  - Forecast sensitivity and adjoint model targeted observations

### IV. Summary

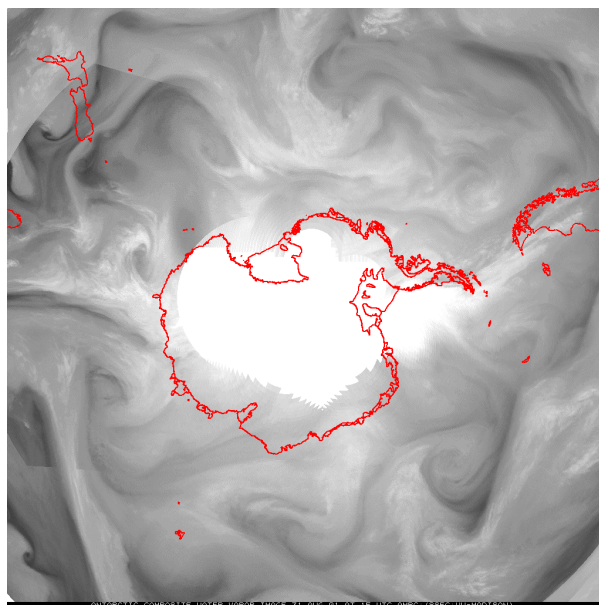


Fig. 1. A sample Antarctic composite water vapor (~6.7 microns) image from 31 August 2001 at 15 UTC using GOES-8, GOES-10, Meteosat-5, Meteosat-7, and GMS-5.



## Applications of Aerosondes for RIME

J.A. Curry, J. Maslanik, J.O. Pinto, S. Drobot, J. Cassano  
University of Colorado

G.H. Holland  
Aerosonde Robotic Aircraft

### 1. Aerosonde Overview

The Aerosonde is an inexpensive, long-endurance unmanned aerial vehicle (UAV) that is an ideal platform for conducting weather observations and scientific research in Antarctica. With endurance of over 30 hours, a single Aerosonde can obtain observations in regions that are inaccessible without expensive ships or manned aircraft. Because of the low cost of the Aerosonde, it can fly in regions that are deemed too dangerous for manned aircraft (such as at low levels under high-wind conditions). A wide variety of instruments are either presently available or scheduled for integration on the Aerosonde during the next few years.

Detailed information on the Aerosonde and its operations can be found in Holland et al. (2001) and at <http://www.aerosonde.com>. The Aerosonde (see Fig. 1) weighs 14 kg and has a wing span of 2.9 m. To date, individual flights have been made in excess of 3000 km and 30 h. The new fuel injected engine (which is undergoing testing in Arctic flights) will extend the duration to substantially. The altitude record of the aircraft is up to 20,000 feet with the new engine ([http://www.aerosonde.com/hamilton\\_2001.htm](http://www.aerosonde.com/hamilton_2001.htm)). To date, almost 3000 flight hours have been flown in operations.

The aircraft operates completely robotically, and can conduct a mission without any communications. However, communications are desirable for air safety issues, monitoring aircraft health, coordinating with other aircraft, and downloading data in real time. Communications to and from the Aerosonde are conducted using a combination of UHF radio and Low-Earth-Orbiting (LEO) satellites. The UHF radio operates in the "meteorological" band of 400-406 MHz, so that no special frequency permits are required. UHF communications are feasible up to a range of about 100 miles. Satellites enable communications over much greater distances than are feasible by radio. After waiting several years for the Iridium system to become operational, Aerosonde decided in early 2000 to initially go with

ORBCOMM to enable both initial flight operations and gain experience with satellite communications. Aerosonde has now demonstrated sustainable operations in the U.S. and in northwestern Australia using ORBCOMM. Aerosonde is reconsidering the revitalized Iridium, which is now providing full data communications at between 2400 and 9600 baud.

Aerosonde's most recent operations are in the NASA CAMEX-4 project to study hurricanes (at [http://www.aerosonde.com/CAMEX4\\_01.htm](http://www.aerosonde.com/CAMEX4_01.htm)). For this project, Aerosonde passed extensive scrutiny by the National Aeronautics and Space Administration (NASA) air safety board.



Fig. 1. Launching the Aerosonde at Barrow.

### 2. High-latitude Operations

Aerosonde operations and development are being undertaken by Aerosonde Robotic Aircraft and Aerosonde North America. Initial high-latitude flights in the northern hemisphere were a record-breaking flight across the North Atlantic from Newfoundland to Scotland in August 1998 and deployment from Barrow during April 1999 in support of the Department of Energy (DOE) Atmospheric Radiation Measurement (ARM) program Single Column Model Experiment. The Aerosonde has now commenced routine operations in the Arctic, based at Barrow, Alaska (funded by the National Science Foundation Office of Polar Programs (NSF-OPP) and DOE-ARM). Notably, the NSF-OPP Arctic Long-Term

Observations (LTO) project has funded the University of Colorado (CU) and Aerosonde for a five-year period to establish a facility at Barrow for deployment and reconnaissance of Aerosondes and to adapt the Aerosonde to make environmental observations in the extreme Arctic environment. These adaptations include ice detection and mitigation, implementation of satellite communications, improved avionics for payload integration, and development of a fuel-injected engine. Additionally, aeroservoelastic simulations are being conducted towards improving the stability of the Aerosonde for remote sensing applications. Through NASA funding, the Aerosonde will also participate in the validation effort for the Advanced Microwave Scanning Radiometer (AMSR) to be launched in early 2002 onboard the Earth Observing System Aqua platform

Under the NSF project, flights based from Barrow have been conducted during August 2000 and April 2001. The next flights are scheduled for February, April/May, and August 2002. Aerosonde is in the process of transitioning to the Mark 3 aircraft, including icing detection, the new fuel injected engine, a more robust airframe, and new avionics including a separate payload computer. A critical issue that remains for operations in high latitudes is aircraft icing mitigation (note: two aircraft were lost due to icing in the April 1999 flights for DOE ARM). Two different deicing methods have been prototyped and are being tested in an icing tunnel. We anticipate testing an active deicing method in the 2002 flights at Barrow.

The Aerosonde is launched from the roof of a moving launch vehicle (automobile) that needs to reach a speed of 45 mph. The Aerosonde can safely be launched in and recovered in winds of up to 20 m s<sup>-1</sup> with the current car-roof launch system, provided there is not a large cross-wind component. A portable catapult launcher is being developed to enable launches from remote sites: a prototype is being built and we expect testing to be completed within the next year. The catapult launcher has the form of a launch rail with a means of accelerating the aircraft to flight speed in 15 meters.

The facilities required for Aerosonde operations consist of the following elements:

Launch site. The launch site usually consists of a runway, road or open grass-land area with minimal ground obstructions. Minimum length required to safely launch and land an Aerosonde is 300 m. If

the catapult launch system is used, then the only requirement is a relatively smooth surface for landing. Note the aircraft lands on its belly without an undercarriage, so a paved surface is not needed. Some temporary infrastructure needs to be established at the launch site to facilitate the launch of the Aerosonde. At a minimum, a shed is needed to provide necessary shelter and power to run the Aerosonde ground station throughout launch and recovery phases. .

Command center. The command center will take control of all Aerosondes once the full check-out has been undertaken by the launch site. This center is usually located in Melbourne, Australia, but can be located anywhere with reliable communications and a small office capable of accommodating 2-3 personal computers and a couple of people

Workshop and storage site. Preferably located close to the launch site, Aerosonde technicians require workspace to assemble and check Aerosondes prior to missions. The site would also be used to store Aerosonde equipment throughout the mission and should have good security. The workshop needs to be a minimum of 5 m x 5 m and preferably has power and lighting..

Issues that are uncertain at present regarding potential operations in Antarctic are regulatory issues and the availability of LEO satellite communications, and the capacity to operated in high katabatic wind conditions.

### **3. Potential Instrument Payloads**

At present, the Aerosonde has the capability to make standard meteorological observations (pressure, temperature, humidity, winds), surface temperature (radiometric) measurements, and surface visible imaging. Vaisala RSS901 sensors are used to measure temperature, humidity, and pressure. Two sensors are included on each aircraft for redundancy. Vector winds are calculated using the Global Positioning System track data and flight track geometry received from the flight computer. This calculation is routinely done on Aerosondes. Real time downlink of this data is required for the mission. To measure the radiometric surface temperature, the Wintronics KT-11.85 infrared pyrometer is currently being used in the Barrow missions. Visible imaging is done with a color Olympus C3030Z00m Camera.

With improved instrumentation, the Aerosonde has considerable potential to provide

the needed observations in the marginal ice zone, both for operations and scientific research.

The Aerosonde development plan provides for a new avionics system, with substantially upgraded computing capacity by 2002. A separate payload computer is used as the interface between the instrument and avionics, which allows new instruments to be incorporated with minimal modifications. The new payload computer will enable up to 13 Gb of data to be stored on board.

For the present Aerosonde configuration, payload selected for each aircraft must satisfy the following criteria:

- *Weight:* The Aerosonde Mark 3 has a total payload capacity of 7 kg, which includes fuel plus instruments. The Aerosonde fuselage is designed so that there can be a direct weight tradeoff between fuel and instrument payload. The maximum range of the Aerosonde Mark 3 (in still air) without payload is over 3000 km; for each kilogram of payload, the range is reduced by 500 km.
- *Volume:* The volume available in the fuselage for instrument payload is 50x125x200 mm (note: the meteorological sensors are mounted on the wing; hence these instruments are not included in the fuselage volume budget). The fuselage can be modified for specialized purposes, if needed.
- *Power:* The power available for the instrument payload is 40 W sustained and 60-100 W peak.

A proposal to the Department of Defense is pending, for purchase and integration of the following instrumentation onto the Aerosonde:

- laser altimetry
- micro-SAR
- microwave radiometer
- cloud physics instrumentation
- shortwave and longwave radiometers
- thermal cameras
- thermal line-scan sensors

Because of the payload limitation of the Aerosonde, particularly for long endurance flights, each Aerosonde flying a mission will carry a different set of instruments. Formation flying can be used to optimize the measurements. For example, aircraft flying at higher altitudes carrying remote sensing instruments and cameras can fly directly over aircraft carrying instruments for in situ flux measurements.

At present, the Aerosonde is not capable of making direct turbulence measurements. This possibility is being investigated, although no funding has been identified for this development.

#### 4. Potential Science Applications

There is a wide variety of potential scientific applications of the aerosonde to RIME. In support of mesoscale modelling research, the Aerosonde could contribute to

- providing initialization and assimilation data for mesoscale models
- validation of mesoscale model simulations, particularly with regards to meteorological variables, cloud properties, and surface fluxes
- evaluation of satellite observations that are being investigated for assimilation
- evaluation and improvement of cloud and radiation parameterizations
- provision of lower boundary conditions for the mesoscale simulations (e.g. surface temperature, sea ice concentration)

For process-oriented research related to mesoscale cyclogenesis, dynamics of katabatic winds near and beyond the end of the terrain slope, barrier wind generation, topographic modification of synoptic-scale cyclones, and adjustments between marine and continental environments, the Aerosondes can make numerous contributions, with using only the standard meteorological instrumentation. Clusters of Aerosondes can be flown in different regions and at different altitudes in the phenomena of interest, during the entire duration of the event. This would provide unprecedented mesoscale coverage of these phenomena.

#### References

- Holland, G.H., P.J. Webster, J.A. Curry, et al., 2001: The Aerosonde robotic aircraft: A new paradigm for environmental observations. Bull. Amer. Meteorol. Soc, 82, 889-901.

# RIME AND THE DOME C TROPOSPHERIC PROGRAM

Paul Pettré<sup>1</sup>

## 1. Introduction

The Dome C tropospheric program considers a broad sector of the Antarctic which extends from 90°E to 150°W of longitude and includes the area of the Ross Island. It is well-known that this area shows a relatively large climatic variability which results from its position in the atmospheric general circulation. In this area, already largely instrumented, the main Antarctic weather phenomena can be observed. Nevertheless, new instruments are developed and will be set up for the Dome C project.

Although the Dome C project aims at the climatic scale, it is clear that the meso-scale is an obliged passage for the study and validation of parameterizations necessary to the coupled ocean-atmosphere climate models. The RIME experiment is a unique opportunity to document and study the coupling on a synoptic scale between the area of Dome C and that of the Ross Sea.

We present below Dome C Tropospheric Program and its connections with the RIME project.

## 2. Scientific objectives

The crucial problem, in term of studies of weather or climate in the polar areas, is the low density of observation stations, and the shortness and the heterogeneity of the climatological series. After the closing of the Vostok station, Dome C will be the only point of measurement representative of the central high plateau of East Antarctica.

Naturally, in these areas there are complex interactions between atmosphere, ocean and sea ice, and icecaps, inducing many processes of forcing and feedback, more or less associated with orographic effects. This occurs on all scales. With regard to the Antarctic, it is generally considered that katabatic circulation is responsible for the formation of a secondary circulation which can modify the large scale pressure field and the distribution of the depressionary systems as well as the cloud cover and precipitation. In addition, the katabatic winds have a dynamic effect on sea ice, moving the ice pack or opening polynyas, which in turn strongly modifies the heat fluxes

between ocean and atmosphere and consequently the large scale atmospheric circulation.

We have then defined three main objectives for the Dome C project which can be shared in the frame of RIME:

1) development of the automatic systems of meteorological observation, mainly making it possible to obtain a profile of wind and temperature from surface to an altitude of several kilometres, and a system to evaluate precipitation and snow drift or sublimation;

2) improvement of physical parameterizations of the cryosphere-atmosphere exchanges on the Antarctic high plateau and the validation of the satellite observations of altimetry necessary to determine mass balance, surface roughness, temperature, and nebulosity;

3) study of the secondary meridional circulation induced by the katabatic winds and the transport of the cold air from the Antarctic plateau towards its periphery and the average latitudes which is at the origin of the Semi-Annual Oscillation in the Southern high latitudes as well as the subsidence in the polar vortex. This study will make it possible to improve our knowledge of the complex processes observed in this area taking into account the interactions between cryosphere, atmosphere, ocean and sea ice. One will also be able to quantify the seasonal cycle of the transport of cold air, aerosols and chemical components.

## 3. Connection of the Dome C project with RIME

Through the atmospheric boundary layer (ABL), typically a few hundreds of meters thick, heat, moisture and momentum fluxes are transferred by turbulent processes to the circulation of the free atmosphere. The wind and temperature profiles observed in the troposphere are then the result of the action of these turbulent ABL processes.

In Antarctica, due to the presence of a strong stable stratification of the air close to the

---

<sup>1</sup> CNRM/GMGEC 42, avenue G. Coriolis 31057 Toulouse Cedex, France ; Email : pettre@meteo.fr

ground, the ABL plays a central role in determining the climate of the entire continent. The large-scale atmospheric circulation in and around Antarctica is influenced by the near-surface katabatic circulation, which can be considered as the lower branch of the secondary circulation which will be studied as the complementary part in the Dome C project. Despite the crucial role of stable boundary layer processes, our lack of knowledge is twofold: first, the Antarctic atmospheric boundary layer is poorly documented in terms of available experimental data, and second, the theoretical understanding of the physical processes taking place is incomplete. Therefore, future research efforts are necessary in both fields.

On the theoretical and modelling side, the stable boundary layer is still the object of several basic studies because its behaviour is quite unpredictable due to the presence of intermittency (i.e. sporadic turbulent activity in an otherwise very stable environment), internal gravity waves and low level-jets. There is a need to evaluate and improve the existing parameterisations, and possibly to develop new ones. The quality of forecasting in the polar regions depends on our experimental and theoretical understanding of the processes taking place in the Antarctic boundary layer.

Collaborations and support will be sought to develop and test recently proposed ABL parameterizations which are expected to considerably enhance the physical basis of meso-scale forecast models in the case of very stable atmospheric conditions. Continued interactions between modellers and experimentalists within the project will insure that models and data are optimally exploited, and if necessary adapted for better use.

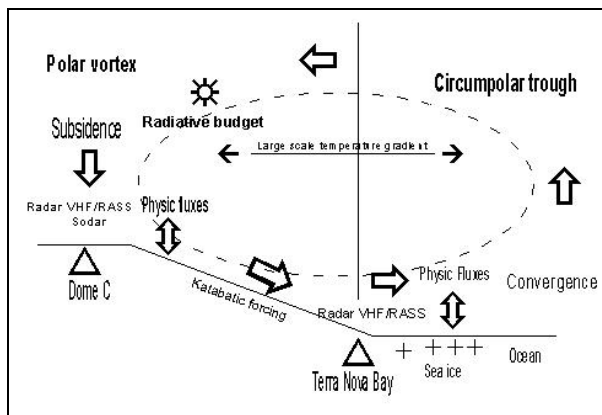


Fig. 1. Conceptual depiction of the Dome C tropospheric experiment.

#### 4. Field experiment

To achieve the above listed scientific objectives an experiment is foreseen in which the following measurements are planned.

##### Radiation

Two radiometers mod.CNR-1 (Kipp and Zonen) will be used for the determination of the radiation budget. These instruments measure separately the short- and long-wave radiation of incoming and outgoing components to derive the net radiation ( $R_n$ ) at the Earth's surface. The short-wave radiation is measured by two pyranometers (CM3), one for the incoming component from the sky, and the other, facing downward, for the reflected component from the snow. From these two pyranometers the albedo is determined. Long-wave radiation is measured by two pyrgeometers (CG3), one for the far infrared radiation coming from the sky, the other from the snow surface. The radiometric data will be recorded by a Campbell CR10 - ET data-logger every minute, averaged every 10 minutes and then stored in a Campbell SM192 memory module. One of these radiometers will be installed on a 2-3m meteo mast (hereafter MM). Another has already been installed at the summit of the 13m tower (hereafter MT) during the 1999/2000 field experiment in Dome C.

##### Turbulent Fluxes and surface layer profiles

Profile relationships are needed, as are the vertical gradients of wind, temperature and humidity, which are related to the turbulent transfer. Both profiles and direct flux measurements have their limitations. It is then advantageous to make possible a large number of measurements in order to compare fluxes and different parameterizations (gradient method, eddy correlation, etc). Thermometers, hygrometers and wind probes will be settled at 1.25, 2.5, 5, 10 and 13 m (top of the meteo tower) in order to obtain the wind and temperature profiles in the surface layer. Two sonic anemo-thermometers model USA - 1 (Metek) and a fast response lyman-alpha-hygrometer will be used in the station for turbulence to estimate the heat and latent fluxes. One of the fast response sensors (anemo-thermometer and fast hygrometer) will be settled on the MM and located in a flat zone with little or no obstruction nearby, the other at the top of MT. The raw-data will be collected by a MeteoFlux computer system performing real-time measurements of the 3 wind components, humidity and sonic temperature at a frequency of 10 Hz. The data will be processed by means of three axis rotations following Sozzi and Favaron (1996).

### **Sub-surface energy fluxes**

During the summer the main sources of heat transfer in the ice is the absorption of solar radiation. In the other seasons, when the solar radiation is negligible, the heat conduction plays a major role. To fully parameterise the energy budget proper measurement of the snow heat fluxes at 5, 15, 50 cm will be done with conventional HFP01 heat flux plates. Also temperature measurements into the snow will be done at 0, 5, 15, 33 and 50 cm in order to test existing parameterisation for energy fluxes into the snow.

### **Automatic weather station data**

The automatic weather station data will be used as a support to the turbulent fluxes and atmospheric profiles studies as well to connect surface data observation in Dome C with other Antarctic stations.

### **Microbarographs**

Internal waves generated topographically or otherwise are one of the sources making difficult the parameterisation of the stable ABL. Internal wave propagation, their velocity and intensity, and the consequent transfer of energy may be studied using 3 microbarographs suitably located in a 1-km area.

### **Minisodar**

A triaxial Doppler sodar will be used to study the thermal structure of the atmosphere, to monitor the boundary layer depth and to measure the horizontal and vertical velocity. The mini-sodar will be located close to the anemological and the radiometer stations.

### **Micro-lidar**

Measurements of aerosol load and phase inside the ABL will be achieved with a remote sensing technique using a two wavelengths (532 and 1064 nm) micro-lidar looking upward from the ground. The system is expected to retrieve a molecular + aerosol profile of about 150-300 m in the ABL and to detect aerosol phase (liquid water or ice crystal), estimating also the particle size distribution. The phase is retrieved by the ratio between the main and the cross-polarised signal at 532 nm (volume depolarisation): zero or very low values of depolarisation indicate aerosols in liquid phase; ratios around 50% are peculiar of well formed (size > 1 micron) ice crystals; intermediate values of depolarisation indicate mixed phases or amorphous particles. Moreover an estimate of the particle size distribution is possible, using the

wavelength dependence of the backscattering ratio, particularly when the mean radius of the particles is comparable with the wavelengths used (in our system for radii < 10 micron). The lasers with polarised emission will have a power of few micro-Joule and a repetition rate of a few kHz. The vertical resolution will be better than 4 m.

### **Microwave radiometer**

The development and break down of atmospheric inversions over the course of the time will be quantitatively estimated using a passive Microwave radiometer (MPT 5) by Kipp and Zonen. MPT 5 is a scanning 5-mm radiometer specially adapted for Antarctic studies. It will use remote sensing to monitor the boundary layer temperature from the ground up to 500 m. The determination of temperature profile is based on thermal radiation measurements at different zenith angles.

## **5. Study of the secondary meridional circulation**

Experiment IAGO (André et al. 1986), performed in 1985, was aimed at studying the katabatic flow on a broad field stretching from 200 km inside the continent to the coast. The results of IAGO showed that, as one could expect, the strongest interactions between the katabatic flow and the general circulation occur in the coastal area. The influence of large-scale forcing on the katabatic regime at Adélie Land has also been studied by Parish et al. (1993) using model simulations, which have indicated that the ambient environment plays a key role in the development and intensity of the katabatic wind regime. As shown by Gallée and Pettré (1998), cold air accumulates at the foot of the slope and can modify the local pressure gradient and induce convergence, parallel to the coast, between the katabatic wind coming from the continent and the flux due to an oceanic perturbation.

The atmospheric circulation in the Antarctic surface is entirely dominated by the katabatic winds, which show very high regularity. Except for relatively rare strong katabatic events and the very calm situations in summer during which local, thermally-forced circulations can occur (Pettré et al. 1993), one can expect to observe in this region very regular conditions throughout the boundary layer. In addition, the transport of cold air by the katabatic winds from the Antarctic high plateau towards its periphery induces a meridional circulation.

The experimental network includes the continental station of Dome C and the coastal stations of Terra Nova Bay (Italy) and Dumont d'

Urville (France). The Dome C station will be equipped with a wind and temperature profiler RIME experiment, the station at Terra Nova Bay could be equipped with another radar VHF/RASS for the study of the secondary circulation induced by the katabatic winds: assessment of the momentum flux through the coast line and of its variability, penetration of the oceanic disturbances on the continent and katabatic response, effect of the extent and concentration of sea ice, formation and height of the tropopause, and position of the polar vortex.

To facilitate the validation of model simulations, the network will be increased with the automatic stations on the transects Dumont d'Urville - Dome C (American AWS) and Casey - Dome C (Australian AWS), and by the weather station at Dumont d'Urville.

### Radar VHF/RASS

Radar VHF configuration: Frequency: 45 MHz; transmitted power: 2.5 KW. Antenna: 16 dipoles, surface: 10x10 m<sup>2</sup>; 3 beams: vertical, north, east.

RASS configuration: 2 sources; Acoustic frequencies: 80 to 110 Hz; Transmission mode: pseudo random by 0.5s steps between 80 and 110 Hz; Working: only in vertical direction beam of the radar and between 06H and 22H LT (3 min every 10 mn; Coverage: 1 to 4-5 km; Range resolution: 300 m.

### Present weather sensor and precipitation measurement

Vaïssala FD12P able to discriminate the type of precipitation (snow, ice, water) and to evaluate the quantity of precipitation.

(radar VHF/RASS) allowing an evaluation of the air subsidence. In the framework of the

### 6. Implementation

We list below the main instruments that will be installed at Dome C and the laboratories involved. Each laboratory takes charge of the development of the instrument, its implementation and the data processing. A database will be created and maintained by the GEOGAA to make it available to the national and international community.

### Bibliography

- André, J.C., Wendler, G., and Zephoris, M., 1986: The IAGO Katabatic programme, *Antarctic Climate Research*, **1**, 17--18.
- Gallée, H., and Pettré, P., 1998: Dynamical constraints on katabatic wind cessation in adélie Land, Antarctica, *J. Atmos. Sci.*, **55**, 1755--1770.
- Parish, T.R., Pettré, P., and Wendler, G., 1993: The influence of large-scale forcing on the katabatic wind regime at Adelie Land, Antarctica, *Meteorol. Atmos. Phys.*, **51**, 165--176.
- Pettré, P., Payan, C. and Parish, T. R., 1993: Interaction of katabatic flow with local thermal effects in a coastal region of Adelie Land, East Antarctica, *J. Geophys. Res.*, **98**, D6, 10,429--10,440.

Table 1. Collaborators and instruments for the Dome C Tropospheric Program

| Laboratory                                   | Instrumentation   | Staff   |
|--|---|---|
| CNR-IFA<br>Roma                              | Turbulent fluxes - Mast/Tower<br>Radiative budget - Mast<br>Mini-Sodar<br>Microwave Radiometer<br>Microbarograph<br>Micro-Lidar | Stefania Argentini<br>Giangiuseppe Mastrantonio<br>Angelo Viola<br>Igor Petenko<br>Francesco Cairo<br>Guido Di Donfrancesco |
| CNR-ISAO<br>Bologna                          | Radiative budget- Tower<br>Turbulent fluxes - Tower   | Marianna Nardino<br>Teodoro Georgiadis<br>Ubaldo Bonafé<br>Francesco Calzolari<br>Giuliano Trivellone                       |
| ENEA-PAS<br>Roma                             | Radio-sounding<br>Automatic Weather Station   | Andrea Pellegrini   |
| CNRM<br>Toulouse<br>CRA/LA/OMP<br>Lannemezan | Radar VHF/RASS<br>Dome C<br>Dumont d'Urville  | Paul Pettré<br>Vladislav Klaus<br>Bernard Campistron<br>Gilbert Despau  |
| LEGOS<br>Toulouse                            | Satellite observations  | Frédérique Remy<br>Benoît Legresy   |
| <b>Modelling</b>                             |   |   |
| CNRM<br>Toulouse                             | Model ARPEGE-Climat<br>Vaïssala PWD11   | Paul Pettré<br>David Salas y Melia<br>Fabrice Chauvin   |
| LGGE<br>Grenoble                             | Model LMD-Z   | Christophe Genthon<br>Gerhard Krinner   |
| <b>Data spreading</b>                        |   |   |
| GEOGAA<br>Toulouse                           | Data base<br>Multidisciplinary aspects  | Paul Pettré   |

# SIMULATION OF THE IRON DUST TRANSPORT IN THE ROSS SEA

Hubert Gallée<sup>1</sup>

Laboratoire de Glaciologie et de Géophysique de l'Environnement, Grenoble, France

## 1. Introduction

Recent scientific developments have shown increased evidence that the natural sulphur cycle in the Southern Ocean plays a fundamental role in regulating the climate. Dimethyl sulphide (DMS) production by the phytoplankton is a major source for oxidized atmospheric by-products that ultimately form cloud-condensation nuclei that strongly impact the Earth's radiative balance. In the high-nutrient, low-chlorophyll waters of the Southern Ocean, productivity, and therefore DMS production, appears to be iron limited. Phytoplankton blooms in the functional environments around Antarctica are at least partially controlled by iron availability. Among the different sources, large inputs of iron are delivered to the ocean surface from melting of the seasonal sea ice. Estimates of the impact of this process range between 2 and 13,000 % of the calculated new production in the area. This clearly demonstrates the urgent need for better estimates of the spatial and temporal variability of iron in the sea-ice cover and to assess the different sources of the element. It also shows the interest in detecting a potential synergy between iron, DMS and biology in the environment.

## 2. Overview of the Project

Antarctic iron is mainly of crustal origin. The supply of atmospheric dust iron originates from four main sources: the deserts of South America, South Africa, Australia, and Transantarctic Mountains.

The aim of this project is to simulate the iron input and redistribution on the sea-ice cover around Antarctica. To reach that goal an ocean-sea ice model will be forced by the output of a regional climate model (RCM) in which the erosion, transport and deposition of dust iron will be included. The coupling between atmosphere, sea-ice and the ocean will be considered later.

This work is closely related to the RIME

program, and provides the opportunity for interaction. It will be a part of the VIDAS project (Spatial and Temporal Variability of Iron and Dimethyl Sulphide -- DMS -- in Antarctic Sea Ice) which will be submitted to the European Community. Other European teams have collected sea-ice samples in the Ross Sea and will analyze their composition. Their results will be used in order to validate the simulations made with the RCM.

## 3. The Models

### 3.1 Ocean-sea ice model

The sea ice model will be that developed by the Institut d'Astronomie et de géophysique G. Lemaitre (Louvain-La-Neuve, Belgium) (Fichefet et al. 1997). It is coupled to the French Community Ocean Model, OPA (Treguier et al., 2001).

### 3.2 Regional climate model

The regional climate model used will be a mesoscale atmospheric model MAR (Modèle Atmosphérique Régional) which was originally developed for process oriented studies of the Antarctic atmosphere, particularly over the Ross Sea (Gallée and Schayes, 1994; Gallée, 1995; Gallée, 1996). This model is now used by the Laboratoire d'étude des Transferts en Hydrologie et Environnement (LTHE) and the Laboratoire de Glaciologie et de Géophysique de l'Environnement (LGGE), from the Observatoire des Sciences de l'Univers de Grenoble (OSUG, France). The model is also adapted to perform longer time scale simulations nested into large scale forcing fields from an analysis or atmospheric general circulation model. It is a hydrostatic primitive-equation model in which the vertical coordinate is the normalized pressure. The vertical subgrid scale fluxes are treated using the E-epsilon model of turbulence, allowing representation of the turbulent mixing length as a function of the local flow

---

<sup>1</sup>Corresponding Author Address: Dr. Hubert Gallée, Laboratoire de Glaciologie et de Géophysique de l'Environnement, 54 Rue Moliere, DU BP 96 F-38402 Saint Martin d'Hères Cedex, FRANCE



characteristics. This enables an accurate representation of the complex katabatic layer structure. The atmospheric model has recently been updated with a sea-ice model (Gallée, 1997) and with a multi-layered thermodynamic representation of the snow pack (Gallée and Duynkerke, 1997), including the snow metamorphism laws of the Centre d'Etudes de la Neige (Grenoble) (Brun et al., 1992). The snow pack albedo and solar extinction coefficient are calculated from the simulated snow grain characteristics which evolve in time depending on the prevailing temperature gradients and liquid water content in the snow pack. Snow drift, a common feature over Antarctica, is also incorporated (Gallée et al., 2001). Blowing snow affects the near-surface atmosphere vertical stability (via density increase and enhanced sublimation) as well as the surface mass balance by redistributing surface snow in the Antarctic ice sheet marginal zones. This upgraded model therefore provides us with an ideal tool to study atmospheric transport as well as deposition of trace elements over Antarctica in a wider climatic context.

Iron particles originating from remote sources and the Transantarctic Mountains are transported by large-scale advection and the katabatic wind regime, respectively. Vertical mixing through the depth of the atmosphere is produced mainly by vertical turbulent diffusion. The mechanisms that are responsible for the deposition of particles from the atmosphere to the surface are dry deposition, wet deposition, as well as fog deposition (Davidson et al., 1996). Dry deposition represents the collection of mechanisms that continually transport particles to the earth's surface even in the absence of clouds or fog. Wet deposition can be caused by nucleation scavenging (particles serving as condensation nuclei) and in-cloud as well as below-cloud scavenging (collecting particles during precipitation). Passive tracer sources, transport, and deposition will be implemented in the atmospheric model. Furthermore, iron transport by drifting snow particles will be added to the blowing snow model. This could be an important additional iron input to the sea ice.

## References

Brun, E., P. David, M. Sudul and G. Brunot, 1992: A numerical model to simulate snowcover stratigraphy for operational avalanche forecasting. *J. Glaciol.* **38** (128), 13-22.

- Davidson, C.I., M.H. Bergin, and H.D. Kuhns, 1996: The deposition of particles and gases to ice sheets, in *Chemical exchange between the atmosphere and polar snow*, edited by E. Woff, and R.C. Bales, pp. 275-306, Springer-Verlag, New-York.
- Fichefet, T., and M.A. Morales Maqueda, 1997: Sensitivity of a global sea ice model to the treatment of ice thermodynamics and dynamics, *J. Geophys. Res.*, **102**, 12609-12646.
- Gallée, H., and G. Schayes, 1995: Development of a three-dimensional Meso-g primitive equation model : katabatic winds simulation in the area of Terra Nova Bay, Antarctica, *Monthly Weather Review*, **122** (4), 671-685.
- Gallée, H., 1995: Simulation of the Mesocyclonic activity in the Ross Sea, Antarctica, *Monthly Weather Review*, **123** (7), 2051-2069.
- Gallée, H., 1996: Mesoscale atmospheric circulations over the southwestern Ross Sea sector, Antarctica, *J. Appl. Meteorol.* **35**, 1142-1152.
- Gallée, H., 1997: Air-sea interactions over Terra Nova Bay during winter: simulation with a coupled atmosphere-polynya model, *J. Geophys. Res.*, **102** (D12), 13835-13849.
- Gallée, H., and P.G. Duynkerke, 1997: Air-snow interactions and the surface energy and mass balance over the melting zone of west Greenland during GIMEX, *J. Geophys. Res.*, **102** (D12), 13813-13824.
- Gallée, H., G. Guyomarc'h, and E. Brun, 2001: Impact of the snow drift on the Antarctic ice sheet surface mass balance : a sensitivity study to snow surface properties, *Bound.-Layer Meteor.*, **99**, 1-19.
- Treguier, A-M., B. Barnier, A. de Miranda, J.-M. Molines, N. Grima, M. Imbard, G. Madec, C. Messenger and S. Michel, 2001: An eddy permitting model of the Atlantic circulation: evaluating open boundary conditions. *J. Geophys. Res.*, in press.